NUREG/CR-4091
SAND84-2291
RV
Printed May 1985

The Effect of Alternative Aging and Accident Simulations on Polymer Properties

L. D. Bustard, J. Chenion, F. Carlin, C. Alba,
G. Gaussens, M. LeMeur

Prepared by
Sandia National Laboratories
Albuquerque, New Mexico 87185 and Livermore, California 94550
for the United States Department of Energy
under Contract DE-AC04-76DP00789

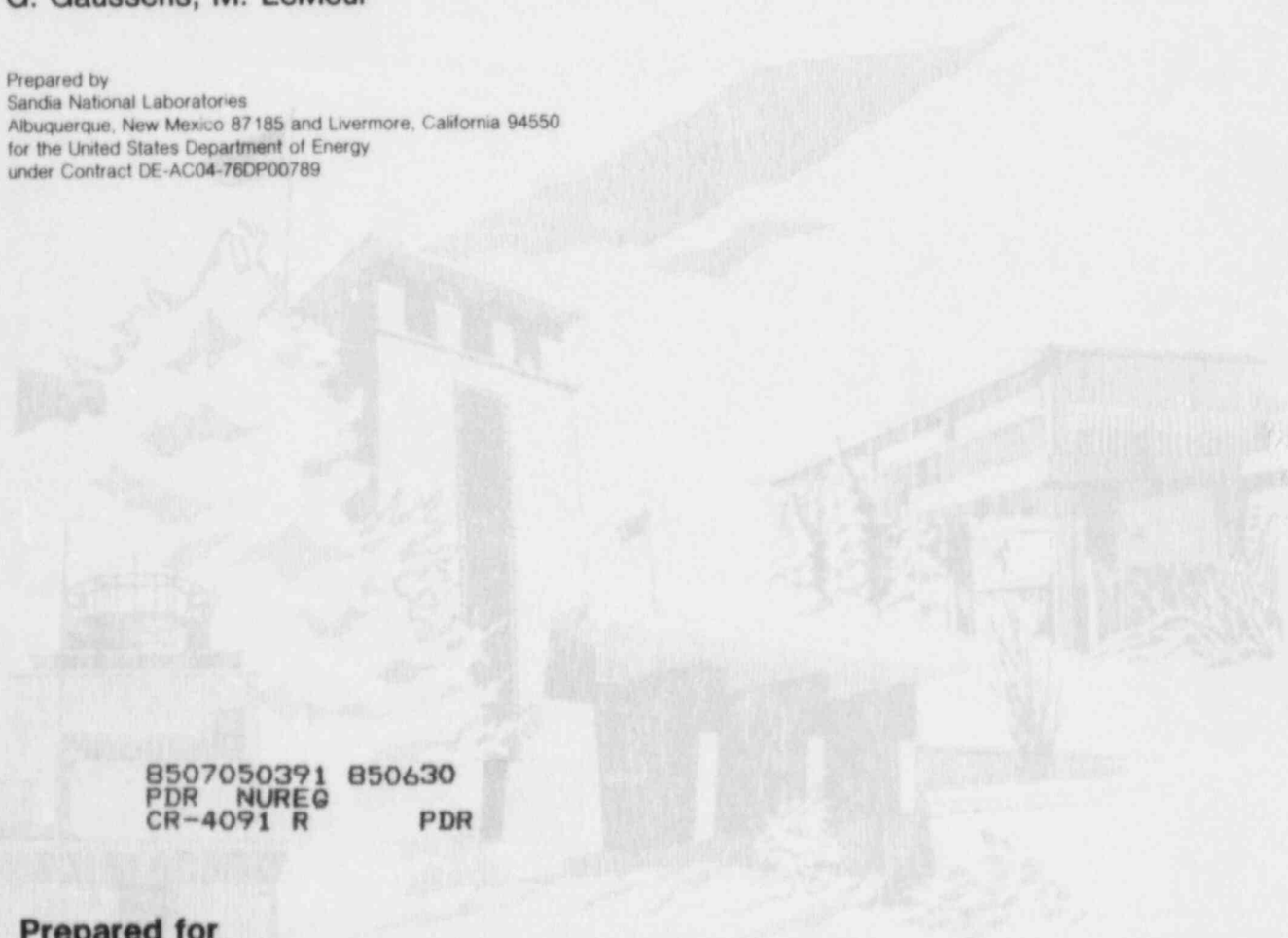

Prepared for
U. S. NUCLEAR REGULATORY COMMISSION

Available from

Superintendent of Documents
U.S. Government Printing Office
Post Office Box 37082
Washington, D.C. 20013-7982

and

National Technical Information Service
Springfield, VA 22161

NUREG/CR-4091
SAND84-2291
RV

THE EFFECT OF ALTERNATIVE AGING AND ACCIDENT SIMULATIONS ON POLYMER PROPERTIES

L. D. Bustard
Sandia National Laboratories
Albuquerque, New Mexico 87185, USA

J. Chenion, F. Carlin, C. Alba, and G. Gaussens
CEA-ORIS LABRA at Saclay
91190 Gif-sur-Yvette, France

M. LeMeur
CEA-DAS-SAF
92260 Fontenay-aux-Roses, France

May 1985

Sandia National Laboratories
Albuquerque, New Mexico
Operated by
Sandia Corporation
for the
U. S. Department of Energy

Prepared for
Electrical Engineering and Instrument Control Branch
Division of Engineering Technology
Office of Nuclear Regulatory Research
U.S. Nuclear Regulatory Commission
Washington, DC 20555
Under Memorandum of Understanding DOE 40-550-75
NRC FIN No. A-1051

PREVIOUS PUBLICATIONS IN THIS SERIES

1. K. T. Gillen, R. L. Clough, G. Ganouna-Cohen, J. Chenion, and G. Delmas, Loss of Coolant Accident (LOCA) Simulation Tests on Polymers: The Importance of Including Oxygen, NUREG/CR-2763, SAND82-1071, July 1982.

2. K. T. Gillen, R. L. Clough, G. Ganouna-Cohen, J. Chenion, and G. Delmas, "The Importance of Oxygen in LOCA Simulation Tests," Nuclear Engineering and Design, 74 (1982), pp. 271-285.

3. L. D. Bustard, E. Minor, J. Chenion, F. Carlin, C. Alba, G. Gaussens, and M. LeMeur, The Effect of Thermal and Irradiation Aging Simulation Procedures on Polymer Properties, NUREG/CR-3629, SAND83-2651, April 1984.

ABSTRACT

The influence of accident irradiation, steam, and chemical spray exposures on the behavior of twenty-three age-preconditioned polymer sample sets (twenty-one different materials) has been investigated. The test program varied the following conditions:

1. Accident simulations of irradiation and thermodynamic (steam and chemical spray) conditions were performed both sequentially and simultaneously.

2. Accident thermodynamic (steam and chemical spray) exposures were performed both with and without air present during the exposures.

3. Sequential accident irradiations were performed both at 28°C and 70°C.

4. Age preconditioning was performed both sequentially and simultaneously.

5. Sequential aging irradiations were performed both at 27°C and 70°C.

6. Sequential aging exposures were performed using two sequences: (1) thermal followed by irradiation and (2) irradiation followed by thermal.

We report both general trends applicable to a majority of the tested materials as well as specific results for each polymer. Our data base consists of ultimate tensile properties at the completion of the accident exposure for three XLPO and XLPE, five EPR and EPDM, two CSPE (HYPALON®), one CPE, one VAMAC, one polydiallylphtalate, and one PPS material. We also report bend test results at completion of the accident exposures for two TEFZEL® materials and permanent set after compression results for three EPR, one VAMAC, one BUNA N®, one SILICONE, and one VITON® material.

TABLE OF CONTENTS

TABLE OF CONTENTS
(continued)

LIST OF FIGURES

LIST OF FIGURES
(continued)

LIST OF FIGURES
(continued)

LIST OF FIGURES
(continued)

LIST OF TABLES

LIST OF TABLES
(continued)

ACKNOWLEDGMENTS

Our appreciation is extended to Stella St.Clair who ably assisted with the measurements of the U.S. samples, the data analysis for all samples, and the graphic display of all data. We also thank Frank Wyant for assisting with the computer graphics display of our data.

EXECUTIVE SUMMARY

The response of twenty-one U.S. and French polymer materials to variations in aging and accident simulation techniques has been determined by a joint U.S.-French experimental program. Twenty-three different sample sets were employed (i.e., two materials were tested both for tensile properties and for permanent set after compression). The test program varied the following conditions:

1) Accident simulations of irradiation and thermodynamic (steam and chemical spray) conditions were performed both sequentially and simultaneously.

2) Accident thermodynamic (steam and chemical spray) exposures were performed both with and without air present during the exposures.

3) Sequential accident irradiations were performed both at 28°C and 70°C.

4) Age preconditioning was performed both sequentially and simultaneously.

5) Sequential aging irradiations were performed both at 28°C and 70°C.

6) Sequential aging exposures were performed using two sequences: (1) thermal followed by irradiation and (2) irradiation followed by thermal.

The individual effect of several of these parameters has previously been reported by numerous authors.[1-11] However, these previous research activities rarely combined accident and aging research into one comprehensive test program. We varied several aging and accident test parameters in one research program.

Our overall research goal was to determine whether some combinations of alternative aging and accident simulation techniques are better suited for qualification activities than other combinations of simulation techniques. To help answer this question, we performed two evaluations on our experimental data base. First, we identified those sequential accident simulation techniques that produced degradation similar to that achieved during simultaneous irradiation and LOCA (with air) accident simulation test exposures. We consider this simultaneous accident simulation to be the best representation among our alternative simulations of postulated design basis event accident conditions. During this evaluation, we also identified those aging techniques that were most conservative (i.e., produced the most degradation) when followed by the simultaneous accident simulation.

Second, we analyzed our experimental data base to identify those aging and accident simulation techniques that severely degraded the polymer mechanical properties. For this evaluation, we only considered materials which had been exposed to all combinations of the alternative aging and accident simulations. We generated tables of all aging and accident simulation combinations. (There were separate tables for French

and U.S. materials.) For each table location, we listed all the U.S. or French materials whose mechanical properties were reduced by that choice of aging and accident simulations to or below a threshhold value. (For example, we listed all materials whose normalized elongation, e/e_o, was reduced to .05 or less). An examination of the table illustrates those combinations of aging and accident simulations affecting the greatest number of our materials. To further analyze our results, we provided each material entry in the table a weight to reflect the material's sensitivity to the choice of aging and accident simulation techniques. A low weight is given to each material entry if that material's degradation is insensitive to the choice of aging and accident simulation techniques. A high weight is given if the material's degradation is very sensitive to the choice of aging and accident simulation techniques. By summing the assigned weights, we evaluated the relative importance of each aging and accident simulation technique.

Both evaluation techniques lead to similar conclusions. For mechanical properties of the materials we tested, the more conservative choice for an aging sequence would be a radiation followed by a thermal exposure.

We also note that the presence or absence of air during accident simulations can influence the degree of degradation in some materials. The U.S. EPR and TEFZEL materials are examples where degradation of ultimate tensile elongation is enhanced when air (oxygen) is present during accident simulations; the U.S. XLPO materials are examples where elongation degradation is reduced by the presence of air. Hence, since most reactor containments are not inerted, a conservative accident simulation for qualifying our materials would include air in the LOCA test chamber.

We noted substantial variability in test results because of differences in either the chemical composition or processing of test samples. For example, the response of the French cross-linked polyolefin material to alternative simulation techniques is different than the response of the two U.S. cross-linked polyolefin materials. Similar variability was noted both within and between other classes of material.

We encourage the development of a larger data base. This will enable our "preliminary" insights to either be solidified or appropriately modified.

It is important to recognize the limitations associated with our study. We monitored only mechanical properties of our polymer materials. Mechanical failure is an important but not the sole method by which polymers can contribute to functional degradation of Class 1E equipment. We also tested a limited number of materials. Many important classes of polymers were not included in our study. Our conclusions represent dominant trends and may not therefore apply to all materials. For some materials, alternative aging and accident simulation techniques may be equally appropriate. Finally, we choose experimental test conditions (radiation dose, steam profiles, etc.) that are not applicable to all nuclear utilities. These limitations should be considered prior to incorporating our "preliminary" conclusions into a qualification program for Class 1E equipment.

1.0 INTRODUCTION

Polymer materials are important components of safety-related equipment both in the United States and France. Some examples are cables, transmitters, and pressure switches. In both countries, safety-related equipment containing polymer constituents is qualified by tests that simulate aging and postulated accident environments. These simulations rarely reproduce the environmental parameters exactly. In fact, it would be impossible to exactly reproduce aging environments because of the long experimental times (approximately 40 years) that would be required. Other constraints also limit the experimental ability to reproduce accident environments exactly. Hence a necessary aspect of each qualification program is the choice of appropriate environmental simulation techniques and parameters.

The response of twenty-three U.S. and French polymer materials to variations in aging and accident simulation techniques has been determined by our joint U.S.-French experimental program. This information will provide the nuclear industry and regulatory bodies in the United States and France a partial data base by which to judge appropriate simulation practices. The test program varied the following conditions:

1. Accident simulations of irradiation and thermodynamic (steam and chemical spray) conditions were performed both sequentially and simultaneously.

2. Accident thermodynamic (steam and chemical spray) exposures were performed both with and without air present during the exposures.

3. Sequential accident irradiations were performed both at 28°C and 70°C.

4. Age preconditioning was performed both sequentially and simultaneously.

5. Sequential aging irradiations were performed both at 28°C and 70°C.

6. Sequential aging exposures were performed using two sequences: (1) thermal followed by irradiation and (2) irradiation followed by thermal.

The individual effect of several of these parameters has been previously reported by numerous authors. For example, we have previously reported on the influence of aging simulation procedures on polymer properties.[1] A recent publication highlights much of the research that has been performed on accelerated-aging tests for predicting radiation degradation of organic materials.[2] Other publications [3-11] report on accident methodology research activities.

These previous research activities rarely combined accident and aging research into one comprehensive test program. Our goal was to vary

several aging and accident test parameters in one research program. Thus the relative importance of each of these parameters could be assessed. Also, test conclusions would be less influenced by arbitrary choices for some test parameters (i.e., we reduced the number of parameters held constant throughout the test program.)

Our study, however, did require a choice of postulated aging and accident environments. Variations in reactor type and containment design make difficult a choice applicable to all reactors. We chose 25 Mrd as an aging radiation exposure and 60 Mrd as an accident radiation exposure. Dose rates of ~0.06 Mrd/h were used for aging of U.S. samples; dose rates of ~.1 Mrd/h were used for the French samples. The accident irradiations for both the French and U.S. samples were done at ~.3 Mrd/h. These doses and dose rates are consistent with those employed in France for qualification purposes at the start of our test program. Our accident simulation of thermodynamic conditions (steam and chemical spray) was also based on French qualification requirements. Table 1.1 lists a typical French qualification exposure sequence. Figure 1.1 illustrates the French accident steam and chemical spray exposure profile. For contrast, Figure 1.2 provides information on a typical U.S. effort as might be employed for qualification of cables.

Irradiations in the United States that simulate aging and accident conditions are typically performed at ambient conditions. In contrast, in France both the aging and accident irradiations are performed at 70°C. This latter choice reflects typical maximum operating temperatures inside containment plus margin. Our test program varied the irradiation temperature to assess the importance of this difference between U.S. and French qualification practices; samples were irradiated at both 27°-28°C and 70°C.

An important parameter not varied during our experimental program was the aging irradiation dose rate. Experimental studies [2,12-14] have demonstrated the importance of physical and chemical contributions to dose rate effects. Physical dose rate effects are caused by diffusion- limited oxidation. Our aging irradiation dose rate of ~0.1 Mrd/h (an order of magnitude less than sometimes used in U.S. qualification efforts) reduces the impact of oxygen diffusion effects, an important cause of dose rate effects.[2] Chemical dose rate effects are most commonly caused by the slow breakdown of intermediate hydroperoxide species. Such a process may be occurring if material properties depend on the test sequence of irradiation and thermal exposures.

In this report we summarize test results and conclusions at completion of our accident simulations. A previous publication [1] summarized our results and conclusions at completion of the aging portion of our research program. The previous publication also provided detailed descriptions of the samples, the aging facilities, and the aging procedures. In this report we only briefly summarize these facts and then discuss in more detail the accident simulation facilities and techniques, test results, and conclusions.

Table 1.1

French Qualification Exposure Sequence
At The Time of Test Program Implementation

1. Thermal Aging

2. Radiation Aging
   25 Mrd at 70°C and approximately 0.1 Mrd/h

3. Accident Irradiation
   60 Mrd at 70°C and approximately 0.3 Mrd/h

4. Accident Steam and Chemical Spray Exposure
   (Figure 1)

5. Post-Accident Exposure
   10 days at 100°C and approximately 95% RH

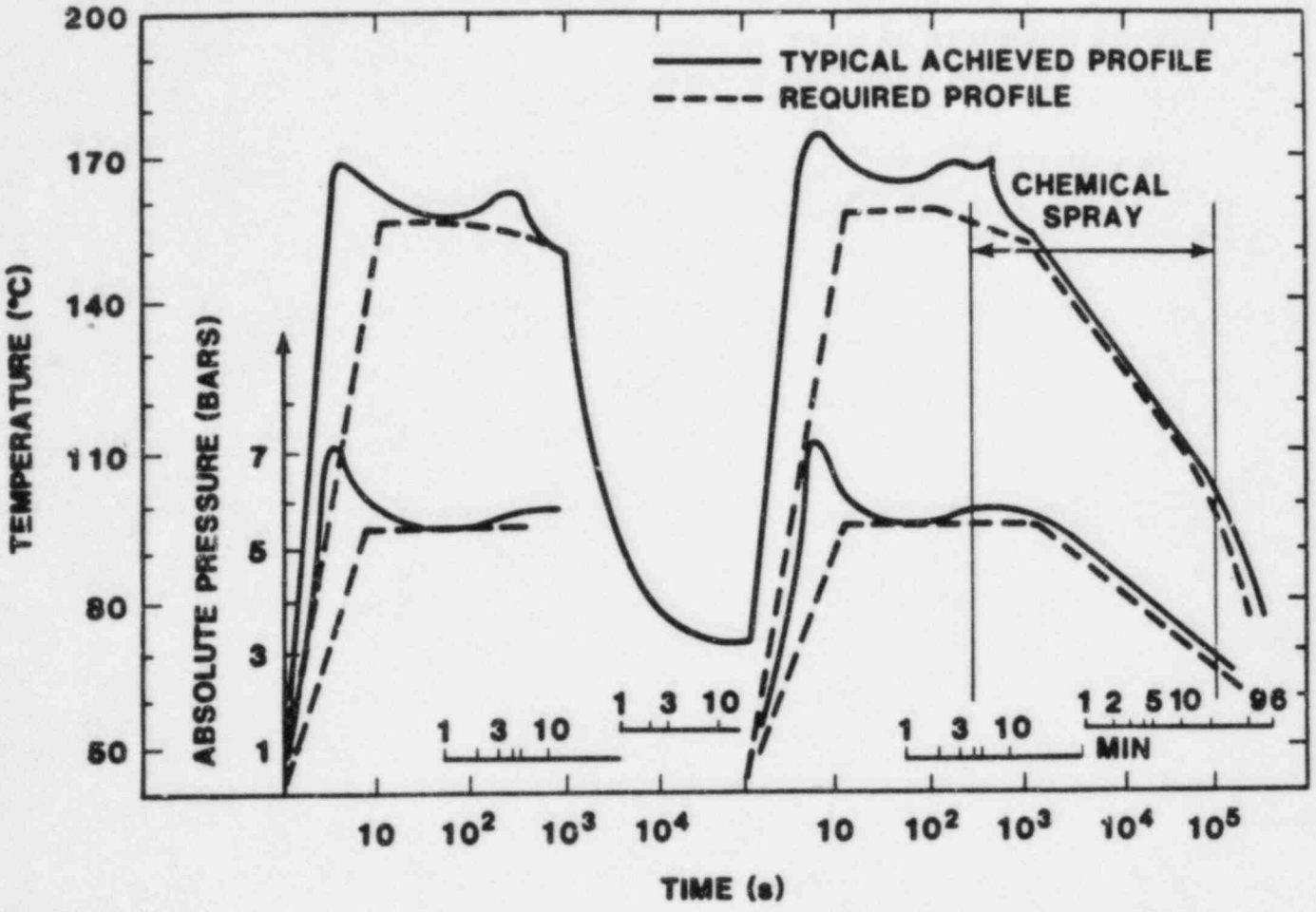

Figure 1.1: French Accident Steam and Chemical Spray Exposure Profile. Table 1.1 summarizes other portions of the French qualification exposure sequence.

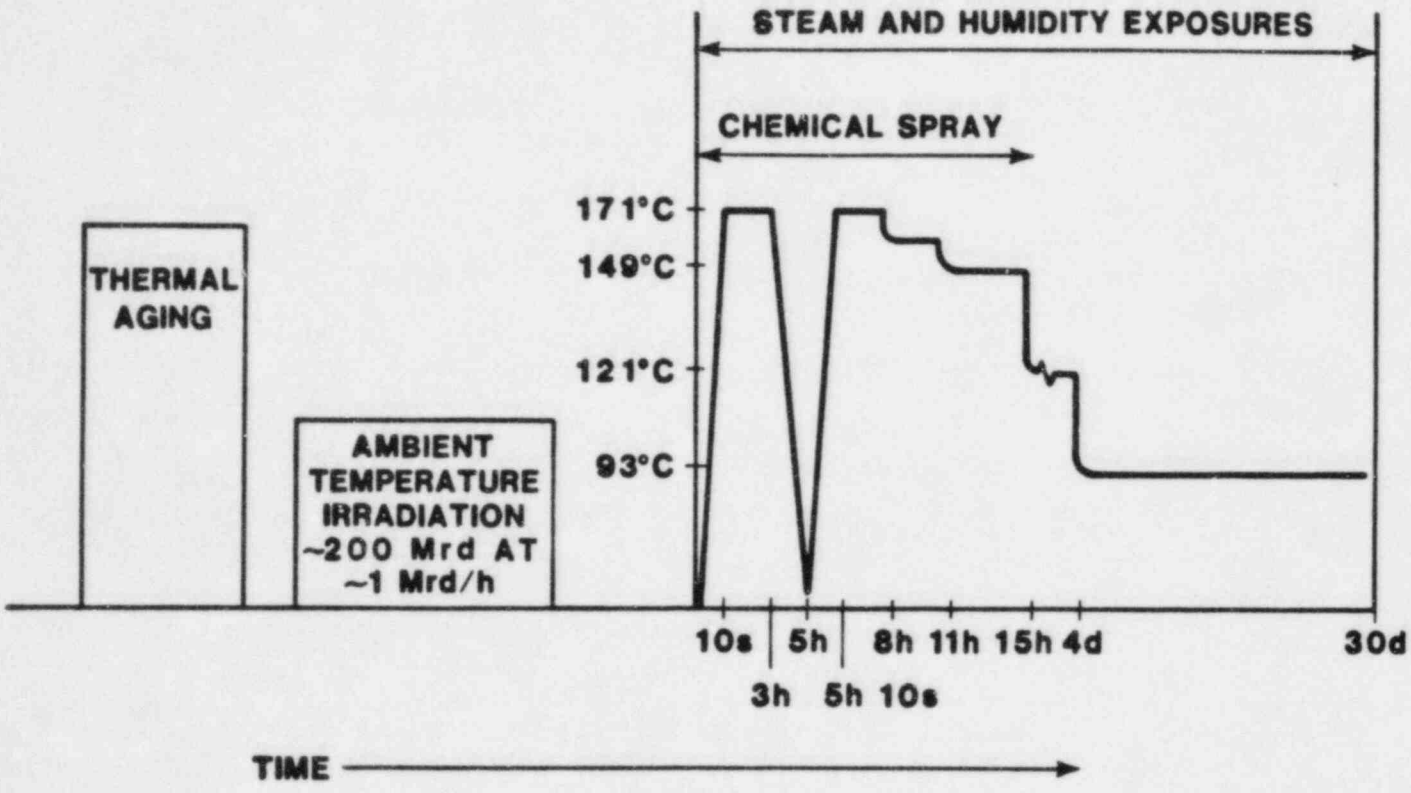

Figure 1.2: Typical U.S. Exposure Sequence for a LOCA Qualification Effort

2.0 SAMPLES

2.1 U.S. Samples

The U.S. samples consisted of six insulation materials, two jacket materials, and five compression materials. The insulation and jacket materials were carefully obtained by disassembling cable received from five U.S. manufacturers of Class 1E cables. The materials are:

EPR 1	A radiation cross-linked fire-retardant EPDM insulation obtained from a shielded instrumentation cable.
EPR 2	A chemically cross-linked fire-retardant EPDM insulation obtained from a 600V, 3-conductor control cable.
XLPO 1	A cross-linked polyolefin insulation obtained from a shielded instrumentation cable.
XLPO 2	A cross-linked polyolefin insulation obtained from a 600V, 3-conductor control cable.
TEFZEL 1	A TEFZEL insulation removed from a thermocouple extension cable.
TEFZEL 2	A TEFZEL insulation removed from a shielded instrumentation cable.
CSPE	A chlorosulfonated polyethylene jacket removed from a 600V, 3-conductor control cable.
CPE	A chlorinated polyethylene jacket removed from a 600V, 3-conductor control cable.

Each of the jacket and insulation specimens were cut to a length of 10.9 $\pm$ .3 cm (except for EPR 1 which had an initial length of 10.2 $\pm$ .3 cm). The insulation specimens were tubular in shape. The nominal insulation thickness (i.e., tube wall thickness) is summarized in Table 2.1. The jacket specimens were cut with a die into rectangular pieces. The width of each specimen was .56 cm. The nominal jacket thicknesses are also presented in Table 2.1.

The five compression materials were obtained from the same U.S. manufacturer. Samples, received from the manufacturer as compression molded sheets with nominal thicknesses of .178 and .191 cm, were cut into small rectangles with approximate dimensions: .6 cm x 1.6 cm. The five materials were: EPR A, EPR B, BUNA N, SILICONE, and VITON.

Table 2.1

Nominal Insulation and Jacket Thicknesses
for U.S. Samples

Material	Nominal Thickness (cm)
EPR 1	.064
EPR 2	.076
XLPO 1	.076
XLPO 2	.076
TEFZEL 1	.038
TEFZEL 2	.051
CSPE	.114
CPE	.114

2.2 French Samples

The French samples consist of six elastomer materials used in the manufacture of electrical cables (insulation and jacket materials), two O-ring seal materials and two thermoplastic and thermosetting materials used in the manufacture of connectors.

The electrical cable materials are in the form of either 110 mm-long pieces of insulating material stripped from the copper conductor (identified by "I"), dumbbells cut from jacket material and identified by "G", or standard dumbbells cut from compression molded sheets (identified by "H"). Elastomer dumbbell dimensions are shown in Figure 2.1. The six cable materials are:

82 I1 PRC — Chemically cross-linked polyethylene in the form of conductor insulation for 3-conductor cables. (Polyethylene compounds are a subset of the more generic term polyolefin.)

82 I2 EPDM — Ethylene propylene diene terpolymer conductor insulation. Samples taken from a 3-conductor cable.

82 I9 EPDM — Bromine-loaded, ethylene propylene diene terpolymer insulation. This material was removed from a 3-conductor cable.

82 G10 HYPALON — Chlorosulfonated polyethylene used in the manufacture of cable jackets.

82 H3 VAMAC — Acrylic polyethylene in the form of sheets from which dumbbells (Figure 2.1) were cut. Material is used in electrical cable jackets, mechanical parts, and connectors.

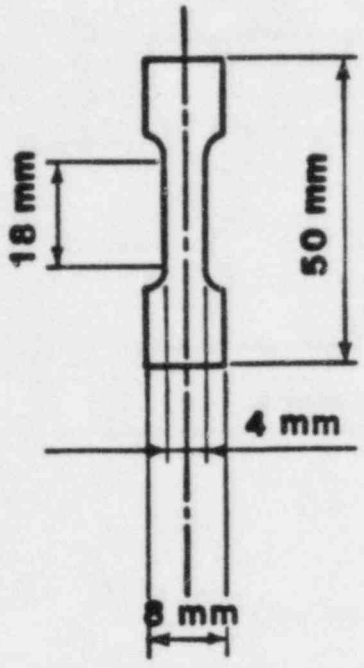

Figure 2.1: Dimensions for 82 G10, 82 H3, and 82 H4 French Dumbbell Samples - H3 French Standard (Commission of Normalization No. NFT 51-034-June 1968)

82 H4 EPR — Copolymer ethylene-propylene rubber in the form of 3 mm sheets from which dumbbells (Figure 2.1) were cut. Material is used in the manufacture of insulation for electrical cables sheathed with fire-proof EPDM.

The two O-ring seal samples (identified by "J") have an inner diameter of 12 mm and an outer diameter of 17 mm. They were enclosed and held under compression in aluminum grooves as shown in Figure 2.2. The O-ring seal materials are:

82 J3 VAMAC — Same material as 82 H3, used in the manufacture of O-ring seals.

82 J4 EPR — Same material as 82 H4, used in the manufacture of O-ring seals.

The two thermoplastic and thermosetting materials used in the manufacture of connectors were in the form of International Organization for Standardization (ISO) dumbbells. The dimensions for these dumbbells are illustrated in Figure 2.3. The two materials are:

82 H5 Polydiallylphtalate	Thermosetting polyester used in connectors and mechanical parts.
82 H6 PPS	Phenylene polysulfide used in the manufacture of switches and connectors.

The French sample identification code (82 I1, 82 H5, etc.) will be used in the remainder of this report. The code presents:

- The year of the starting investigation,
- The sample shape code letter,
- A number identifying the material type.

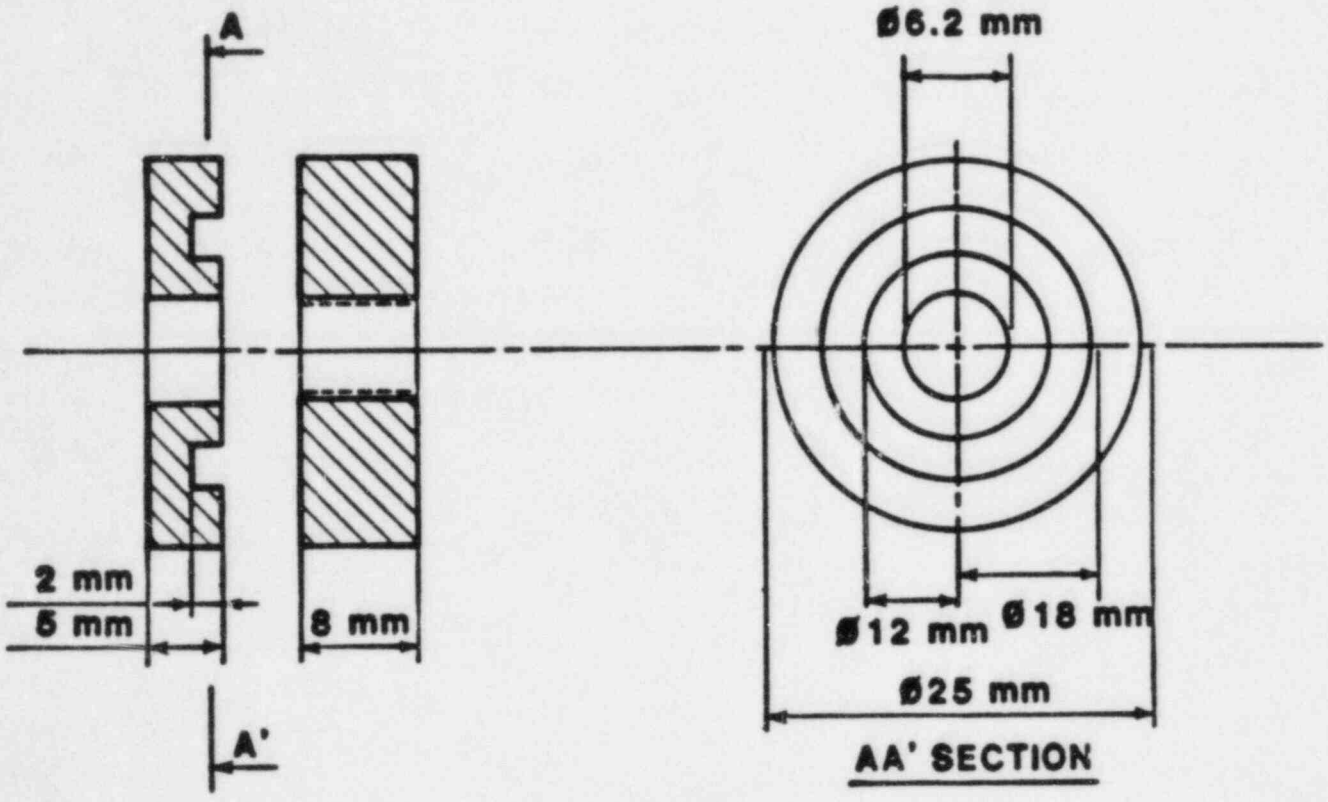

Figure 2.2: Compression Set Fixture Used for 82 J3 and 82 J4 French O-ring Seal Samples

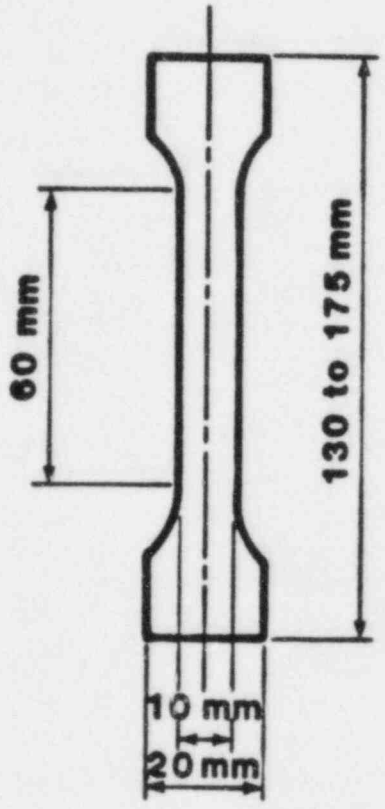

Figure 2.3: Dimensions for 82 H5 and 82 H6 ISO Dumbbell Samples

3.0 FACILITIES

3.1 Aging Facilities

Aging of all U.S. and French samples was performed in the United States at Sandia National Laboratories. Sandia's Low Intensity Cobalt Array (LICA) was employed for the irradiation exposures. Thermal aging was performed using air circulating ovens each of which had been modified to accommodate a number of self-contained aging cells. Both facilities are described in more detail in Reference 1.

3.2 Accident Simulation Facilities

All accident simulations were performed in France in the laboratories of the ionizing radiation office (ORIS-LABRA) at Saclay (the radiation biological application laboratories). The accident simulation was comprised of three elements:

- the accident irradiation
- the thermodynamic (steam and chemical spray) exposures
- the post-accident exposure

The thermodynamic exposure was applied either simultaneously with the accident irradiation, or sequentially.

3.2.1 Irradiation Facilities

Three different irradiations were employed as part of the experimental program. Some samples were irradiated in air at ambient temperatures (28°C); other samples were irradiated in air at elevated temperature (70°C); and some samples were irradiated simultaneously with the thermodynamic (steam and chemical spray) exposures. These latter simultaneous tests were performed with either air or nitrogen as the background gas environment.

All irradiations were carried out in the hot cave of the POSEIDON irradiator (Figure 3.1). The POSEIDON facility is a high intensity installation with a capacity of one million curies of Cobalt-60. The cobalt sources are stocked in a 5.5 m deep pool of water. Half the pool is open to the outside atmosphere, the other half is covered by a overhanging concrete hot cave.

Cobalt source carriers are positioned on transfer trollies at the bottom of the water pool. The appropriate number of cobalt sources for the desired power and geometry are placed on the trolly which is then brought beneath the hot cave. A lift then positions the trolly above the water level (inside the hot cave) at the appropriate location for the irradiation. It is possible to simultaneously irradiate equipment and materials at two temperatures: ambient and 70°C $\pm$ 3°C. Either cylindrical ovens or a large size rectangular CALINE chamber (2.6 x 1.9 x 1.6 meters) are employed. In the CALINE chamber, irradiation can take place at 70°C $\pm$ 3°C. Alternatively, the CESAR (Reference Accident Simulation Test Cell)

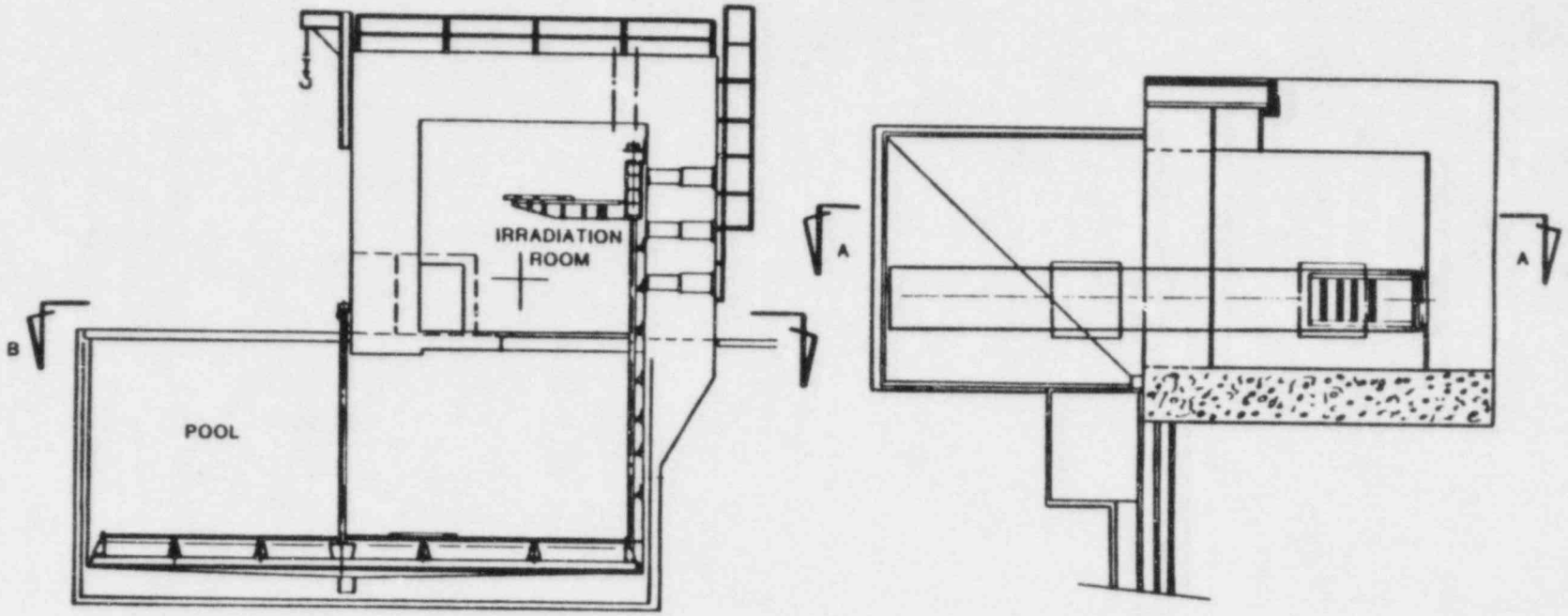

Figure 3.1: Schematic of POSEIDON Irradiation Facility

can be positioned in the hot cave. The CESAR cell allows for simultaneous irradiation, steam and chemical spray exposures. For our experimental program, non-ambient accident irradiations were performed using either the cylindrical ovens or the CESAR cell.

3.2.1.1 Ovens and Containers

French and U.S. samples were placed, either in cylindrical ovens for irradiation at 70°C, or in containers for irradiation at ambient temperature. Ovens and containers were placed parallel to the cobalt source planes inside the irradiation hot cave (Figure 3.2). The strength of the cobalt sources at the time of the irradiation was equal to 192,000 curies.

3.2.1.2 Temperature Measurement

The ovens are stainless steel tubes, 1 meter long and 10 cm in diameter, covered with a heating band and thermal insulation. A temperature sensor fitted between the metal tube and the heating band is linked to a Staticor-R5 type CORECI temperature regulator, calibrated by the manufacturer. Temperature measurement inside each oven is provided by a chromel-alumel thermocouple linked to a MECI type L39084E recorder, via a compensation cable. The recorder is checked and calibrated every six months by the MECI company.

Though the oven length was 100 cm, only 70 cm was used for sample placement, so as to limit the thermal gradient. The end of each oven was covered by polyester gauze material which ensures regular renewal of air inside the ovens, while limiting its flow and hence heat loss. Thermocouples were also fitted in the containers containing the ambient irradiated samples.

3.2.1.3 Measurement of Irradiation Dose Rate

Inside each oven and each container the irradiation dose rate was measured using:

Type MN606 No. 187 ionization chambers calibrated by ORIS-LMRI. The calibration certificate bears the number 2986 dated November 21, 1983 (Table 3.1). The accuracy of an individual dose rate measurement using this instrument is $\pm$ 5%.

Dosimetric films. These were used to display the variation in dose rate along the length of each oven and each container. These films are made of a cellulose triacetate base material whose blackening under radiation is measured by spectrophotometry at a wavelength of 280 nanometers. The accuracy of dose rate measurement using this film is $\pm$ 15%.

3.2.2 Thermodynamic (Steam and Chemical Spray) Exposures

Simulation of thermodynamic conditions was carried out in a CESAR chamber (Reference Accident Simulation Test Cell). For sequential tests, this 200 liter test cell (Figure 3.3) is located outside the POSEIDON

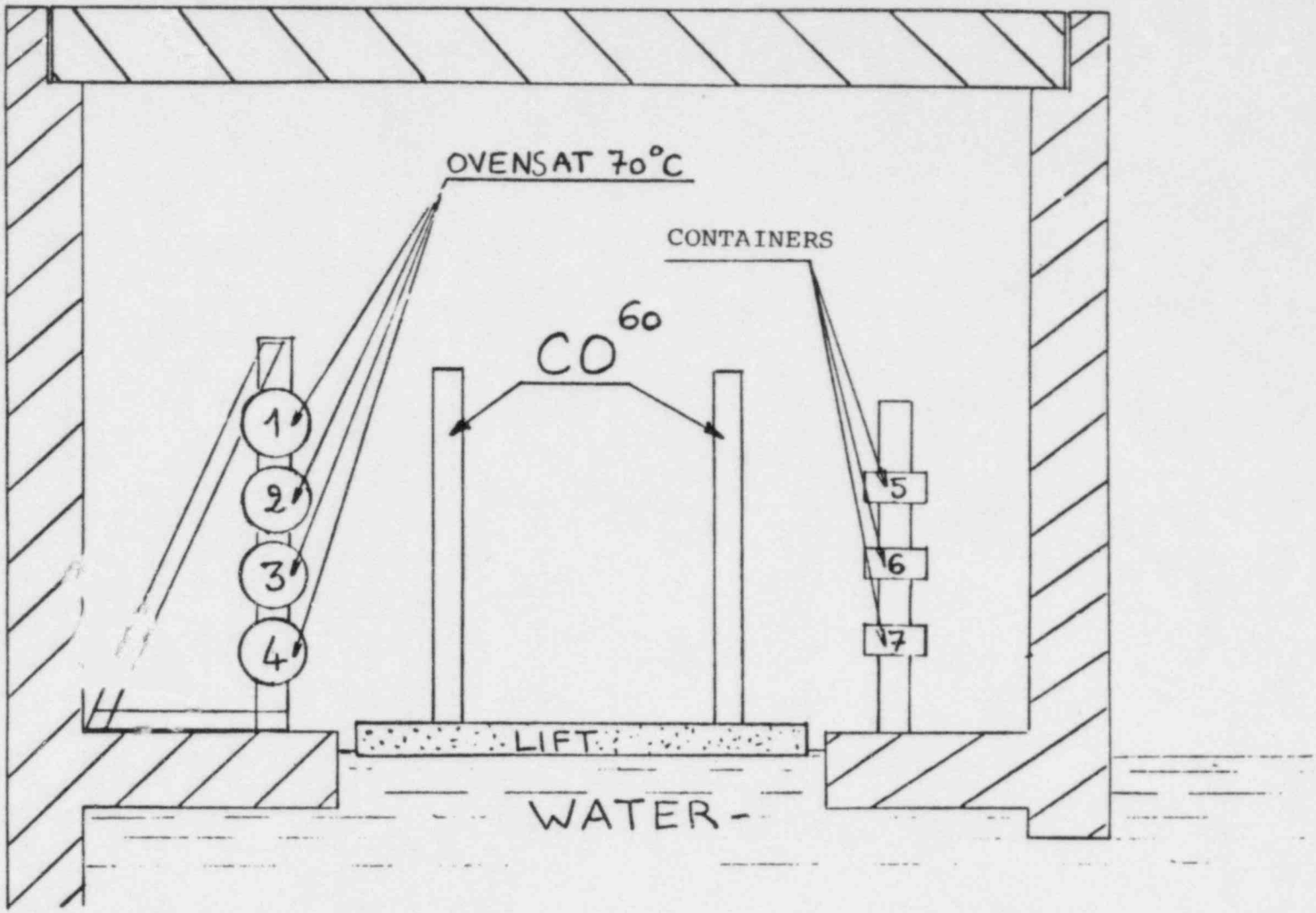

Figure 3.2: Gamma Accident Irradiation of U.S. and French Polymeric Samples (Sequential Accident Simulations)

Table 3.1

Calibration Certificate: Ionization Chamber Employed to Map Accident Irradiation Dose Rates

Certificat n° 2986

Suite n° 8

V.2.3. Chambre d'ionisation MN 606 n° 187.

Après mise en place du bouchon de codage MN 606 et du capuchon d'équilibre électronique, l'instrument est réglé de façon telle que l'indication fournie, corrigée pour les conditions atmosphériques spécifiées, corresponde à la valeur vraie de l'exposition exprimée en roentgen.

	FACTEURS D'ETALONNAGE	
	Facteurs d'étalonnage pour les conditions de référence : θ_o = 20 °C P_o = 101,325 kPa	Incertitude
FONCTION DEBIT	N_X = 2,58.10^{-4} C.kg^{-1}.min^{-1} par unité de lecture	± 3,1 %
	N_X = 1,00 R.min^{-1} par unité de lecture	± 3,1 %
FONCTION INTEGRATION	N_X = 2,58.10^{-4} C.kg^{-1} par unité de lecture	± 2,9 %
	N_X = 1,00 R par unité de lecture	± 2,9 %

Le Chef du L. M. R. I

J.P. SIMOEN

Le Responsable du Centre d'Etalonnage (dosimétrie et neutronique)

M. CANCE

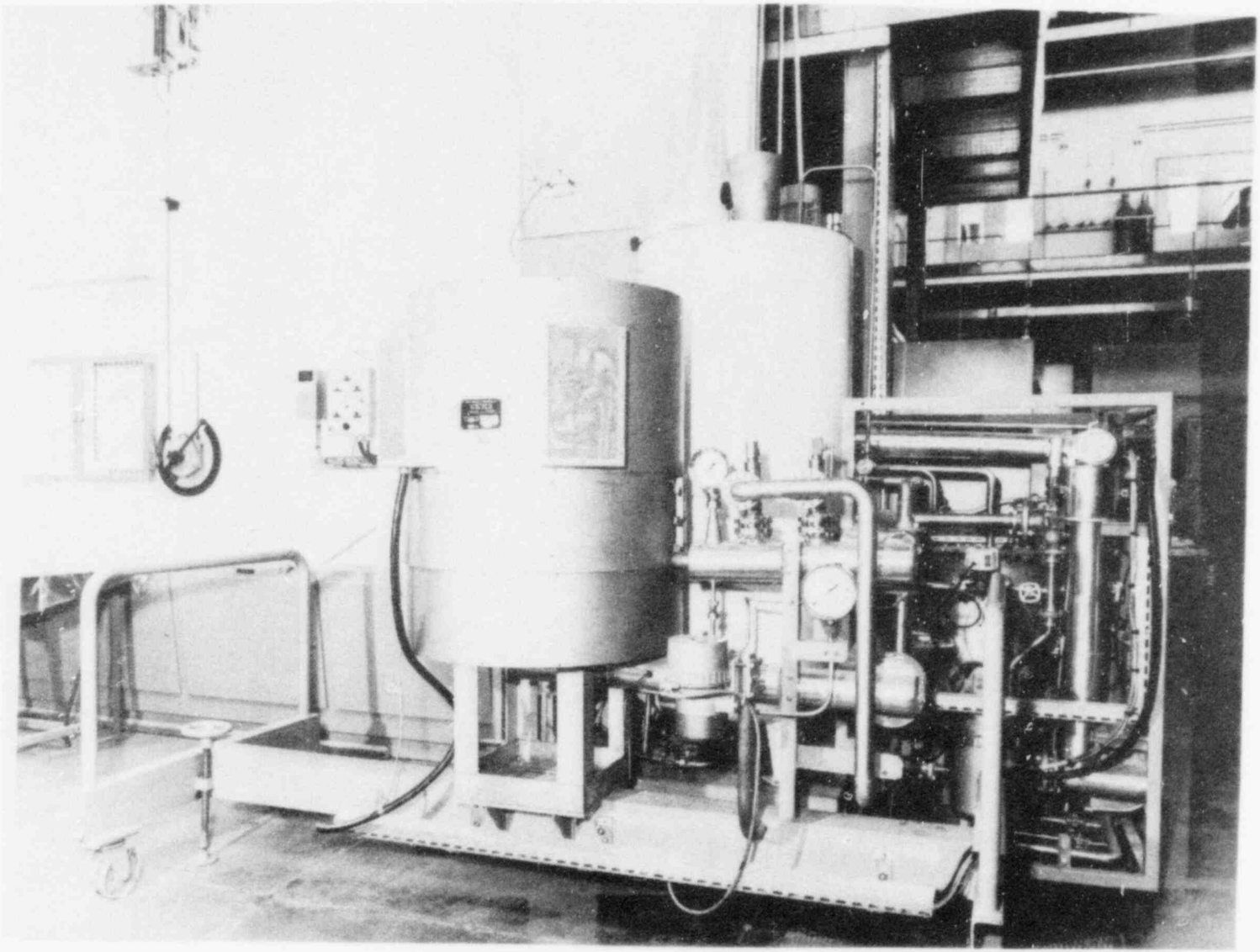

Figure 3.3: CESAR Experimental Chamber

irradiator. For simultaneous simulations of irradiation and thermodynamic conditions, the cell is positioned inside the POSEIDON hot cave as explained in Section 3.2.1. With this cell, it is possible to reproduce on equipment and materials the effects of a PWR accident, including the very rapid rises in pressure and temperature postulated for inside the containment.

For a postulated pipe break in the primary circuit of a PWR, the equipment located in the containment would be subjected to the effects of vapor produced by the expansion of pressurized water. The simultaneous release of fission products from the reactor core into containment building would subject the same equipment to considerable irradiation. The CESAR assembly (Figure 3.4), which is constructed in the ORIS-LABRA laboratories in Saclay, enables simultaneous or sequential simulation of the thermodynamic and irradiation accident conditions.

Thermodynamic shock was obtained by the rapid expansion of dry superheated steam in the chamber. The steam was previously heated and maintained in a storage tank. The rest of the temperature and pressure sequence is provided by a boiler and appropriately placed resistance heaters located in the experimentation cell. A calibration conduit enables measurement of the thermodynamic state prior to the start of the test.

A chemical unit sprays borated water into the CESAR cell. The unit is comprises of two tanks, one containing a concentrated solution and the other a diluted solution. Diluting and spraying are provided by two doser pumps (Figure 3.5). The assembly is controlled by a computer programmed with the desired experimental profile. A console is used to communicate with the computer and introduce test parameters. After the operator has given the test start command, the computer monitors the test chamber temperature and pressure and compares them with the experimental profile stored in its memory. It then actuates electromagnetic valves which control the supply of vapor and compressed gas (air or inert gas), or the release of gas from the test chamber (Figure 3.6). The temperature and the pressure of the test chamber were also measured by instruments independent of those used for regulation. All data were recorded on a plotter.

In addition, conformance with the desired profile was visually checked both before and during the test, using probes whose data were transmitted to digital monitors and printed on a teletype console. The following parameters were recorded:

- the temperature and pressure of vapor in the superheater, before the start of the test,
- the pressure of vapor in the boiler,
- the temperature of the vapor in the calibration piping,
- the temperature of the vapor piping in the test chamber,
- the temperature inside the test chamber during the tests,
- the pressure in the test chamber.

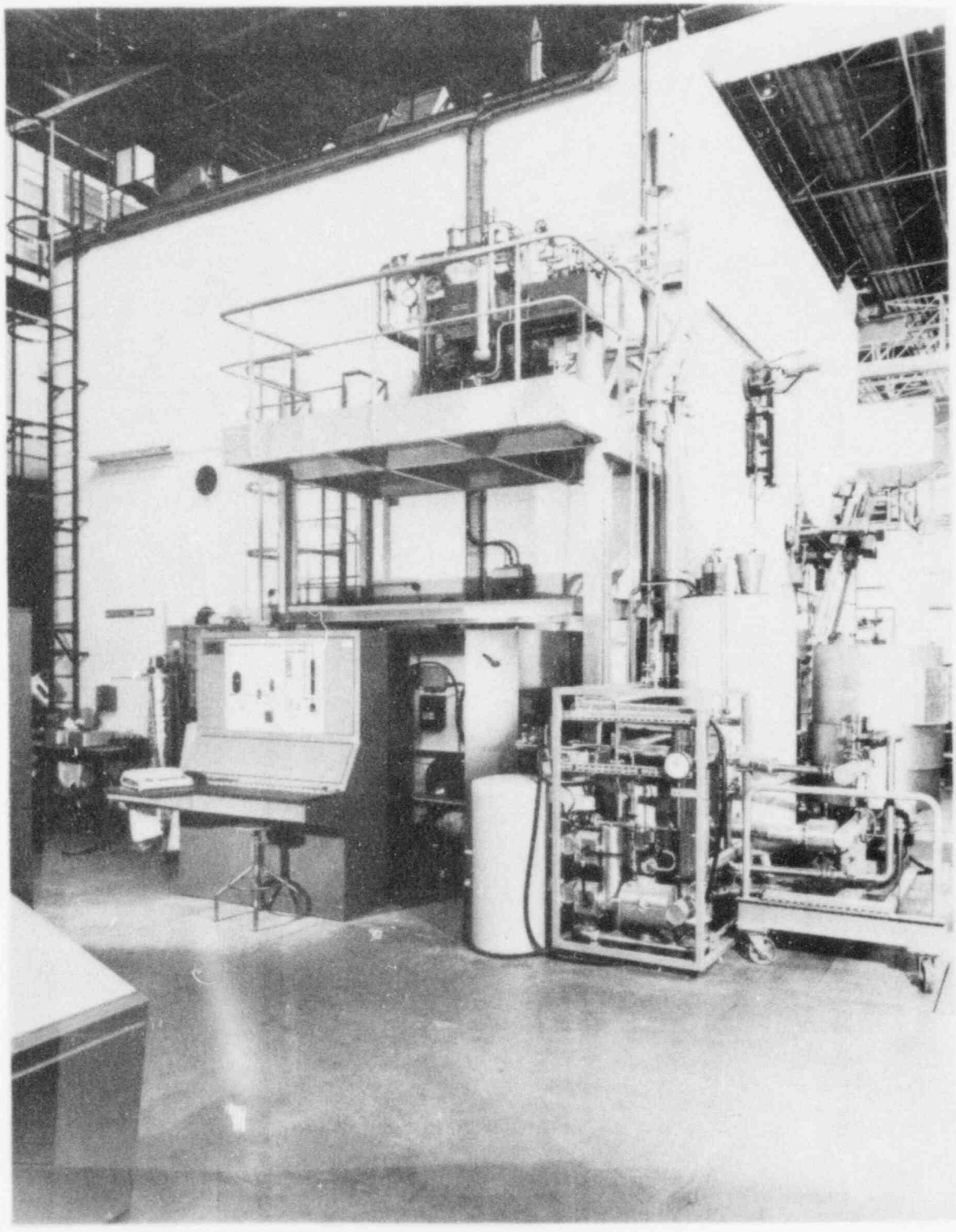

Figure 3.4: The CESAR Facility

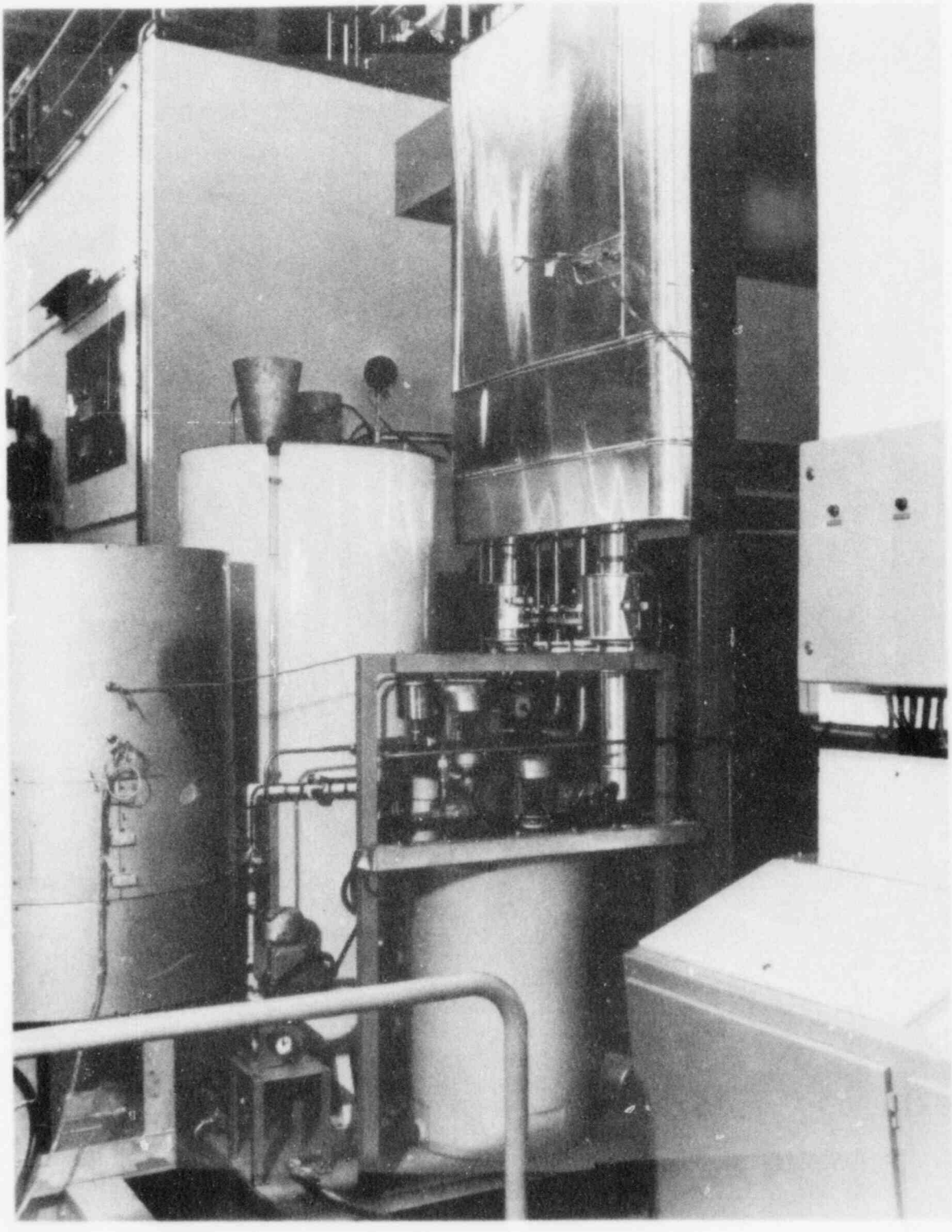

Figure 3.5: Borated Solution Spray Preparation

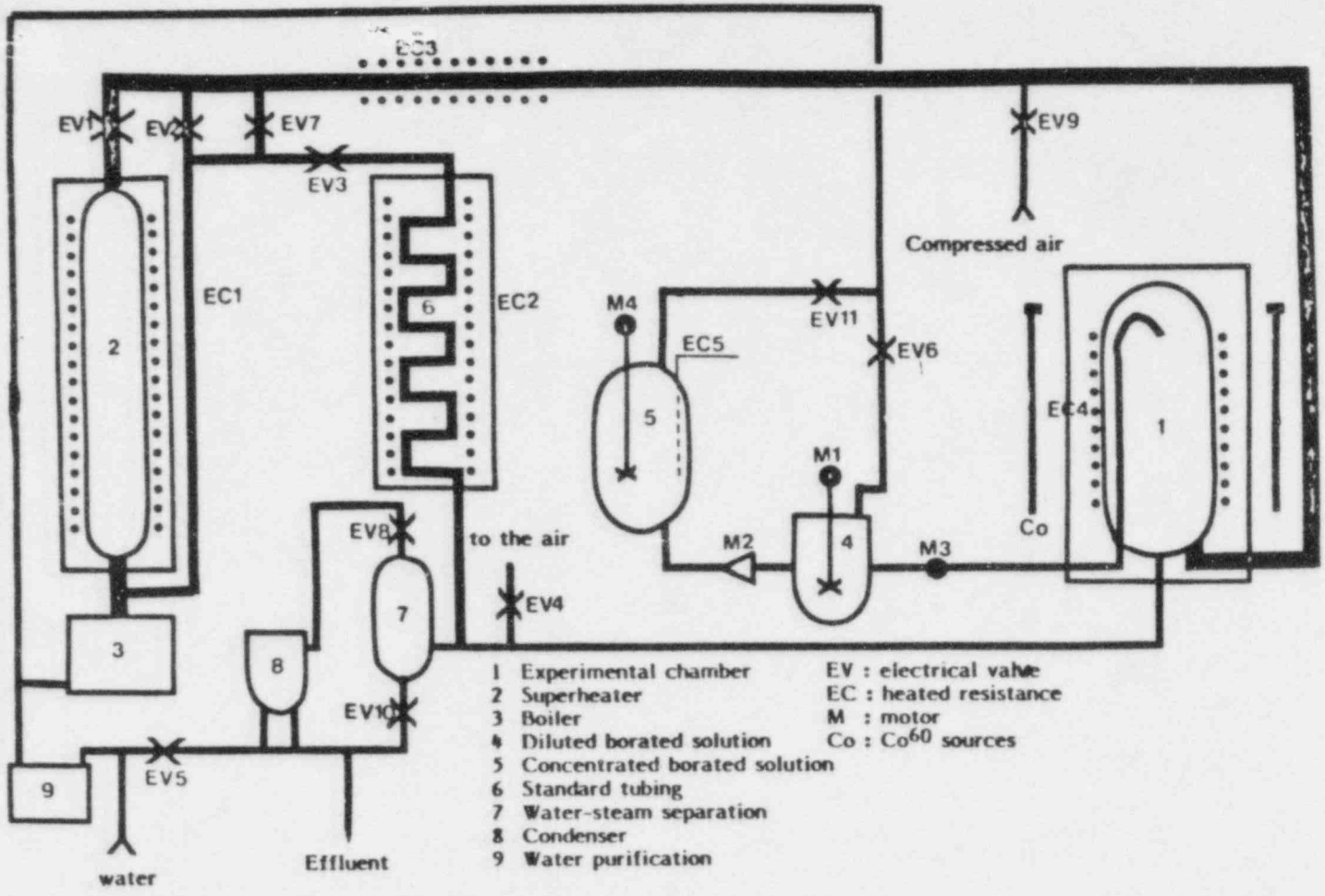

Figure 3.6: CESAR Facility Schematic

The temperature measurement instruments in the test cell are calibrated annually by the operators. A MECI ref. IP 2254 temperature calibrated voltage source (certificate No. 13541) was applied to the input of the plotter and to the corresponding analog input of the computer.

3.2.3 Post-Accident Period

The post-accident period was also simulated in the CESAR chamber. The temperature of the experimentation chamber is controlled throughout the test by the thermocouple measurements described in the previous section (3.2.2). The relative humidity inside the experimentation cell is not measured. However, the temperature is maintained at approximately 100°C by the frequent injection of vapor from the boiler. The relative humidity is therefore that of the vapor dew point at operating temperature (approximately 100%).

3.3 Measurement Equipment and Facilities

3.3.1 Measurement of the Length of U.S. Samples

At the end of the accident simulation tests, the lengths of the U.S. samples were measured. This measurement was performed using Roche slide calipers, with an accuracy of 1/50 mm. Each U.S. sample group contained four samples. One sample was chosen at random for measurement. It was laid out to its full length on a sheet of paper; its length was measured at room temperature.

3.3.2 Weighing of U.S. Samples

At the end of the accident simulation tests, the U.S. samples were weighed. They were then dried and weighed again. These weights were compared to measurements made on the same samples prior to the accident simulations.

3.3.2.1 Weighing

A batch of four samples for each sample group were weighed on Metler scales with a sensitivity of 10^{-4} grams. The scales are kept in a thermostatically controlled room. The four samples were weighed intact, or if degraded by the accident simulation, all sample pieces were reassembled prior to weighing.

3.3.2.2 Drying

Polymer samples were dried at 60°C $\pm$ 1°C in a ventilated oven for six hours. The rise from ambient temperature to 60°C took approximately 30 minutes. The samples were removed from the oven approximately one hour after the electrical supply had been cut, when the oven temperature was approximately 40°C.

3.3.3 Measurement of Mechanical Properties

At the end of each test phase, tensile strength and elongation at break measurements are made on the French and U.S. samples. The French samples were measured in the French laboratories of ORIS-LABRA. The U.S. samples were measured at Sandia National Laboratories.

3.3.3.1 U.S. Measurements

Tensile measurements were performed on the CSPE, CPE, EPR 1, EPR 2, XLPO 1, and XLPO 2 samples. In general, when tensile tested, the weights were not more than ~2% greater than the weights of the samples prior to the LOCA exposures. (We allowed moisture absorbed by our samples during the LOCA simulation to desorb prior to performing tensile measurements). Tensile measurements were performed using Instron® tensile testing machines. Samples were gripped using pneumatic jaws; initial jaw separation was 5.1 cm and the samples were strained at 12.7 cm/min. The strain was monitored with an Instron electrical tape extensometer clamped to the sample. The measurement accuracy for U.S. tensile mechanical properties was generally much better than one standard deviation evaluated from a population of four samples. The Appendix lists all U.S. data with associated errors (i.e., $\pm$ one standard deviation).

Bend tests were performed on the TEFZEL 1 and TEFZEL 2 samples rather than tensile tests since aged specimen tubes shattered when gripped by the pneumatic jaws of the Instron tensile testing machine. Bend radii between 75 and 6 times the radii of the TEFZEL specimens were employed. Each specimen was successively bent around tubes of smaller diameter until insulation cracking was visually observed.

Permanent set after compression measurements were performed on the U.S. EPR A, EPR B, BUNA N, VITON, and SILICONE compression set specimens. The compression set specimens were exposed using the fixture illustrated in Figure 3.8. Each layer of the fixture contained three .127 $\pm$ .001 cm spacers and four compression set samples. Each of the five layers of one fixture was used for a different compression sample material; namely, EPR A, EPR B, BUNA N, VITON, or SILICONE.

The compression set samples ranged in thickness between .165 and .205 cm. Prior to compression, each individual sample was measured for thickness using a Starret dial indicator with a .64 cm diameter flat plate probe. The sample's thickness and position in the fixture was noted. After exposures to aging and accident simulations (~2 years later), the sample thickness was again measured using a Scherr-tumico, Model AL15 dial indicator with a .56 cm diameter flat plate probe. Prior to the final measurements, the fixture was disassembled (releasing the compressive strain) and a 30-minute recovery time allowed.

Our compression set samples have much smaller thicknesses than those recommended by ASTM Standard D395-78.[15] This Standard recommends (for Method B) test specimens with 1.25 cm thicknesses. Our sample thicknesses more realistically simulate use conditions, but generate much larger errors in the calculated values for compression set. Absolute error for

our compression set values is ± 0.1. Compression set values can range between 0.0 and 1.0. Our data tables (see Section 5.1.9) report statistical variations (± 1 σ) evaluated for the four specimens of each material type contained in a compression set fixture.

3.3.3.2 French Measurements

The French measurements were carried out on a Zwick traction machine (Figure 3.8), Model 7025/3 placed in a thermostatically controlled room at 21°C. The samples, in the form of dumbbells or wiring insulation were clamped into the jaws of the test machine. The space between the jaws was 4.0 cm for dumbbells 82G10, 82H3 and 82H4, approximately 15.0 cm for dumbbells 82H5 and 82H6, and approximately 11.0 cm for insulations 82I1, 82I2 and 82I9.

An extensometer was placed in the center of each sample. Its initial separation was 1.0 cm. The traction speed was 5.0 cm per minute for elastomers and thermoplastics. Traction speed was reduced to 0.8 mm per minute for the thermoset sample (French Standard No. NFT 51034).

Measurements of permanent set after compression were carried out at ORIS-LABRA on French elastomer O-ring samples 82J3 and 82J4. Measurement of the initial and final diameters of the core were carried out using Roche slide calipers, with an accuracy of 0.02 mm (French Standard No. NFT 46011).

The measurement accuracy of French mechanical properties is as follows:

a) Tensile Strength
The accuracy for tensile strength measurements is basically dependent upon the variations in size from one sample to the next; it is equal to:

± 5% for dumbbells
± 15% for wiring insulation

b) Elongation at Break
Accuracy is determined by both the variation in the size of the samples, and the accuracy of extensometer measurements; it is equal to:

± 5% for dumbbells
± 5% for conductors

Elongation at break measurements for the thermoplastic and thermoset materials, 82H5 and 82H6, which were less as unaged samples then the equipment accuracy have therefore not been recorded.

c) Permanent Set After Compression
Measurements were taken with an accuracy of ± 9%.

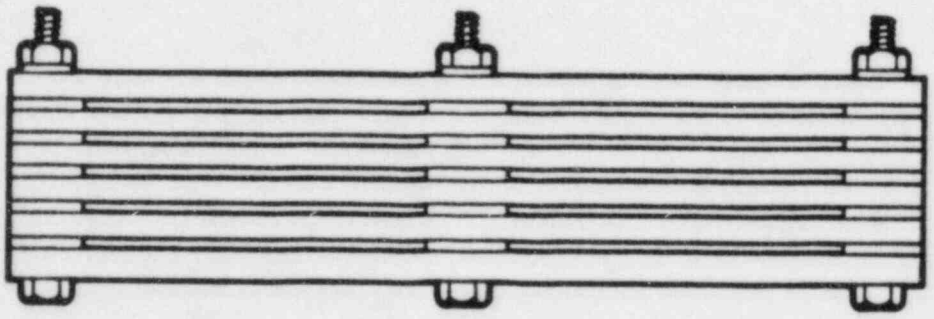

Figure 3.7: U.S. Compression Set Fixture

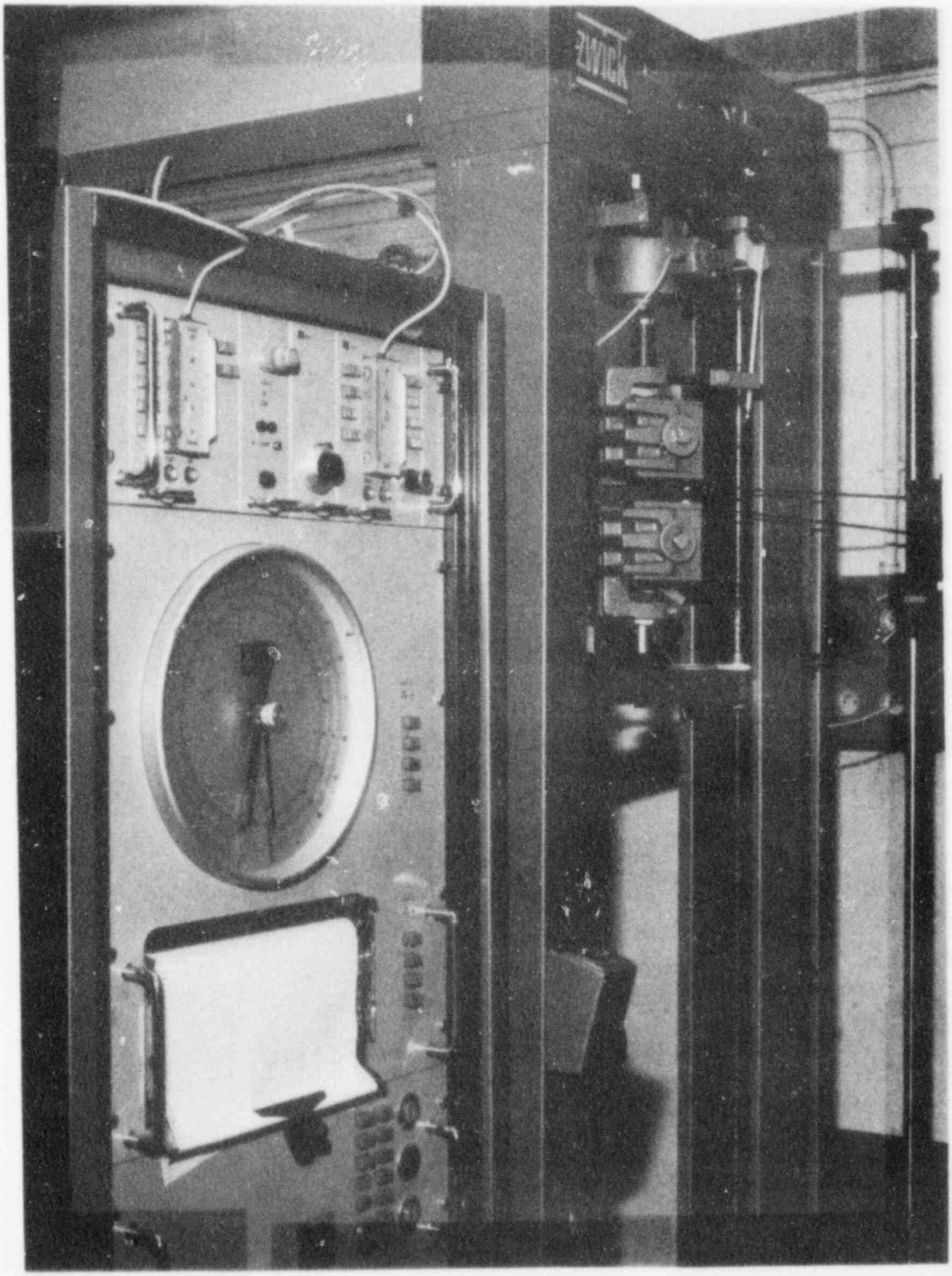

Figure 3.8: Zwick, Model 7025/3, Tensile Test Machine Employed for French Measurements

4.0 EXPERIMENTAL PROCEDURES

4.1 Aging Method

4.1.1 U.S. Samples

The U.S. insulation and jacket samples were exposed to five different aging procedures. In addition, unaged samples were exposed to the accident simulation. These procedures (and the shorthand codes used in the rest of the report to describe them) are:

A = R70→120°C.: A 16-day irradiation at ~65 krd/h and 70°C followed by a 16-day thermal exposure at 120°C.

B = R27→120°C: A 16-day irradiation at ~65 krd/h and ambient temperatures (~27°C) followed by a 16-day thermal exposure at 120°C.

C = 120°C→R70: A 16-day thermal exposure at 120°C followed by 16-day irradiation at ~65 krd/h and 70°C.

D = 120°C→R27: A 16-day thermal exposure at 120°C followed by a 16-day irradiation at ~65 krd/h and ambient temperatures (~27°C).

E = R120: A 16-day simultaneous exposure to 120°C thermal and ~65 krd/h irradiation environments.

F = Unaged.

The U.S. Compression Set Samples were exposed to four different aging procedures. These procedures (and the shorthand used in the rest of the report to describe them) are:

B = R27→120°C: A 16-day irradiation at ~60 krd/h and ambient temperatures (~27°C) followed by a 16-day thermal exposure at 120°C.

D = 120°C→R27: A 16-day thermal exposure at 120°C followed by a 16-day irradiation at ~60 krd/h and ambient temperatures (~27°C).

E = R120: A 16-day simultaneous exposure to 120°C thermal and ~60 krd/h irradiation environments.

U = Unaged.

The 120°C, 16-day elevated temperature exposure was chosen based on Arrhenius calculations which assumed a 40-year service operation at 45°C and material activation energy of 1.0 eV. Table 4.1 summarizes the total

radiation dose and the thermal exposure time for each sample group. Additional details concerning the aging techniques are provided in Reference 1.

4.1.2 French Samples

The French samples were exposed to four different aging procedures. In addition, unaged samples were exposed to the accident simulations. These aging procedures (and the shorthand codes used in the rest of the report to describe them) are:

A = T→R70: A 10-day thermal exposure followed by a 9- or 10-day irradiation at ~115 krd/h and 70°C.

B = R70→T: A 9- or 10-day irradiation at ~115 krd/h and 70°C followed by a 10-day thermal exposure.

C = T→R27: A 10-day thermal exposure followed by a 9- or 10-day irradiation at ~115 krd/h and ambient temperatures (~27°C).

D = R27→T: A 9- or 10-day irradiation at ~115 krd/h and ambient temperatures (~27°C) followed by a 10-day thermal exposure.

U = Unaged.

The 10-day thermal exposure temperature depended on the specimen material. Table 4.2 lists each of the French samples and the appropriate thermal aging temperature. Various sample groups were irradiated over a several month period. Co-60 decay during this time period necessitated varying the irradiation exposure time from 9 days to 10 days so that each sample group was irradiated to a similar dose (~25 Mrd). Table 4.3 summarizes the total radiation dose and the thermal exposure time for each group of French samples. Additional details concerning the aging techniques are provided in Reference 1.

4.2 Accident Simulation

The purpose of the tests was to observe the effect of the following parameters on polymer behavior during accident simulations:

- the aging simulation method,
- the order of accident simulation phases,
- the comparison of reference accident simultaneous or sequential simulation,
- the accidental phase irradiation temperature,
- the gas surrounding the materials during the LOCA (nitrogen or air).

Table 4.1

Aging Radiation Dose and Thermal Exposure Time
for U.S. Insulation, Jacket, and Compression Set Specimens

Sample Group	Total Radiation Dose [Mrd(air equiv.)]	Thermal Exposure Time (Hrs)
Cable and Jacket Materials		
XLPO 1A	24.2	385
XLPO 1B	24.2	385
XLPO 1C	23.4	384
XLPO 1D	23.1	385
XLPO 1E	24.3	386
XLPO 2A	22.7	386
XLPO 2B	24.2	385
XLPO 2C	23.4	384
XLPO 2D	23.0	385
XLPO 2E	24.3	385
EPR 1A	25.7	385
EPR 1B	25.5	385
EPR 1C	25.0	384
EPR 1D	25.3	384
EPR 1E	25.7	384
EPR 2A	25.7	385
EPR 2B	25.5	385
EPR 2C	25.0	384
EPR 2D	25.3	384
EPR 2E	25.7	384
CSPE A	25.0	389
CSPE B	25.4	380
CSPE C	24.2	389
CSPE D	24.2	389
CSPE E	24.6	384
CPE A	23.9	389
CPE B	23.4	389
CPE C	23.1	385
CPE D	23.1	385
CPE E	23.4	384
TEFZEL 1A	22.3	386
TEFZEL 1B	22.9	377
TEFZEL 1C	22.3	383
TEFZEL 1D	22.3	384
TEFZEL 1E	22.4	381
TEFZEL 2A	22.3	386

Table 4.1
(continued)

Aging Radiation Dose and Thermal Exposure Time
for U.S. Insulation, Jacket, and Compression Set Specimens

Sample Group	Total Radiation Dose [Mrd(air equiv.)]	Thermal Exposure Time (Hrs)
TEFZEL 2B	22.9	377
TEFZEL 2C	22.3	383
TEFZEL 2D	22.3	384
TEFZEL 2E	22.4	381
Compression Set Specimens		
Unaged:		
#15	NA	NA
#16	NA	NA
#25	NA	NA
#26	NA	NA
#28	NA	NA
#39	NA	NA
#40	NA	NA
#46	NA	NA
B:		
#3	23.8	386
#4	23.8	386
#9	22.2	386
D:		
#18	22.0	386
#19	23.4	386
E:		
#29	23.0	383
#30	23.0	383

Table 4.2

Thermal Exposure Temperatures For French Samples

	Sample Description	Sample Code	Exposure Temperature (°C)
1.	PRC Insulation	82 I1	140
2.	EPDM Insulation	82 I2	140
3.	EPDM Insulation	82 I9	140
4.	PPS Dumbbells	82 H6	160
5.	Polydiallylphtalate Dumbbells	82 H5	160
6.	VAMAC Acrylic Polyethylene Dumbbells	82 H3	120
7.	EPR Dumbbells	82 H4	140
8.	HYPALON Dumbbells	82 G10	140
9.	VAMAC Acrylic Polyethylene O-ring Seal Samples	82 J3	120
10.	EPR O-ring Seal Samples	82 J4	140

Table 4.3

Total Radiation Dose and the Thermal Exposure Time
for Each Group of French Samples

	Radiation Exposures	
	Radiation Dose	Thermal Exposure Time
82 I1 A	24.7 Mrd	240.5 hours
B	24.7 Mrd	240.2 hours
C	24.7 Mrd	240.5 hours
D	24.9 Mrd	240.2 hours
82 I2 A	24.7 Mrd	240.5 hours
B	24.7 Mrd	240.2 hours
C	24.7 Mrd	240.5 hours
D	24.9 Mrd	240.2 hours
82 I9 A	24.0 Mrd	258.5 hours
B	25.3 Mrd	238.8 hours
C	23.9 Mrd	258.5 hours
D	25.6 Mrd	241.1 hours
82 H6 A	26.0 Mrd	238.6 hours
B	26.0 Mrd	238.7 hours
C	25.8 Mrd	238.6 hours
D	26.2 Mrd	238.7 hours
82 H5 A	24.1 Mrd	240.2 hours
B	24.6 Mrd	238.6 hours
C	23.8 Mrd	240.2 hours
D	24.0 Mrd	241.0 hours
82 H3 A	25.4 Mrd	240.0 hours
B	25.4 Mrd	240.2 hours
C	25.4 Mrd	240.0 hours
D	25.4 Mrd	240.2 hours
82 H4 A	25.1 Mrd	258.5 hours
B	25.1 Mrd	268.8 hours
C	24.9 Mrd	258.5 hours
D	24.9 Mrd	268.8 hours
82 G10 A	25.5 Mrd	239.0 hours
B	25.5 Mrd	243.9 hours
C	24.4 Mrd	239.0 hours
D	24.4 Mrd	243.9 hours

Table 4.3
(continued)

Total Radiation Dose and the Thermal Exposure Time
for Each Group of French Samples

	Radiation Exposures	
	Radiation Dose	Thermal Exposure Time
82 J3 A	25.4 Mrd	240.0 hours
B	25.4 Mrd	241.3 hours
C	24.5 Mrd	240.1 hours
D	24.5 Mrd	240.2 hours
82 J4 A	24.0 Mrd	245.5 hours
B	24.6 Mrd	243.9 hours
C	24.1 Mrd	245.5 hours
D	24.3 Mrd	239.0 hours

Hence, the following four accident simulations were performed on each of the five groups of preaged French samples (A, B, C, D, or non-aged, U) identified in Section 4.1.2:

L1 = Accident irradiation at 70°C followed by thermodynamic and post-accident exposures with air (R70→LOCA(air)).

L2 = Thermodynamic and post-accident exposures with air followed by an accident irradiation at 70°C (LOCA(air)→R70)).

L3 = Simultaneous accident irradiation and thermodynamic exposures with air followed by a post-accident exposure with air (R + LOCA(air)).

L4 = Accident irradiation at 28°C followed by LOCA and post-accident exposures with air (R28→LOCA(air)).

Experimentally, the LOCA simulation included both a thermodynamic (steam and chemical spray) and post-accident exposures.

For the U.S. samples (preaged by the six methods identified in Section 4.1.1: A, B, C, D, and E, and non-aged, F), the reference accident simulation cycles were as follows:

L5 = Accident irradiation at 70°C followed by thermodynamic and post-accident exposures with air (R70→Steam(air)).

L6 = Accident irradiation at 70°C followed by thermodynamic and post-accident exposures with nitrogen (air was replaced by nitrogen) (R70 → Steam(N_2)).

L7 = Accident irradiation at 28°C followed by thermodynamic and post-accident exposures with air (R28→Steam(air)).

L8 = Accident irradiation at 28°C followed by thermodynamic and post-accident exposures with nitrogen (air was replaced by nitrogen) (R28→Steam(N_2)).

L9 = Simultaneous accident irradiation and thermodynamic exposures with air followed by a post-accident exposure with air (R + Steam(air)).

L10 = Simultaneous accident irradiation and thermodynamic exposures with nitrogen (air was replaced by nitrogen) followed by a post-accident exposure with nitrogen (R + Steam (N_2)).

Experimentally, the LOCA simulation included both a thermodynamic (steam and chemical spray) and post-accident exposures. The terminology LOCA (air) and steam (air) refer to similar accident simulations. LOCA (air) is the terminology used for French samples while steam (air) refers to U.S. samples.

The various test phases are summarized in Table 4.4.

Some parts of the French and U.S. accident sequences were identical, but were performed on different materials. They were therefore combined to limit the number of tests. All accident irradiations (both at 70°C and at ambient) were performed together. Since several of the accident test sequences differed only by the choice of accident irradiation temperature, the accident thermodynamic exposures (steam and chemical spray) as well as the post-LOCA exposures were combined into one test. The following list documents chronologically the individual tests for all French and U.S. samples:

- L10
- L2 Thermodynamic and post-LOCA exposures
- Gamma irradiation of all French and U.S. samples
- L5 + L7 Thermodynamic and post-LOCA exposures
- L1 + L4 Thermodynamic and post-LOCA exposures
- L9 + L3 Thermodynamic and post-LOCA exposures
- L6 + L8 Thermodynamic and post-LOCA exposures

4.2.1 Irradiation

For the sequential accident simulation tests (L1, L2, L4, L5, L6, L7, and L8), the French and U.S. samples were placed into four tubular ovens for irradiation at 70°C and three containers for irradiation at 28°C (See section 3.2.1.1). Tables 4.5 and 4.6 give the distribution of the samples in each of the ovens and containers during the POSEIDON irradiation. Irradiation was performed from May 18-27, 1983.

4.2.1.1 Dose Rates

The dose rate at the longitudinal midpoint of each oven and each container was measured using the ionization chamber described in Section

Table 4.4

Accident Exposures

French Cycle

L1: R 70°C→LOCA(air)
L2: LOCA(air)→R 70°C
L3: R + LOCA(air)
L4: R 28°C→LOCA(air)

U.S. Cycle

L5: R 70°C→steam(air)
L6: R 70°C→steam(N_2)
L7: R 28°C→steam(air)
L8: R 28°C→steam(N_2)
L9: R + steam(air)
L10: R + steam(N_2)

3.2.1.3. The accuracy of each measurement was therefore ± 5%. The measurement results are given in Table 4.7. The samples were distributed over a length of 70 cm, while the source configuration had a length of 100 cm. The dose rate gradient was measured for the entire length of the tubes and containers using cellulose triacetate films. The accuracy of measurements is ± 15%. The dose rate gradient curves are given for each of the ovens and containers in Figure 4.1. All the dose rates fall within a range of ± 40 krad/h. The irradiation time was calculated to obtain a maximum of 60 Mrad at the midpoint of each oven and each container.

4.2.1.2 Temperature

The temperature during irradiation was measured at several points along the axis of each oven. The maximum variation in temperature was ± 1°C. The temperature gradient diagram is given in Figure 4.2. Square section containers are open in their upper section. A thermocouple placed along the samples at different points inside the container indicates that the temperature does not vary from one sample to the next during irradiation. Before irradiation, the temperature inside the containers was 25 ± 3°C. During irradiation, the temperature reached 28 ± 3°C.

Table 4.5

Location of French Samples In Ovens and Containers During Accident Irradiation. A, B, C, D refer to the four groups of aged samples and U refers to unaged samples. L1 through L4 refer to the four French groupings of samples for accident simulations.

		Unirradiated	CONTAINERS			OVENS			
			5	6	7	1	2	3	4
82I1	A			L4					L2-L1
	B			L4				L1-L2	
	C			L4					L2-L1
	D		L4					L1	L2
	U	L2		L4					L1
82I2	A			L4				L1	L2
	B			L4					L2-L1
	C			L4					L2-L1
	D			L4				L2	L1
	U	L2			L4			L1	
82I9	A			L4				L1	L2
	B			L4				L2	L1
	C			L4					L1-L2
	D			L4				L2	L1
	U	L2			L4	L1			
82H3	A		L4					L2-L1	
	B		L4					L2-L1	
	C		L4				L2	L1	
	D			L4				L2-L1	
	U	L2		L4					L1
82H4	A			L4				L1-L2	
	B			L4			L2	L1	
	C			L4			L2	L1	
	D		L4				L2	L1	
	U	L2		L4				L1	
82H5	A		L4				L1-L2		
	B		L4				L2	L1	
	C		L4				L2	L1	L1-L2
	D		L4				L2		
	U	L2		L4			L1		
82H6	A		L4				L2-L1		
	B		L4				L1		L2
	C		L4				L2	L1-L2	
	D			L4			L2-L1		
	U	L2			L4		L1		
82G10	A			L4			L2	L1	
	B			L4				L2-L1	
	C			L4			L2	L1	
	D		L4						L1-L2
	U	L2		L4				L1	
82J3	A		L4				L2	L1-L2	
	B		L4					L1-L2	
	C		L4				L2	L1	
	D		L4					L1-L2	
	U	L2		L4			L1		
82J4	A			L4			L2-L1		
	B		L4				L2		L1
	C		L4				L2		L1
	D			L4			L1	L2	
	U	L2		L4			L1		

Table 4.6

Location of U.S. Samples In Ovens and Containers During Irradiation. A through E refer to the five groups of U.S. aged samples, F refers to unaged samples. L5 through L10 refer to the six U.S. grouping of samples for the accident simulations.

		CONTAINERS			OVENS			
		5	6	7	1	2	3	4
TEFZEL	1A			L7 L8	L6		L5	
	1B			L7 L8	L6		L5	
	1C		L8	L7	L5		L6	
	1D			L7 L8			L5 L6	
	1E		L8	L7	L6			L5
	1F		L8	L7	L5		L6	
	2A		L8	L7	L5		L6	
	2B			L7 L8	L5 L6			
	2C		L7	L8	L5		L6	
	2D		L8	L7	L5 L6		L5	
	2E			L7 L8	L5 L6			
	2F			L7 L8	L5 L6			
EPR	1A			L7 L8	L5			L6
	1B		L7	L8			L6	L5
	1C			L7 L8	L5		L6	
	1D			L7 L8	L5 L6			
	1E		L7	L8	L5 L6			
	1F		L7 L8		L5 L6			
	2A		L8	L7	L6			L5
	2B	L7	L8		L5			L6
	2C		L8	L7	L5 L6			
	2D			L7 L8	L5 L6			
	2E			L7 L8	L5			L6
	2F		L7 L8		L6	L5		
CPE	A			L7 L8	L5		L6	
	B		L8	L7	L5 L6			
	C		L7	L8	L5			L6
	D		L7	L8	L5			L6
	E		L7	L8	L5		L6	
	F			L7 L8	L5		L6	
CSPE	A			L7 L8	L5 L6			
	B		L7 L8		L6			L5
	C			L7 L8	L5 L6			
	D		L8	L7	L5 L6			
	E			L7 L8	L5 L6			
	F		L8	L7	L5 L6			
XLPO	1A			L8	L7	L5 L6		
	1B			L8	L7	L5	L6	
	1C				L7 L8	L5		L6
	1D			L8	L7	L5 L6		
	1E				L7 L8	L5	L6	
	1F			L8	L7	L5 L6		
	2A			L8	L7	L5	L6	
	2B		L7		L8	L5 L6		
	2C				L7 L8	L5		L6
	2D		L7		L8	L5		L6
	2E				L7 L8	L6		L5
	2F			L8	L7	L5	L6	
Compression set fixtures exposed to L7			n°3	n° 18 n° 26 n° 30				

	Number	Maximum dose rate (Krad/h)	Average dose rate (Krad/h)	Irradiation time (hours)	Total dose Mrad
Ovens	1	325	293	184,6	54
	2	303	276	198,0	54
	3	303	265	198,0	52
	4	310	274	193,5	53
Containers	5	300	287	200,6	57
	6	322	304	186,9	57
	7	325	296	184,6	55

Table 4.7

Irradiation Conditions for U.S. and French Sequential Accident Simulations

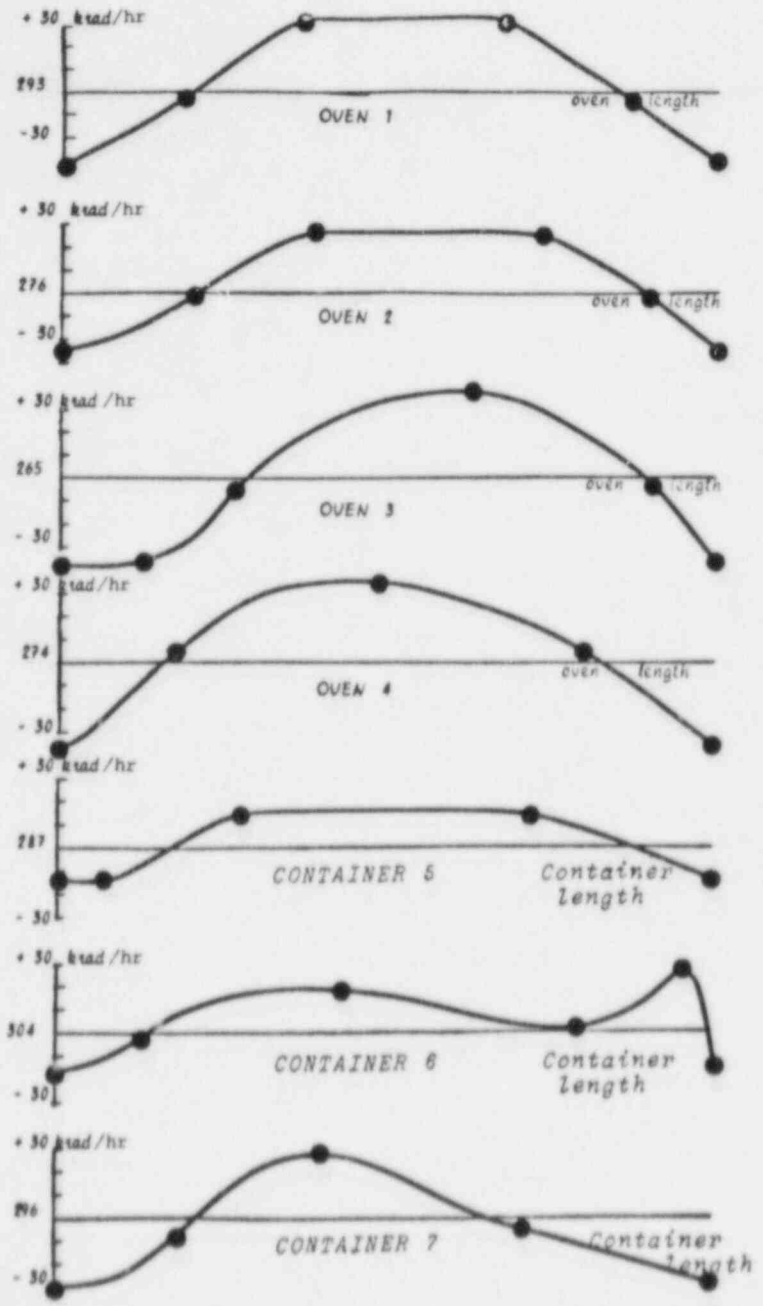

Figure 4.1: Dose Rate Gradient Curves for Each Oven and Box Employed for Sequential Accident Irradiations

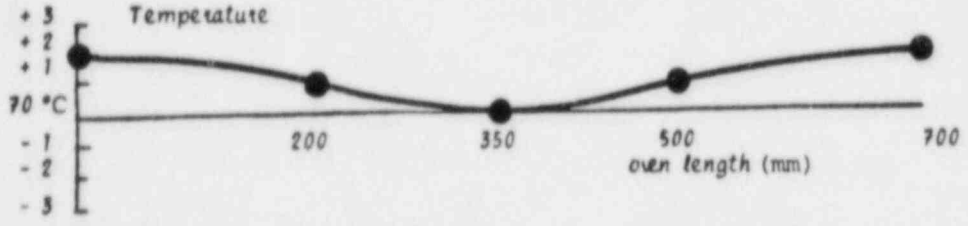

Figure 4.2: Temperature Gradient Diagram for Each Oven Used During the 70°C Irradiations

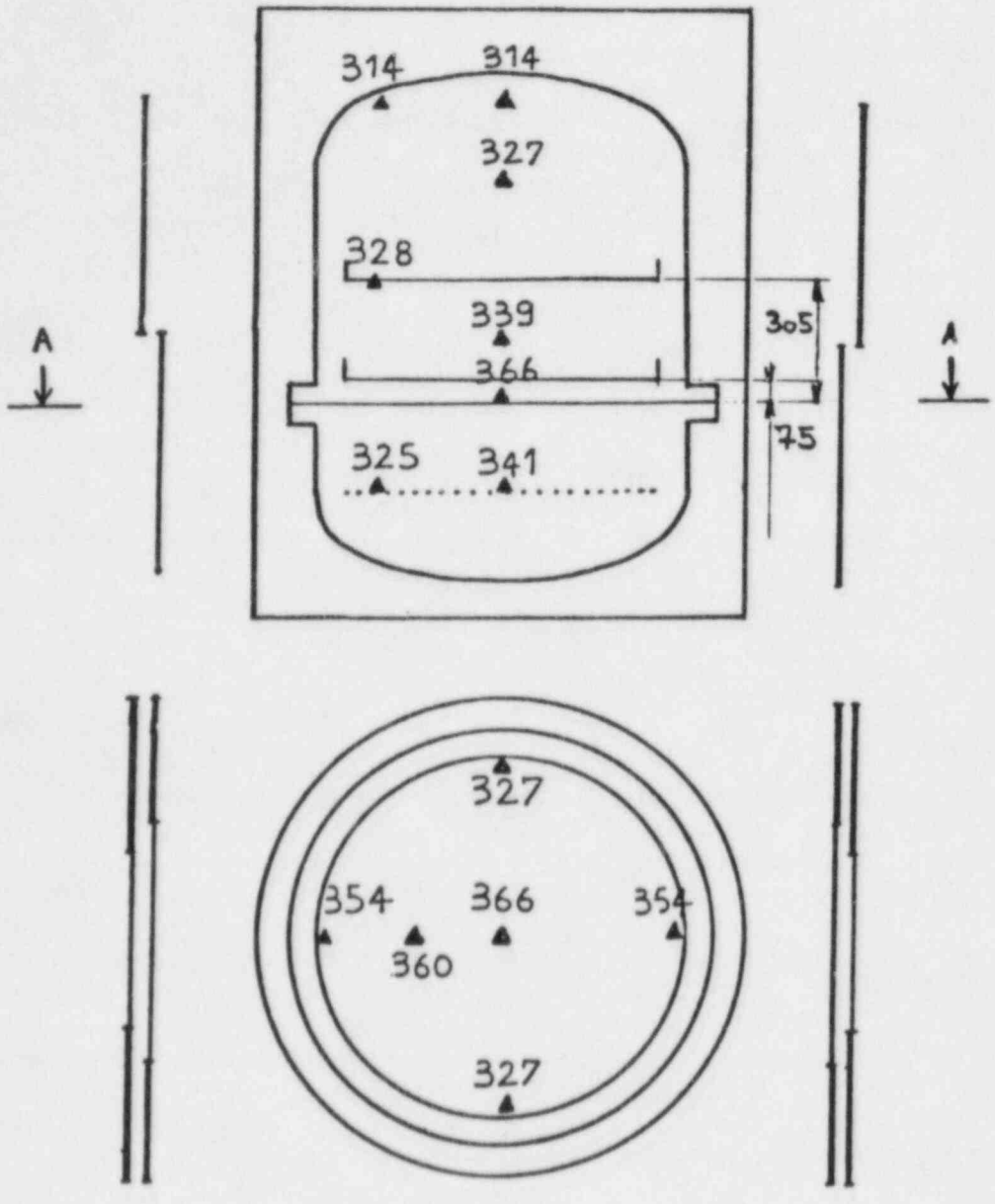

Figure 4.3: Dose Rate Measurements (krd/h) in Air (June 29, 1982) for the CESAR Test Chamber (Used for Simultaneous Accident Simulations)

During the L3, L9, and L10 tests, irradiation was carried out simultaneously with the LOCA, inside CESAR, within the POSEIDON irradiation chamber.

Figure 4.3 shows the dose rate measurements in air at different points of the CESAR experimentation cell taken on June 29, 1982. All readings are within a dose rate deviation of $\pm$ 10% of the average value. The maximum value occurs in the vertical axis of the chamber at sealing ring level; it was equal to 366 krds per hour.

The dose absorbed in the air at the time of each test was calculated taking into account the 5.27 year half-life of the Cobalt 60.

Irradiation began several minutes before the first thermodynamic transient. It continued between the two transients, then during the temperature and pressure development of the second thermodynamic profile. The interval between the two transients was calculated to obtain a total exposure of 60 Mrad. Additional irradiation at the end of LOCA exposure compensated for test deviations.

During irradiation, the rate of air or nitrogen renewal in the CESAR chamber is greater than four geometric volumes per hour, under normal temperature and pressure conditions.

4.2.2 LOCA

4.2.2.1 Position of Samples

The French and American samples were placed in the CESAR chamber on perforated plates with wide holes, ensuring free passage of the water vapor, gases and borated solutions. Figure 4.4 shows the sample positions for the U.S. materials CPE and CSPE during tests L6 and L8.

The insulation samples were placed in supports provided by Sandia National Laboratories (Figure 4.5). The supports are fitted to a plate pierced with holes. The plates were placed one above the other, separated by stainless steel threaded rods. To avoid the rising gas pressure from forcing the insulation samples out of their holders inside the experimentation chamber, a stainless steel trellis is placed over the samples on the last perforated plate (Figure 4.6).

4.2.2.2 Samples

In each sequential test, L1, L2, and L4, the following French samples were tested:

	Aging	Number		Aging	Number
	A	10		A	10
	B	10		B	10
82I1	C	10	82H4	C	10
	D	10		D	10
	U	10		U	10
	A	10		A	10
	B	10		B	10
82I2	C	10	82H5	C	10
	D	10		D	10
	U	10		U	10
	A	4		A	14
	B	4		B	10
82J3	C	4	82H6	C	10
	D	4		D	10
	U	4		U	10
	A	4		A	10
	B	4		B	10
82J4	C	4	82I9	C	10
	D	4		D	10
	U	4		U	10
	A	10		A	10
	B	10		B	10
82H3	C	10	82G10	C	10
	D	10		D	10
	U	10		U	10

All the samples were exposed to the first phase of tests (irradiation or LOCA), after which half were removed for mechanical testing. The remaining half of the samples were exposed to the complete two phases of accident simulation, after which they are also mechanically tested.

During simultaneous accident simulation, L3, only half the number of samples listed above are subjected to the simulation. They were then mechanically tested.

In each sequential test, L5, L6, L7, and L8, the following U.S. samples were tested:

8 Samples TEFZEL 1 A	8 Samples TEFZEL 2 A
8 Samples TEFZEL 1 B	8 Samples TEFZEL 2 B
8 Samples TEFZEL 1 C	8 Samples TEFZEL 2 C
8 Samples TEFZEL 1 D	8 Samples TEFZEL 2 D
8 Samples TEFZEL 1 E	8 Samples TEFZEL 2 E
8 Samples TEFZEL 1 F	8 Samples TEFZEL 2 F
8 Samples EPR 1 A	8 Samples EPR 2 A
8 Samples EPR 1 B	8 Samples EPR 2 B
8 Samples EPR 1 C	8 Samples EPR 2 C
8 Samples EPR 1 D	8 Samples EPR 2 D
8 Samples EPR 1 E	8 Samples EPR 2 E
8 Samples EPR 1 F	8 Samples EPR 2 F
8 Samples XLPO 1 A	8 Samples XLPO 2 A
8 Samples XLPO 1 B	8 Samples XLPO 2 B
8 Samples XLPO 1 C	8 Samples XLPO 2 C
8 Samples XLPO 1 D	8 Samples XLPO 2 D
8 Samples XLPO 1 E	8 Samples XLPO 2 E
8 Samples XLPO 1 F	8 Samples XLPO 2 F
8 Samples CSPE 1 A	8 Samples CSPE 2 A
8 Samples CSPE 1 B	8 Samples CSPE 2 B
8 Samples CSPE 1 C	8 Samples CSPE 2 C
8 Samples CSPE 1 D	8 Samples CSPE 2 D
8 Samples CSPE 1 E	8 Samples CSPE 2 E
8 Samples CSPE 1 F	8 Samples CSPE 2 F

All the samples were exposed to the first phase of tests (irradiation), after which half were removed for mechanical testing. The remaining half of the samples were exposed to the complete two phases of accident simulation, after which they were also mechanically tested.

During simultaneous tests L9 and L10, half as many of the samples were tested.

4.2.2.3 Thermodynamic Conditions

The vapor temperature, pressure, and chemical spray experimental profiles were recommended by the French nuclear safety organizations. Each test was comprised of two thermodynamic transients, followed by temperature, pressure, and chemical spray exposures. Table 4.8 summarizes the desired regulatory temperature and pressure conditions for the thermodynamic exposures. During the second thermodynamic exposure, beginning 220 seconds after the start of the test, the samples were sprayed with borated solution having the following composition:

H_3BO_3 = 15 g/ℓ
NaOH = 6 g/ℓ

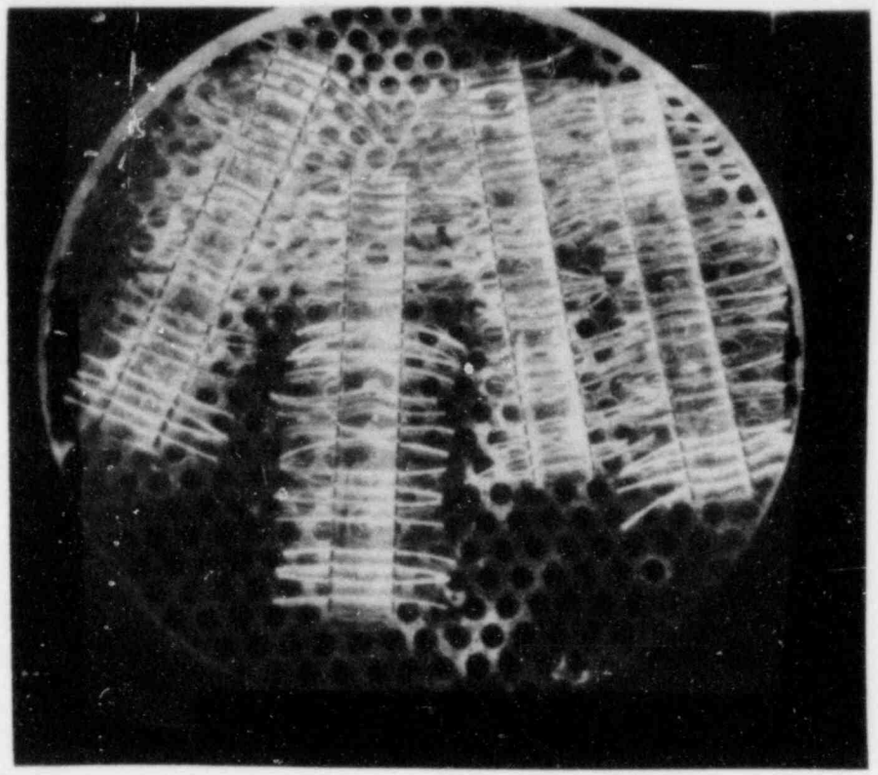

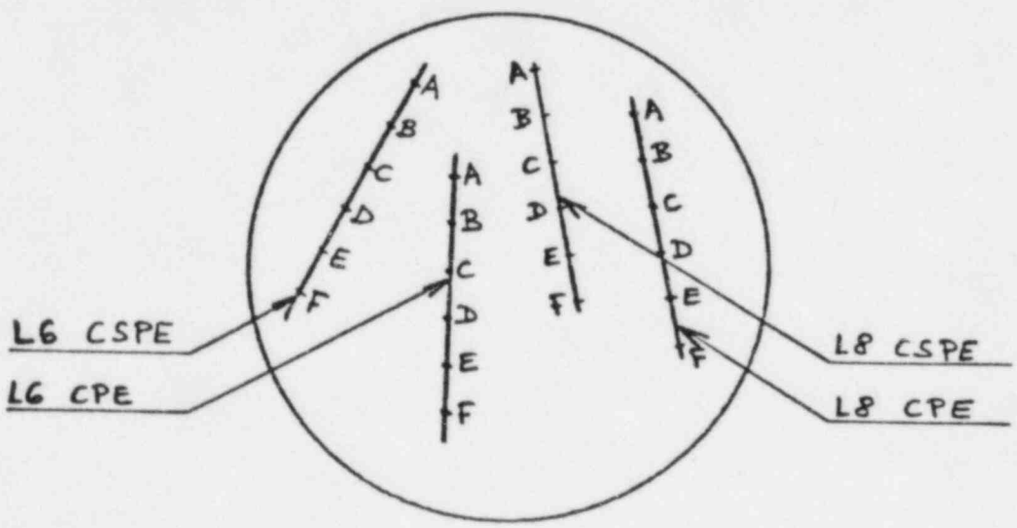

Figure 4.4: U.S. CSPE and CPE Sample Position on Perforated Plate in CESAR Facility During L6 + L8 Thermodynamic Exposure

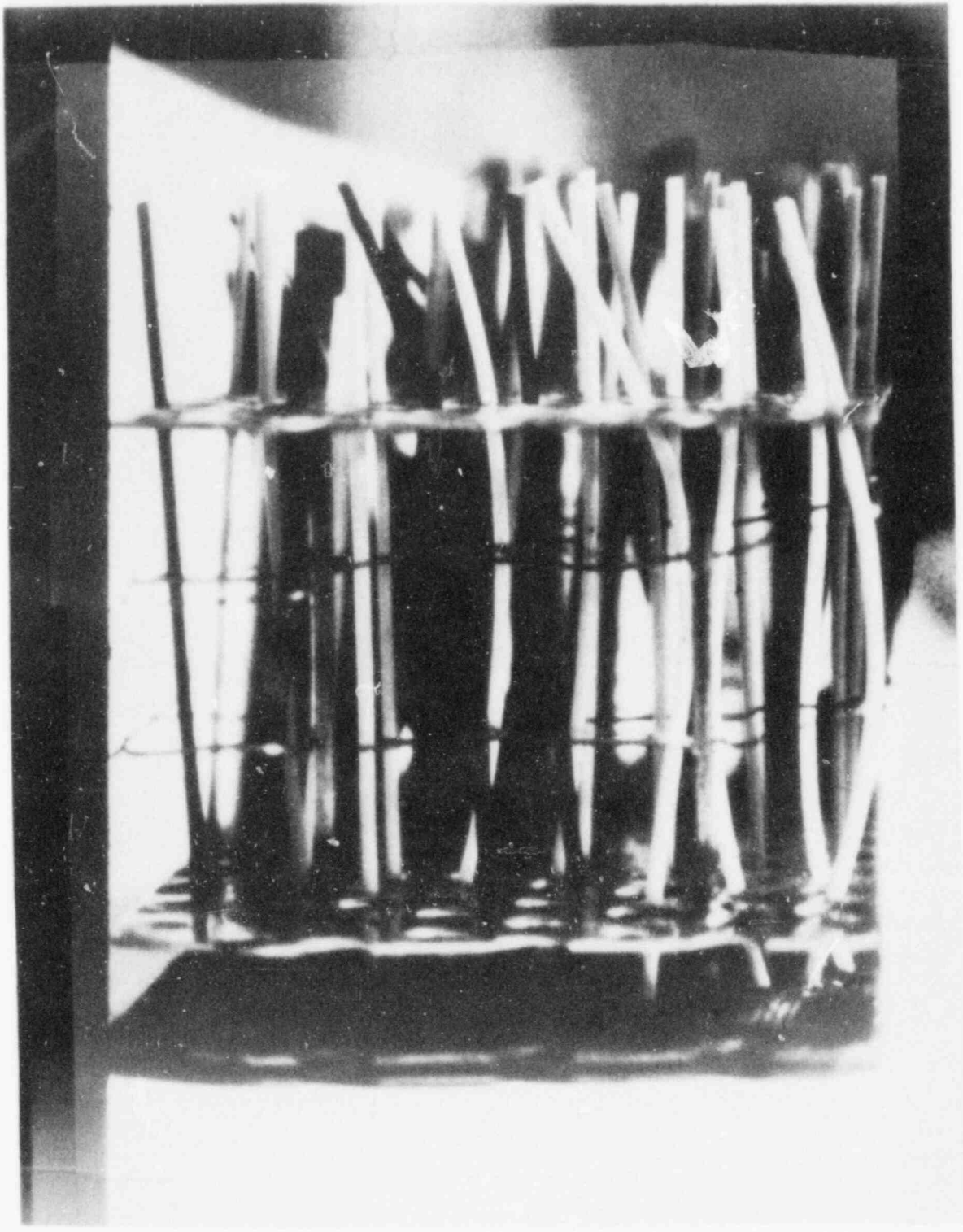

Figure 4.5: U.S. Polymer Samples Supported by Fixtures as Used for Accident Thermodynamic Simulations

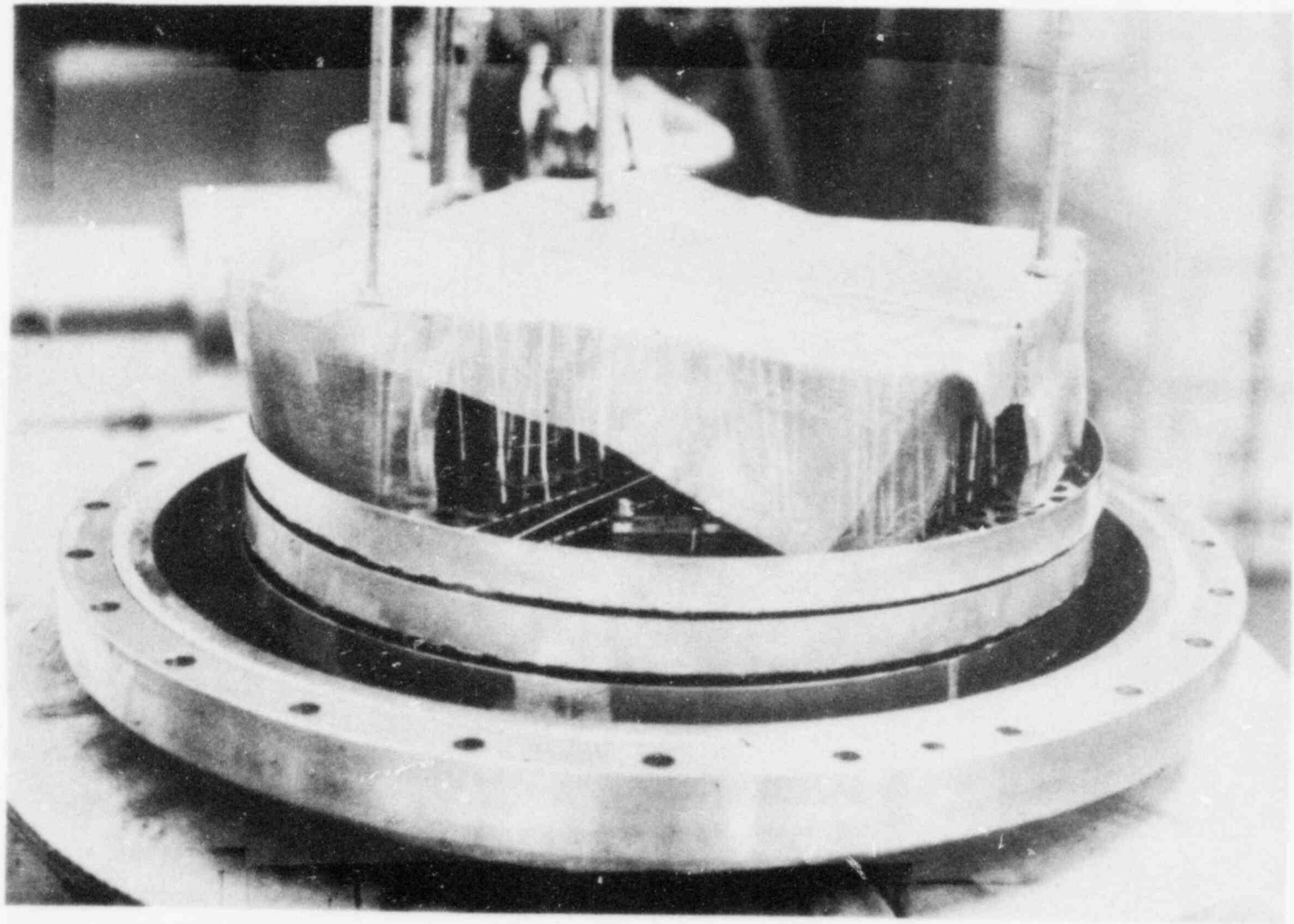

Figure 4.6: Samples Prepared for Thermodynamic Exposures

Table 4.8

French Regulatory Recommendations for
Temperature and Pressure Profiles

Transient	Time	Temperature °C	Pressure (bar)
	to	50	1.0
	to + 10 sec	156	5.7
1	to + 100 sec	156	5.7
	to + 720 sec	150	5.7
	to + 24 hours	50	1.0
	to	50	1.0
	to + 10 sec	156	5.7
	to + 100 sec	156	5.7
	to + 1200 sec	150	5.7
	to + 2800 sec	140	5.0
2	to + 2 hours	130	4.2
	to + 4 hours	121	3.3
	to + 10 hours	110	2.8
	to + 18 hours	100	2.3
	to + 2.5 days	80	1.7
	to + 4 days	73	1.6

The pH value of the solution is maintained at 9.25. The spray rate was 6.1 liters per minute and per square meter of horizontal section of the chamber. The spraying duration was 24 hours; French regulations allow for a 96-hour spray exposure.

4.2.2.4 Achieved Thermodynamic Conditions

Figures 4.7 through 4.12 illustrate the achieved thermodynamic conditions for pressure and temperature. The desired temperature and pressure profiles are also shown. For each thermodynamic transient, the temperature and pressure rise were far greater and much faster than required. The temperature reached between 165 and 175°C in 5 to 6 seconds. During the same time period, the pressure achieved between 6.8 and 7.5 bar absolute (98 and 109 psia). For the first 100 seconds, the temperature remained at approximately 10°C above the required profile.

Only for tests L5 + L7 and L3 + L9 did the temperature quickly approach the theoretical profile. During the second thermodynamic transient a temperature overshoot appears approximately 200 seconds after the start of the test. This overshoot corresponds to the passage from dry vapor pressure to saturated vapor with a corresponding release of 600 calories of energy per gram of vapor. Very rapidly after the initiation

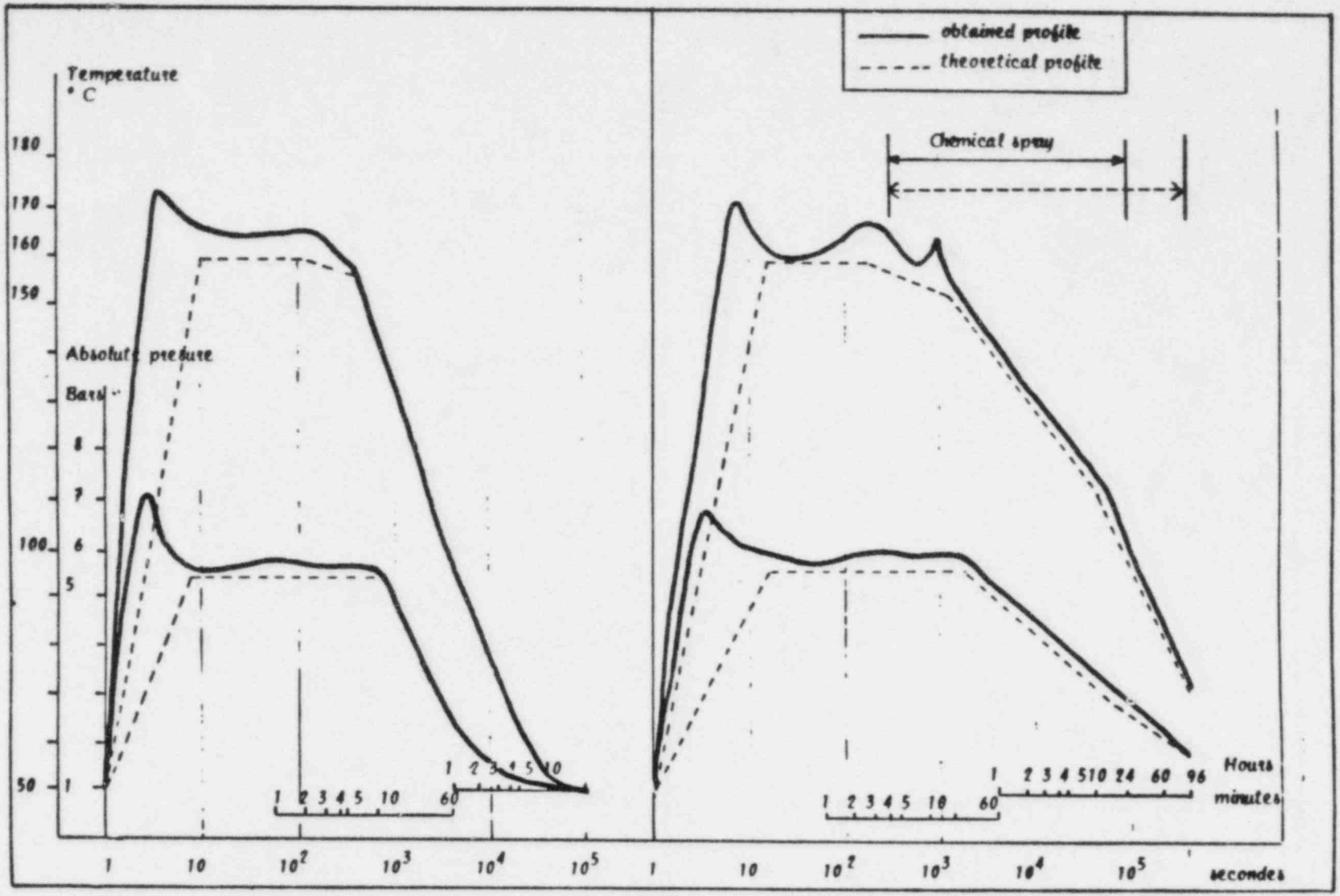

Figure 4.7: Temperature and Pressure Profiles for L1 + L4 CESAR Test

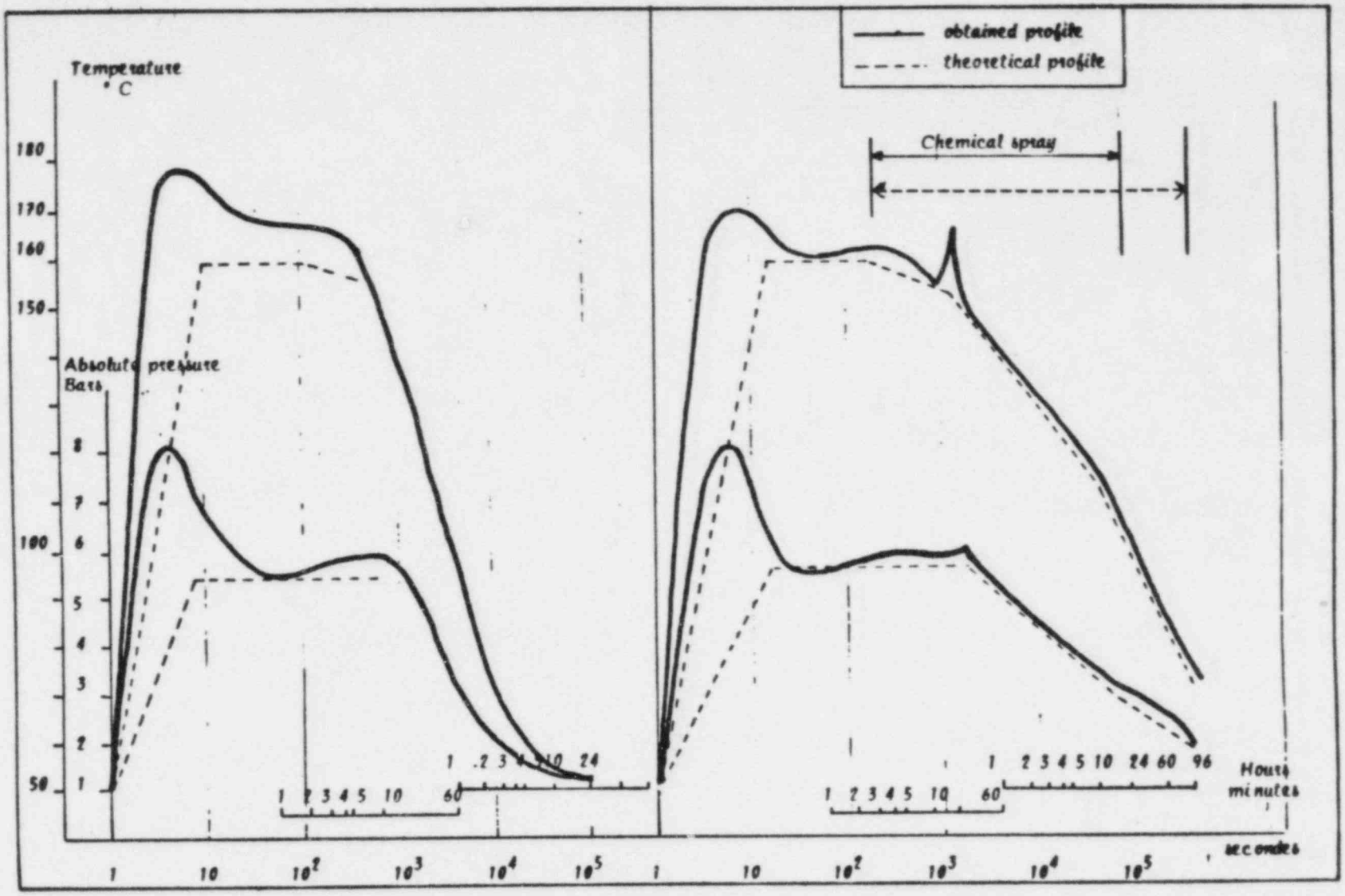

Figure 4.8: Temperature and Pressure Profiles for L2 CESAR Test

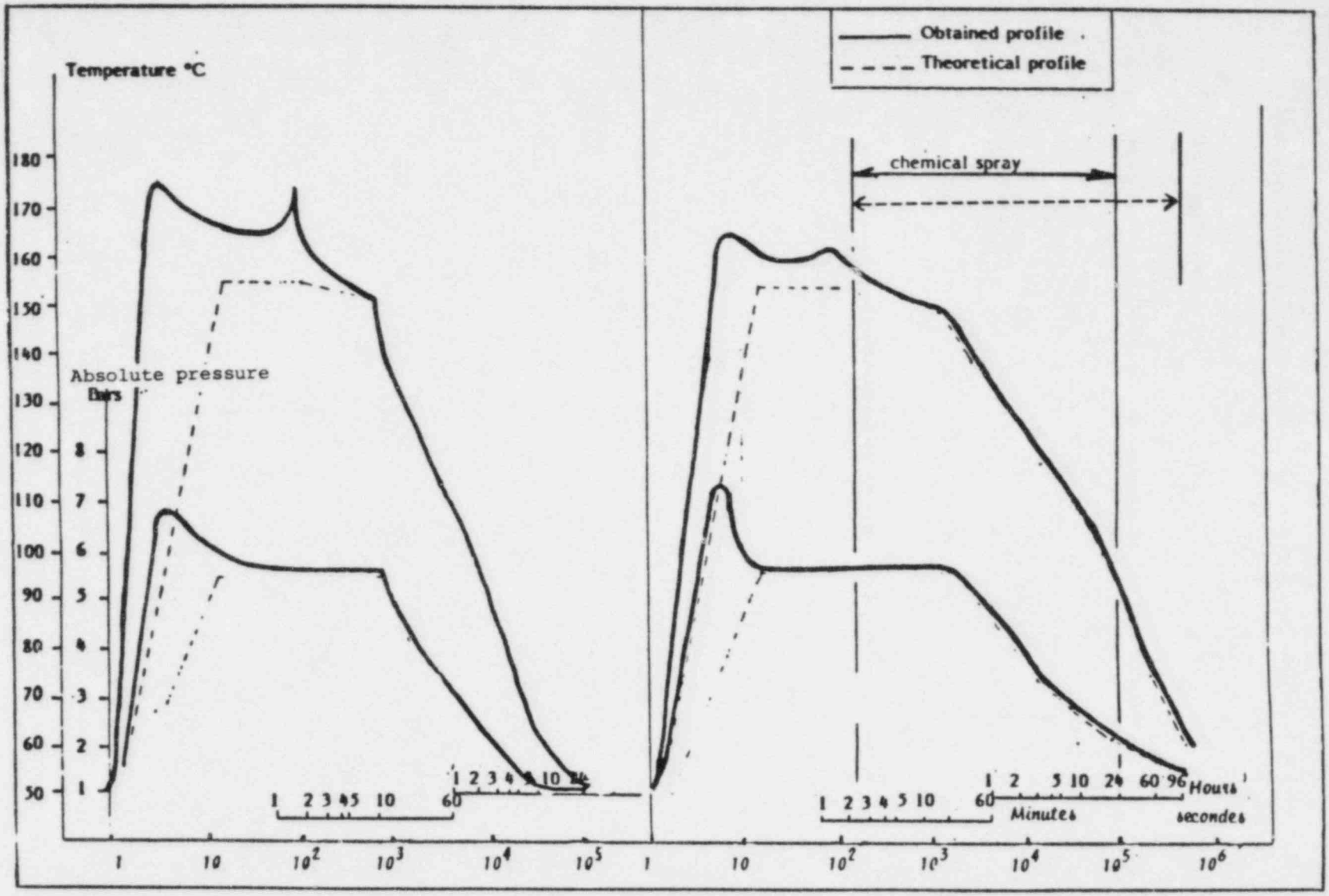

Figure 4.9: Temperature and Pressure Profiles for L6 + L8 CESAR Test

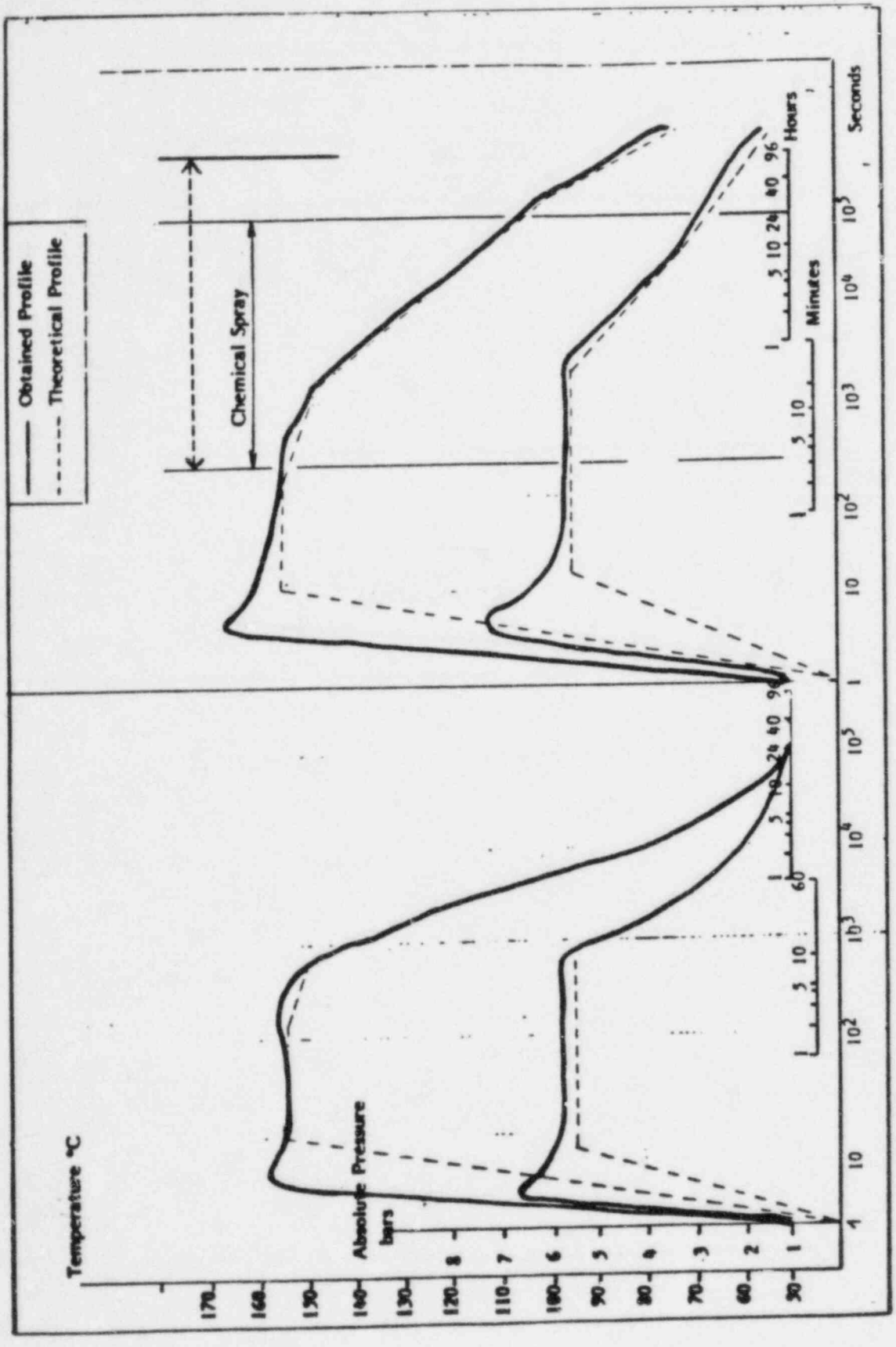

Figure 4.10: Temperature and Pressure Profiles for L5 + L7 CESAR Test

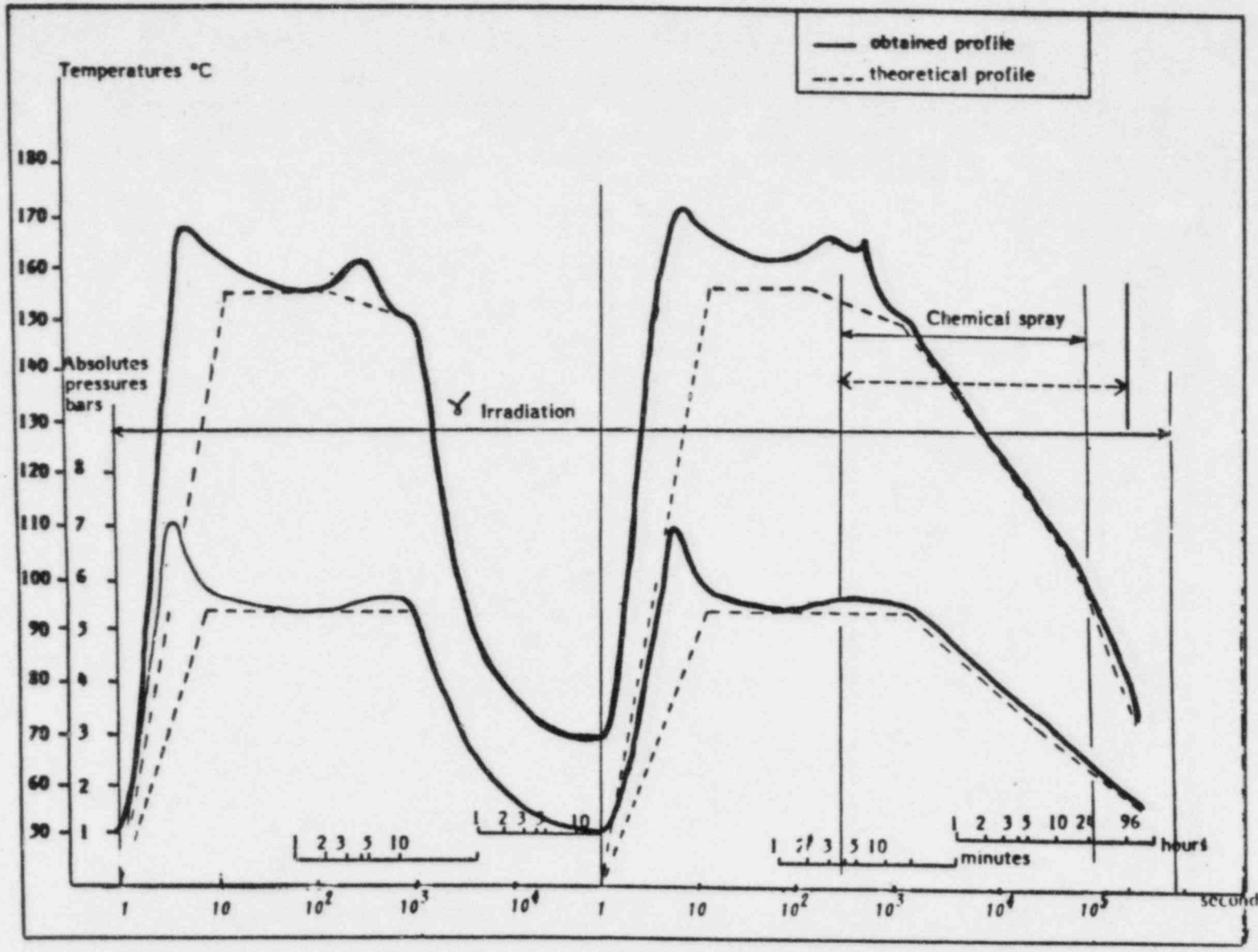

Figure 4.11: Temperature and Pressure Profiles for L3 + L9 CESAR Test

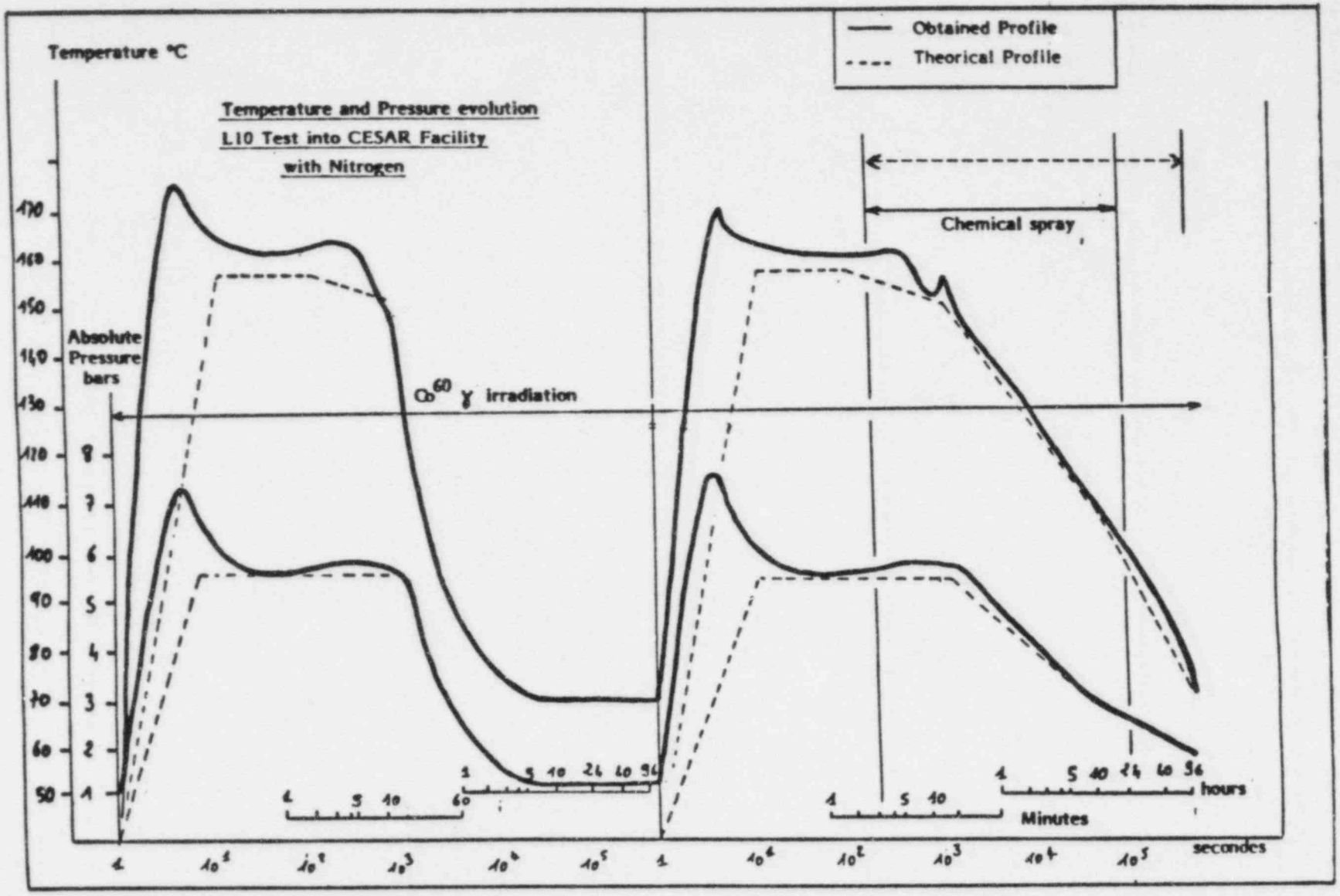

Figure 4.12: Temperature and Pressure Profiles for L10 CESAR Test

of chemical spraying, the achieved temperature profile follows the required profile for the remainder of the test. Approximately 10 seconds after the start of each thermodynamic transient, the achieved pressure matches the required pressure profile.

For the simultaneous thermodynamic and irradiation exposures, irradiation continued during the cooldown between the two thermodynamic transients. The interval between the two transients was adjusted so that the total experimental exposure time corresponded to a 60 Mrd dose. (Experimental deviations were accounted for by adding additional dose at the completion of the two profiles.) Hence the time interval separating the two simultaneous thermodynamic transients was not the same as that employed during the sequential test exposures where irradiation was not a consideration.

For the L3 + L9 simultaneous test the total irradiation time was 188.7 hours corresponding to a center of chamber dose of 60.4 $\pm$ 9.1 Mrd(air-equiv.). The irradiation was stopped three times during the L3 + L9 test due to irradiation hot cave operating incidents. The first incident lasted 19 hours, 35 minutes. The other two interruptions were short, i.e., 0.5 hours for the first and 1 hour for the second. The samples of this test were exposed to additional irradiation after the second thermodynamic profile to compensate for these deviations. For the L10 simultaneous test the total irradiation time was 174.4 hours corresponding to 60.2 $\pm$ 9.0 Mrd(air-equiv.). 6.4 hours of this exposure was performed after completion of the thermodynamic exposures.

Since the irradiation caused heating within the CESAR cell, the test chamber temperature did not fall below 70°C during the natural cooling between the two simultaneous thermodynamic transients. For the sequential test exposures, natural cooling to approximately 50°C was achieved.

4.2.3 Post-Accident Exposures

After completion of the LOCA exposure, a post-LOCA exposure was performed. It lasted ten days and consisted of a 100°C, approximately 100% relative humidity exposure. The exposure was performed in the CESAR chamber; the temperature was maintained by the frequent injection of vapor from the boiler.

4.3 Post-Test Weight and Length Measurements

The weight gains and length increases experienced by the U.S. samples during the accident simulations were measured. For each group of samples, the weight was measured prior to the start of the accident simulations and also at the completion of the post-LOCA 10-day, 100°C, 100% relative humidity exposure. Measurements were performed prior to the six hour 60°C drying exposure. Weight and length measurements for the L10 (R + steam(N_2)) exposure were not obtained prior to drying. For this test exposure, weight and length measurements were only obtained at completion of the drying exposure.

The weight and length measurements were performed 13 to 20 days after completion of the post-LOCA exposure. Hence some moisture desorption had occurred. Cross comparisons between different accident simulation data should not be attempted because of the different desorption times. Comparison within a single accident simulation is meaningful. The specific time intervals for each test were: L5 + L7 was 15 days; L9 was 13 days; L6 was 15 days; and L8 was 20 days.

5.0 RESULTS

We report test results for twenty-three polymer sample sets; eight U.S. insulation and jacket materials, five U.S. O-ring and gasket materials, and ten French elastomer, O-ring, thermoplastic and thermosetting materials. Test results at completion of the aging exposures have previously been reported in Reference 1. In this publication we report on test results at completion of various phases of the aging and accident simulations. Compression set results for the five U.S. O-ring and gasket materials are presented in tabular form in this section. The appendix presents in tabular form all tensile and bend test results for the remaining eighteen materials. In this section of the report we graphically display some of the results. Specifically, we plot the normalized mechanical properties as a function of the aging and accident procedures. Our plots are constructed as follows. A mechanical property (such as normalized elongation) is plotted on the y-axis. The aging technique employed is displayed via the x-axis. The measurement location in the test sequence is indicated by the plotting symbol (+, x, etc.). For the U.S. samples, all plotted measurements are for the completion of the accident simulation. For the French samples, additional measurement locations (such as "After Aging") are also displayed.

We also present the graphical analysis two ways. First, we plot the mechanical property normalized by its unaged value. This plotting technique allows for evaluation of the most conservative combinations of aging and accident simulation techniques. Second, we plot the mechanical property normalized by its after aging value. This plotting technique illustrates the accident contribution to the mechanical property degradation. These latter plots are identified as "Accident Effect Only" and complement the aging results presented in Reference 1.

5.1 U.S. Samples

5.1.1 CSPE

At completion of aging, CSPE tensile properties depended strongly on the aging sequence. For example, the ultimate tensile elongation had decreased to between 6% and 45% of its initial value. Figure 5.1 illustrates these aging results for CSPE as originally presented in Reference 1. Figure 5.2 presents ultimate tensile elongation data at the completion of the accident exposures relative to the initial unaged values. There is not a large difference in results between alternative accident exposure techniques. The influence of aging technique is more pronounced; the R70→T and the R120 aging exposures lead to the most severe degradation. Figure 5.3 illustrates the influence of the accident exposure on the after aging elongation values. In general, the accident exposures reduced the after aging elongation values by approximately 70%. The major exception to this trend was for those samples preconditioned by the R70→T aging sequence. At completion of this aging sequence, the elongation was already substantially degraded (to 6% of the original value); hence large scatter in additional degradation might be expected.

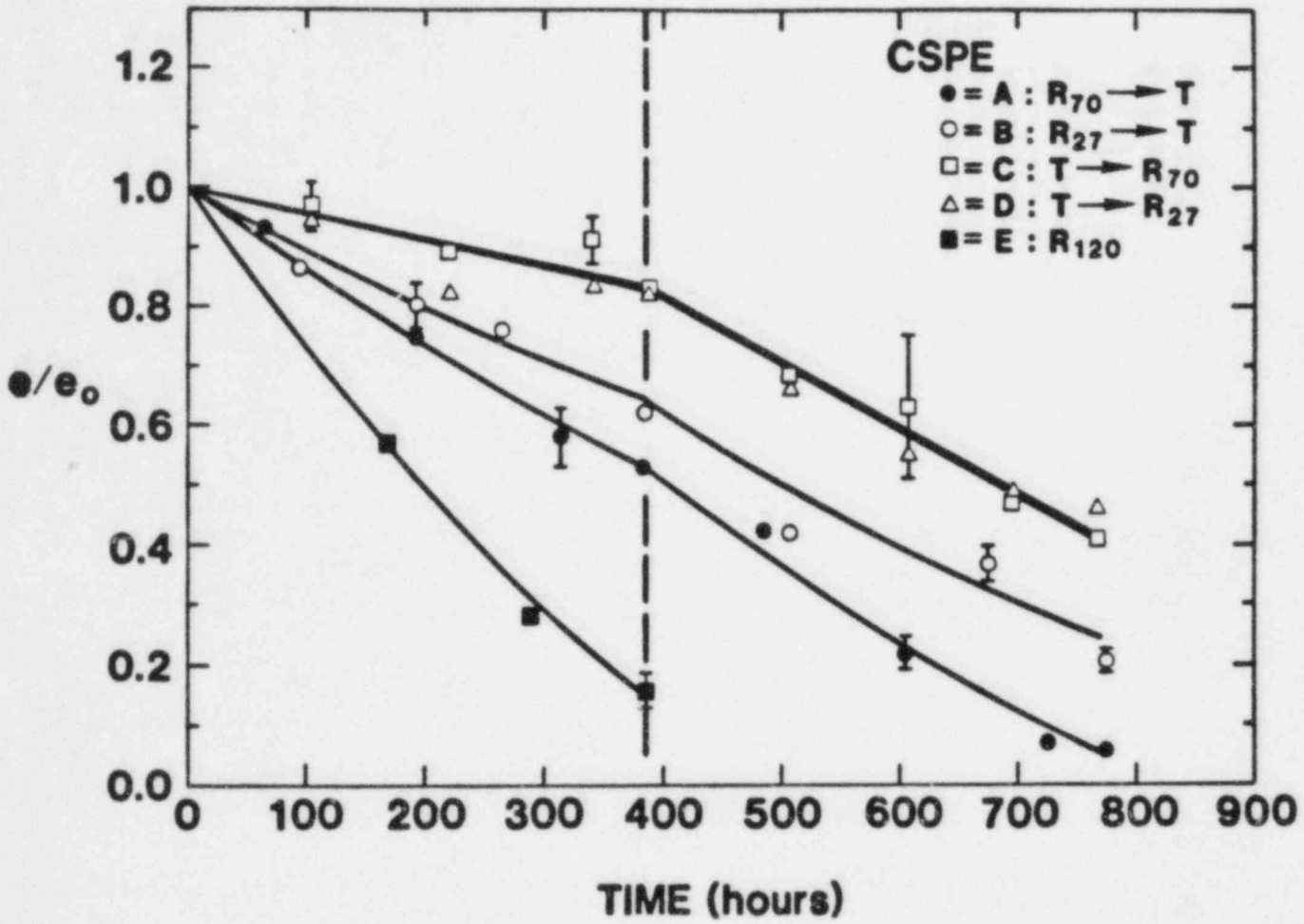

Figure 5.1: Ultimate Tensile Elongation of CSPE During Various Aging Environments. Sample tensile elongation divided by initial (unaged) elongation is plotted versus aging time. Each portion of the sequential exposures lasted ~380 hours.

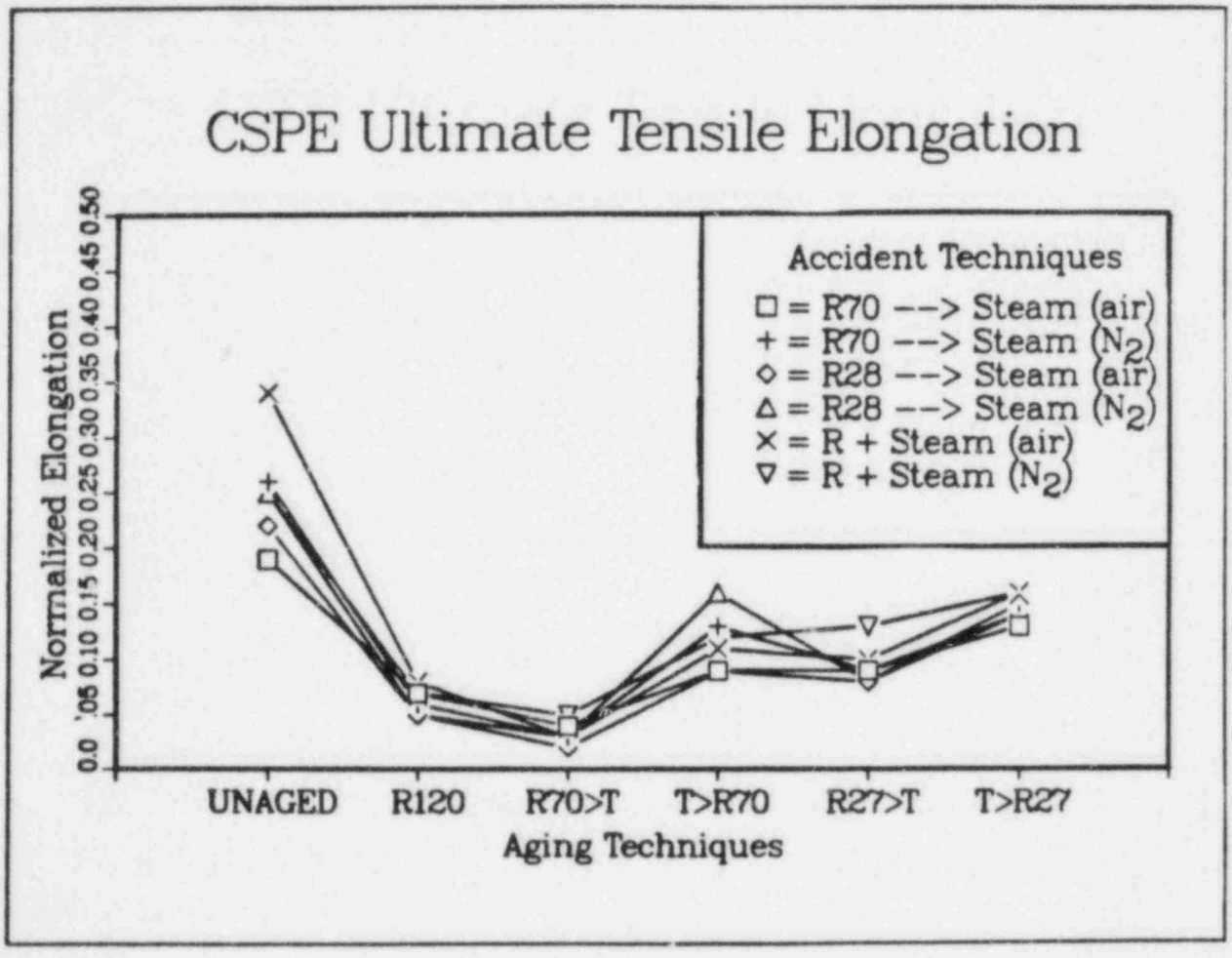

Figure 5.2: Ultimate Tensile Elongation of CSPE at Completion of the Accident Exposure. Sample tensile elongation divided by the initial (unaged) elongation is plotted for several aging and accident simulation techniques.

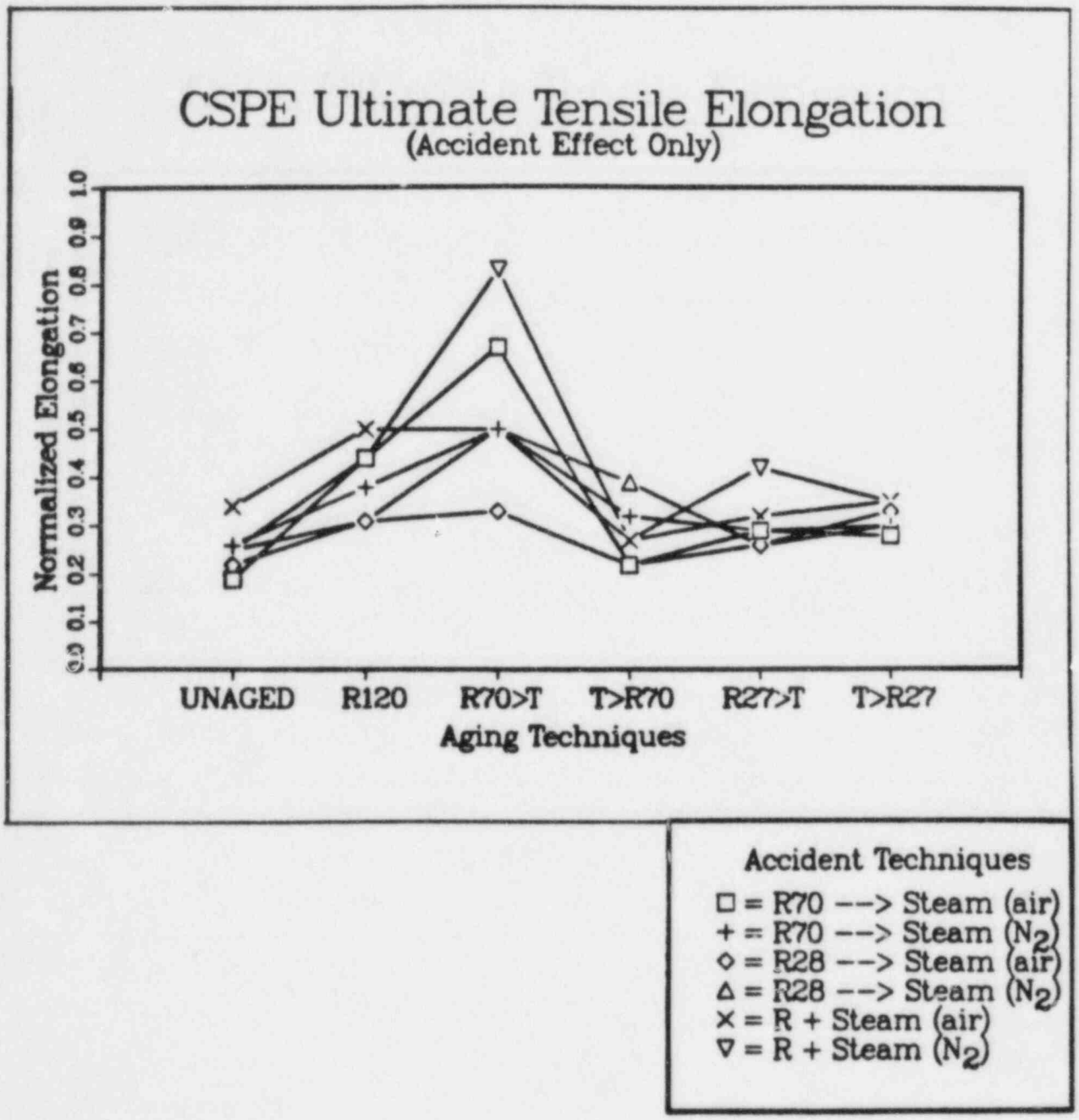

Figure 5.3: Ultimate Tensile Elongation of CSPE at Completion of the Accident Exposure. Sample tensile elongation divided by the after aging elongation is plotted for several aging and accident simulation techniques.

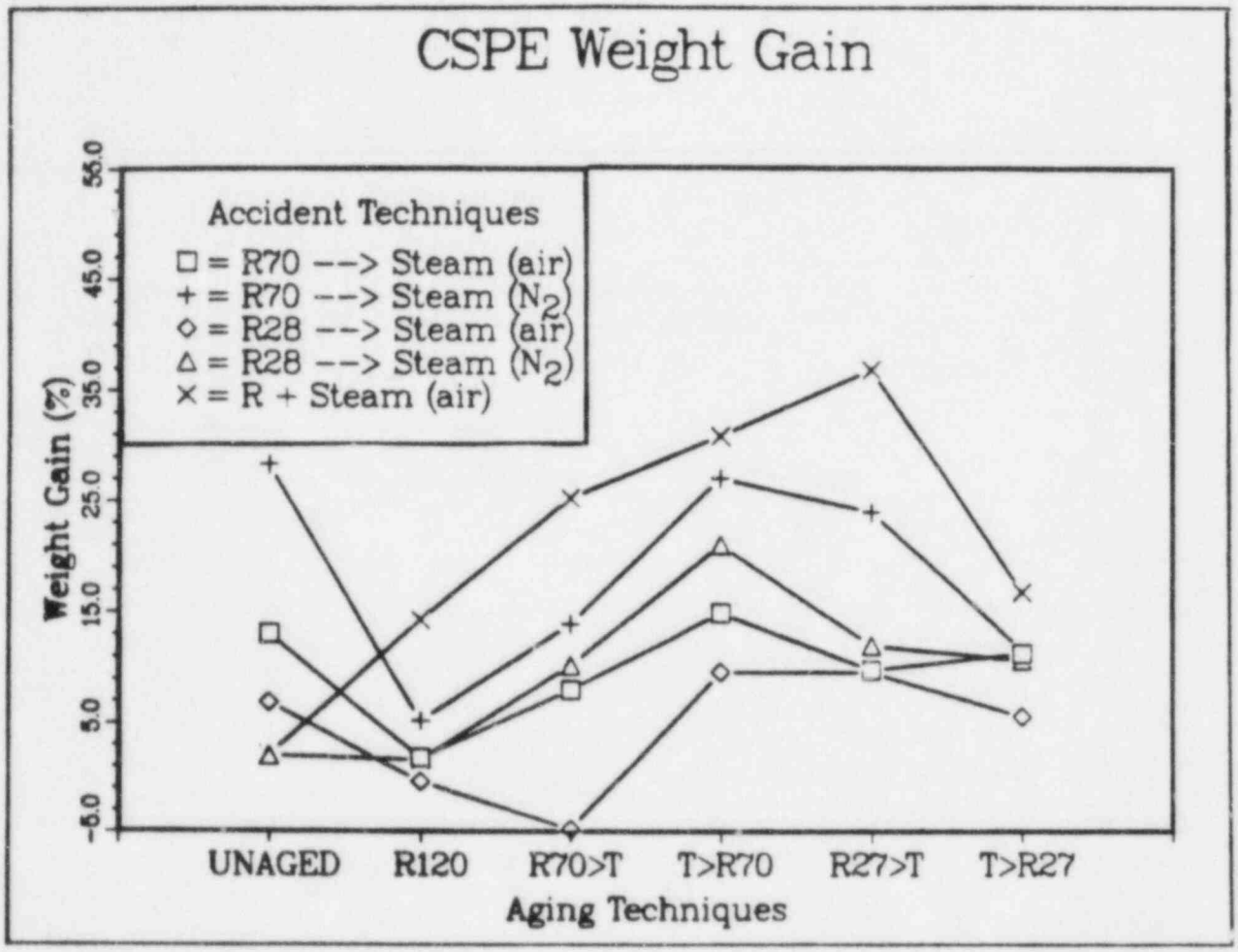

Figure 5.4: CSPE Weight Gain for Several Aging and Accident Simulation Techniques

Moisture absorption data for CSPE is shown in Figure 5.4. Substantial weight gains (up to 35%) were experienced by some of the samples.

5.1.2 CPE

At completion of aging, CPE tensile properties also depended on the aging sequence. For example, the two R→T aging sequences had degraded the ultimate tensile elongation to approximately 10-15% of its initial value. In contrast, the two T→R sequences produced e/e_0 values of approximately 25%. Reference 1 aging results for CPE are illustrated in Figure 5.5.

By completion of the accident exposures, most CPE samples had e/e_0 values less than or equal to 0.1 (See Figure 5.6). Generally, the lowest values were achieved for those samples preconditioned by the R70→T aging sequence; the highest e/e_0 values corresponded to the unaged samples. Samples preconditioned by R120, T→R70, R27→T, and T→R27 yielded similar e/e_0 values. Figure 5.7 presents the influence of the accident exposure on the after aging elongation values; i.e., the e/e_{aging} values are plotted.

Moisture absorption data for CPE is shown in Figure 5.8. The weight gains generally appear to be independent of the preconditioning technique employed prior to the start of the accident simulations.

5.1.3 EPR 1

At completion of aging EPR 1's tensile elongation values did not have a large dependence on the aging technique: the e/e_0 variation was less than 50%, ranging from .52 to .74 (Figure 5.9). However, by completion of the accident exposure, the e/e_0 variation was much larger, ranging from .02 to .35 (excluding the unaged samples from consideration). Figures 5.10 and 5.11 illustrate the e/e_0 values at completion of the accident exposure. Generally the most consistent least degrading accident exposure was the R + steam(N_2) simulation. The most consistent degrading exposures were the R + steam(air) and R70→steam(air) accident simulations. The R28→steam(N_2) and R70→steam(N_2) accident simulations both exhibited increased elongation degradation as the preconditioning aging temperature was lowered from 120°C to 27°C. This effect is also evident in the aging data of Figure 5.9. The irradiation degradation of aging sequences E, A, and B (R120, R70, and R27) becomes more pronounced as the temperature is decreased. Moisture absorption data for EPR 1 is presented in Figure 5.12.

5.1.4 EPR 2

At completion of aging, EPR 2's tensile elongation did not have a large dependence on the aging technique: The e_{aging}/e_0 variation was less than 50%, ranging from 0.34 to 0.50. The most degradation was for the R120 aging exposure. The sequential aging techniques yielded

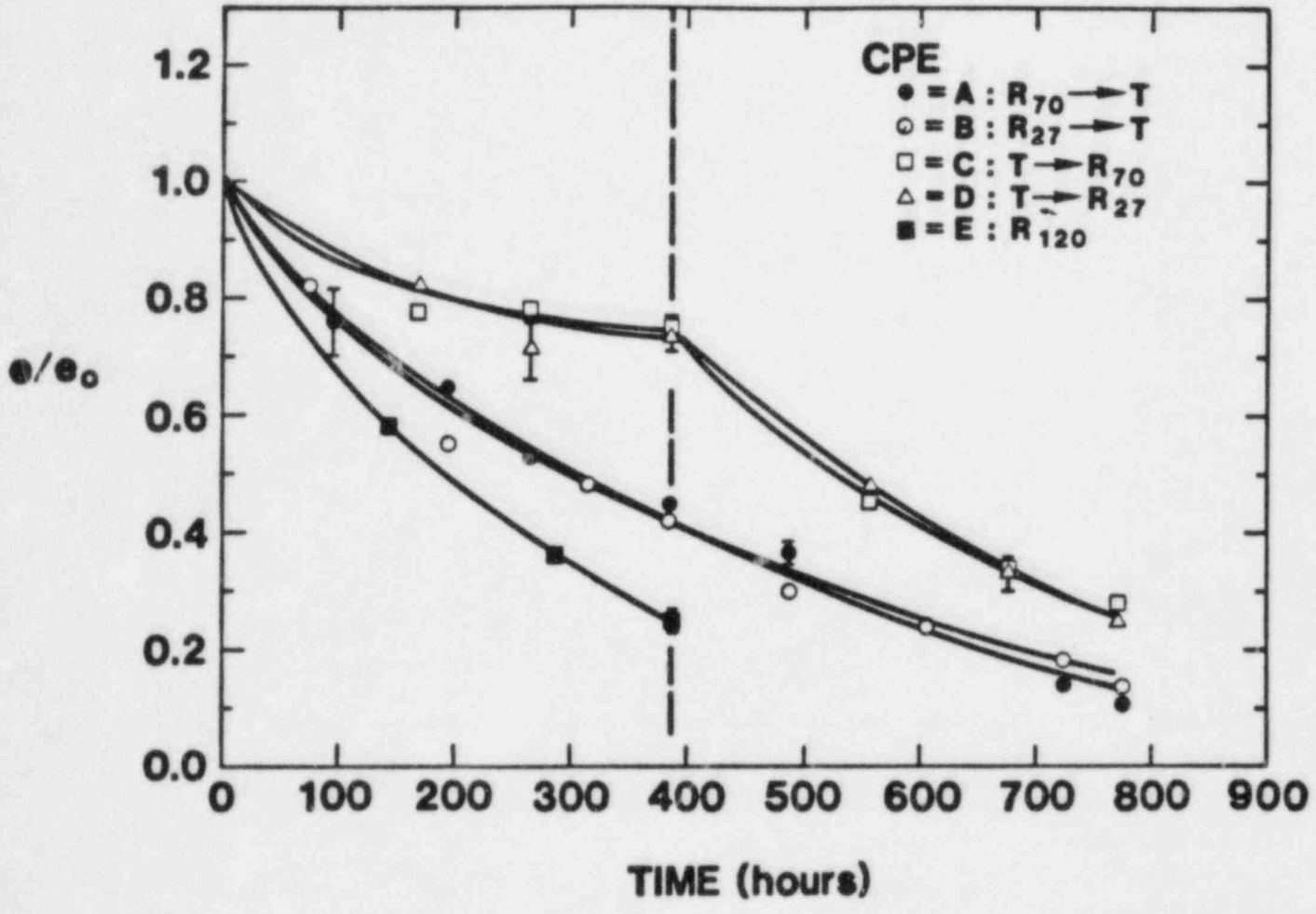

Figure 5.5: Ultimate Tensile Elongation of CPE During Various Aging Environments. Sample tensile elongation divided by initial (unaged) elongation is plotted versus aging time. Each portion of the sequential exposures lasted ~380 hours.

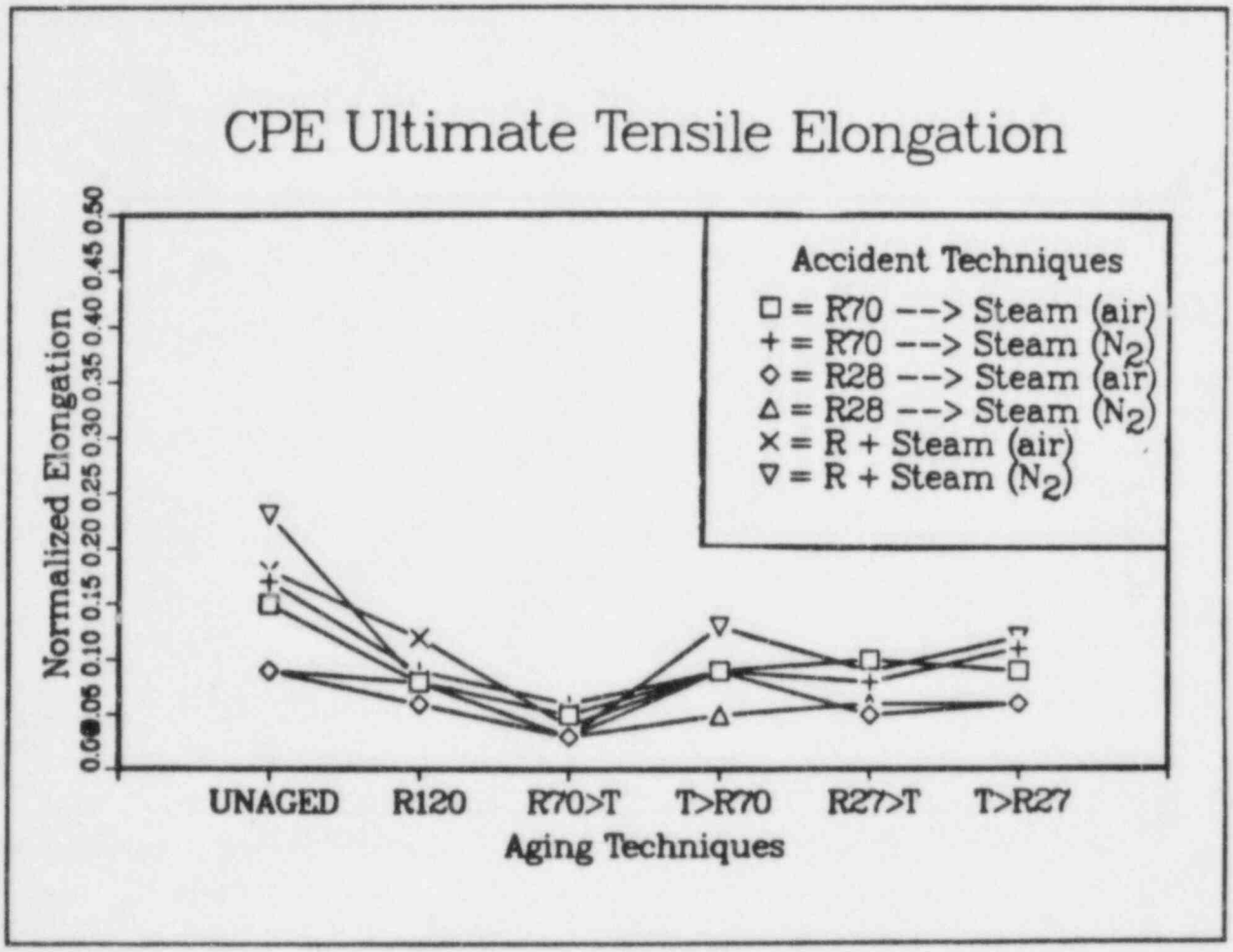

Figure 5.6: Ultimate Tensile Elongation of CPE at Completion of the Accident Exposure. Sample tensile elongation divided by the initial (unaged) elongation is plotted for several aging and accident simulation techniques.

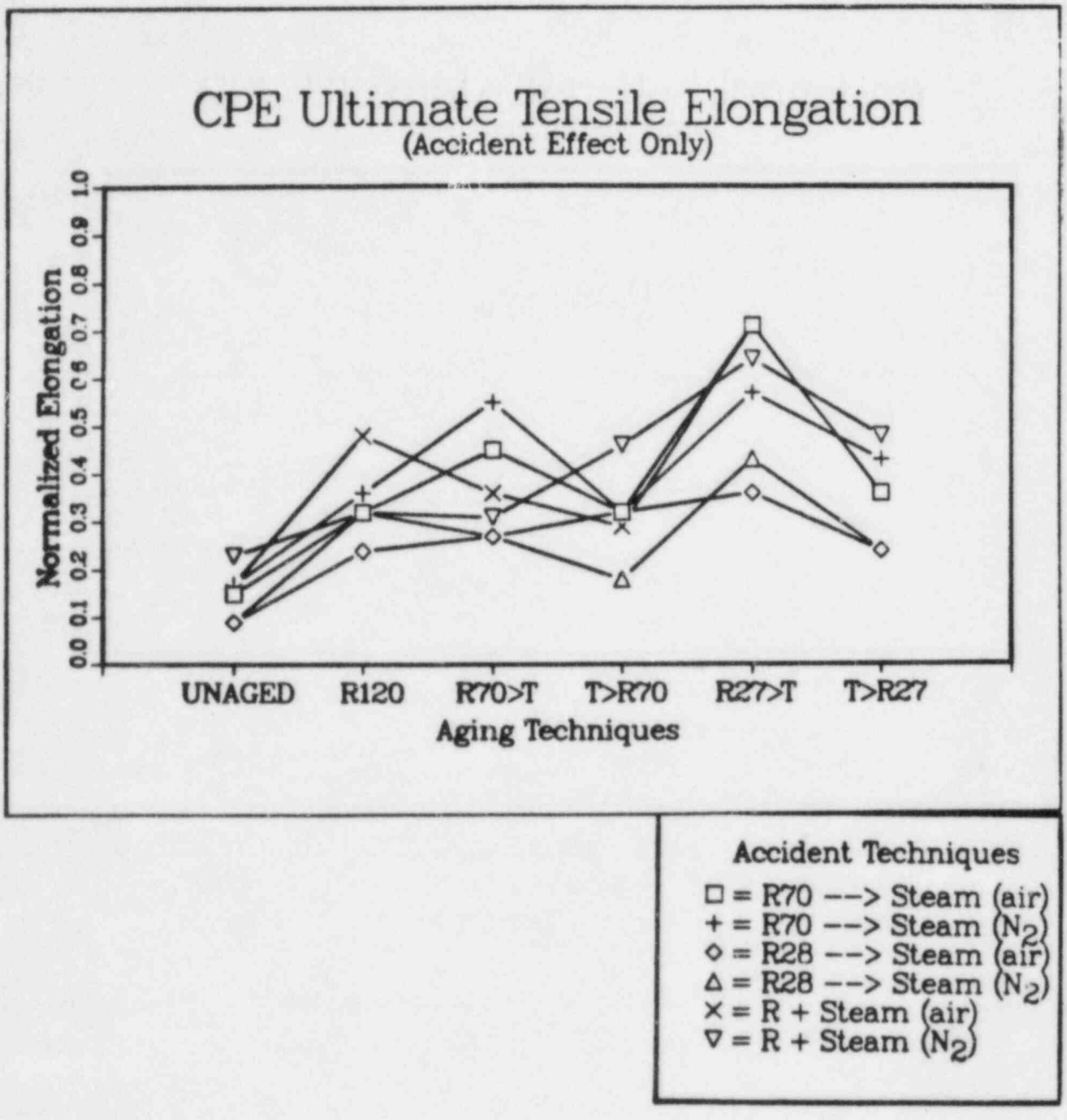

Figure 5.7: Ultimate Tensile Elongation of CPE at Completion of the Accident Exposure. Sample tensile elongation divided by the after aging elongation is plotted for several aging and accident simulation techniques.

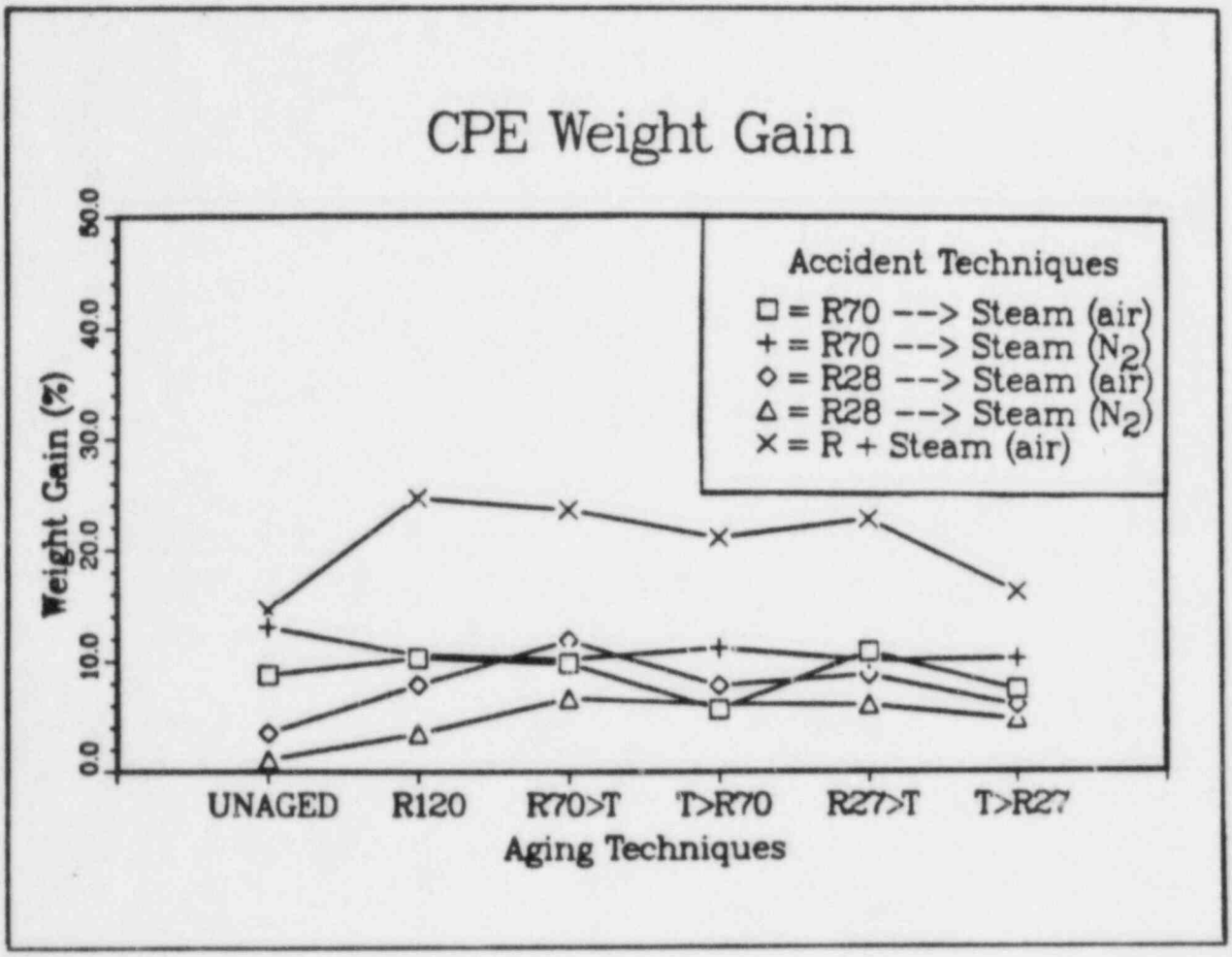

Figure 5.8: CPE Weight Gain for Several Aging and Accident Simulation Techniques

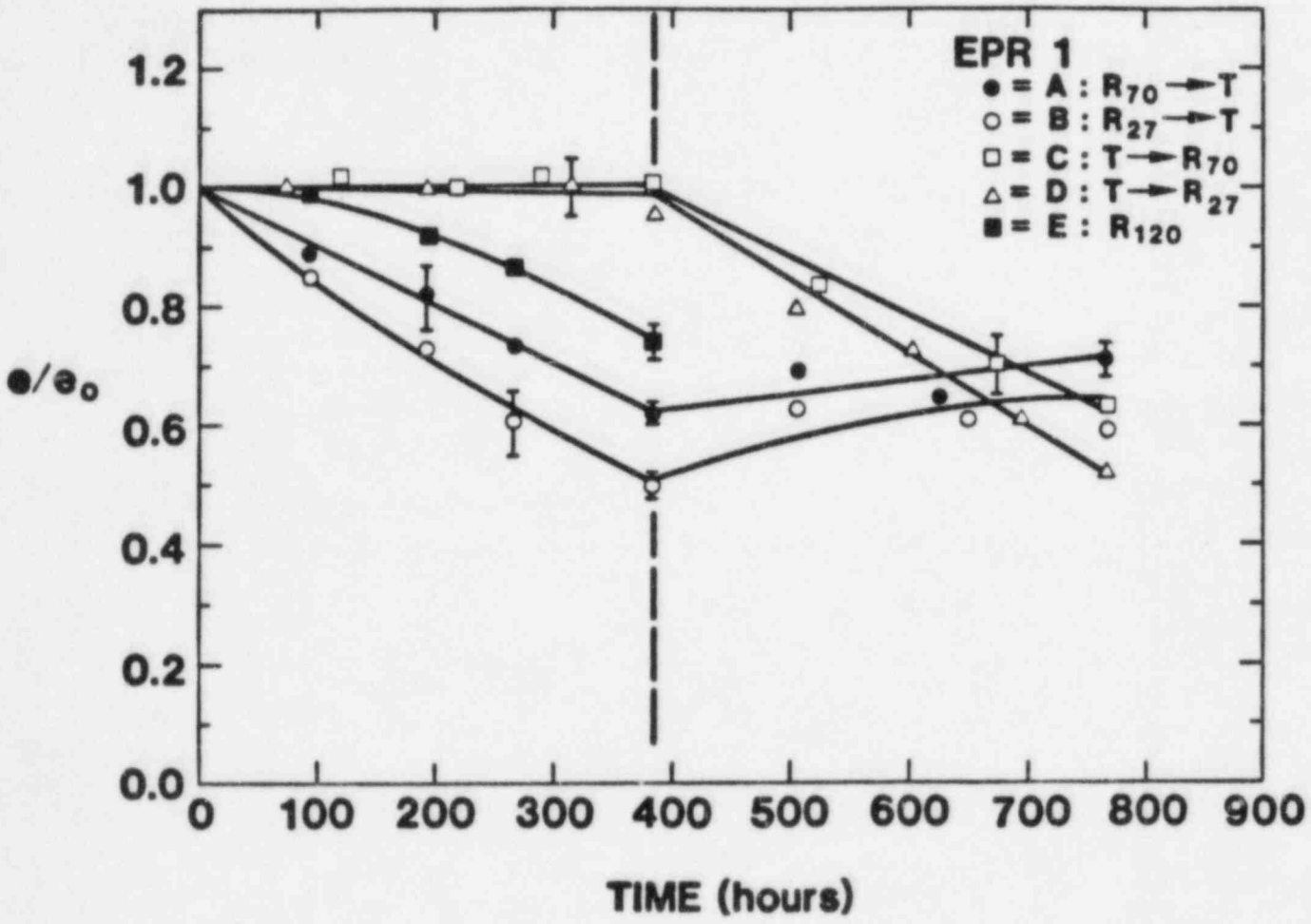

Figure 5.9: Ultimate Tensile Elongation of EPR 1 During Various Aging Environments. Sample tensile elongation divided by initial (unaged) elongation is plotted versus aging time. Each portion of the sequential exposures lasted ~380 hours.

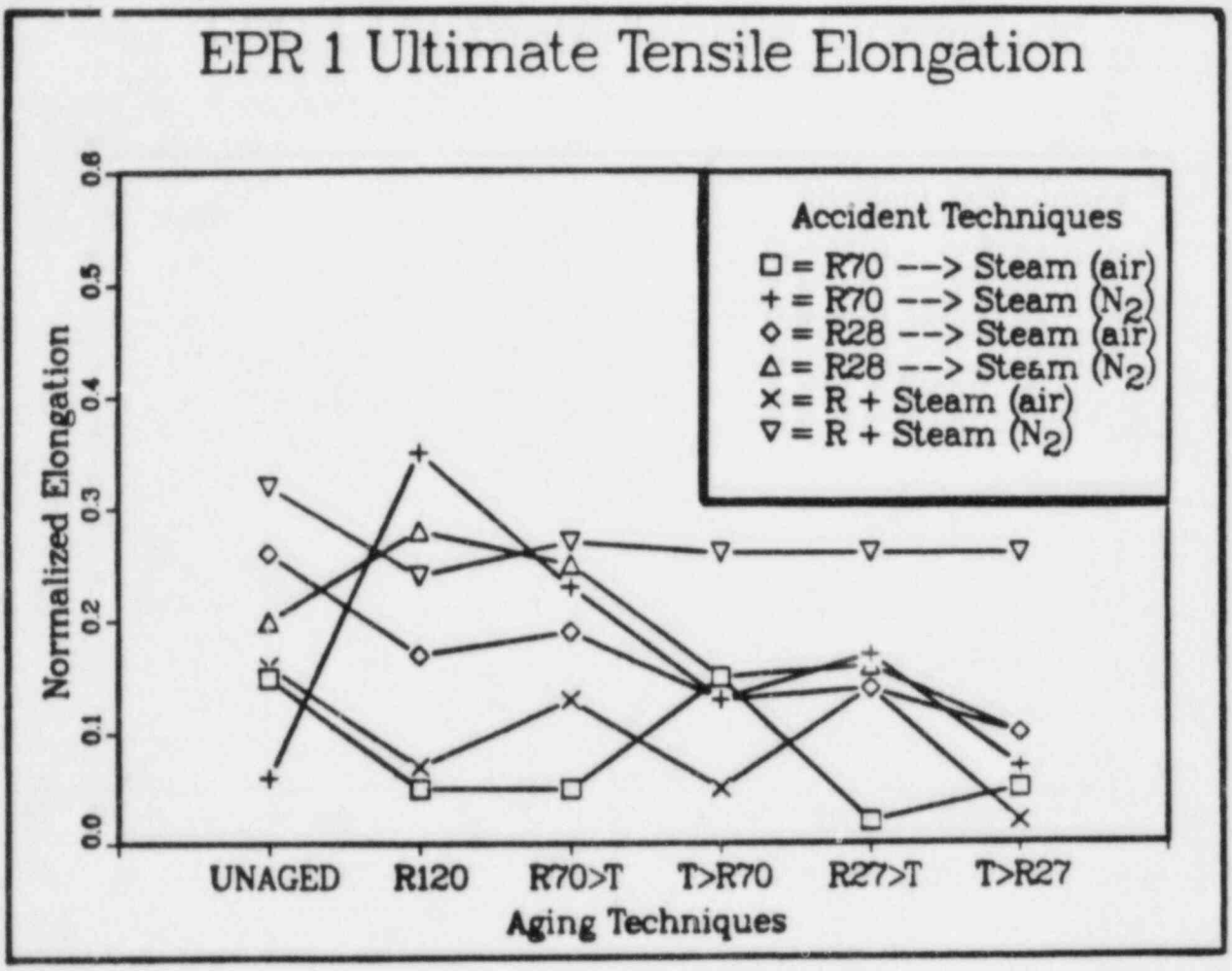

Figure 5.10: Ultimate Tensile Elongation of EPR 1 at Completion of the Accident Exposure. Sample tensile elongation divided by the initial (unaged) elongation is plotted for several aging and accident simulation techniques.

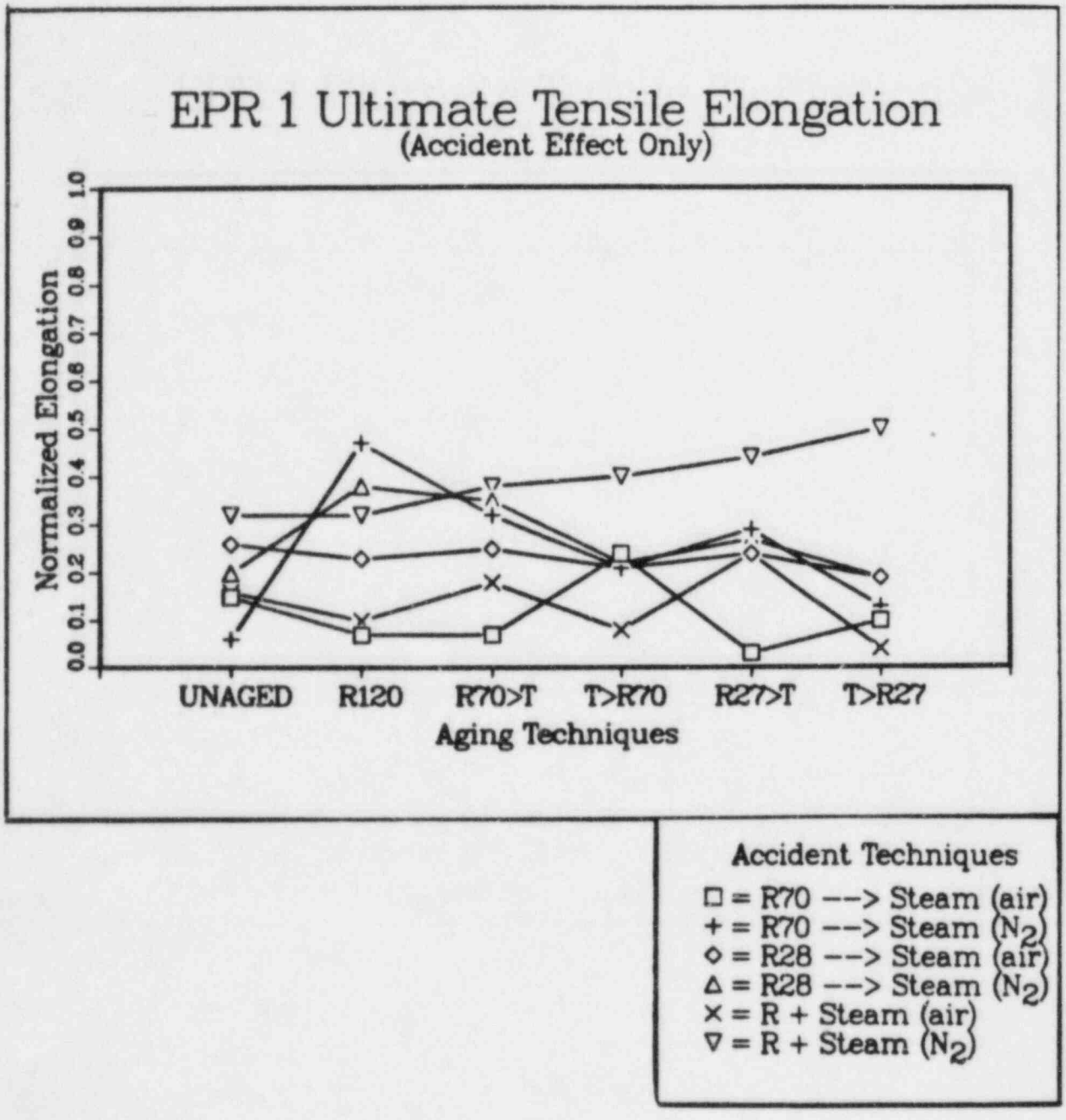

Figure 5.11: Ultimate Tensile Elongation of EPR 1 at Completion of the Accident Exposure. Sample tensile elongation divided by the after aging elongation is plotted for several aging and accident simulation techniques.

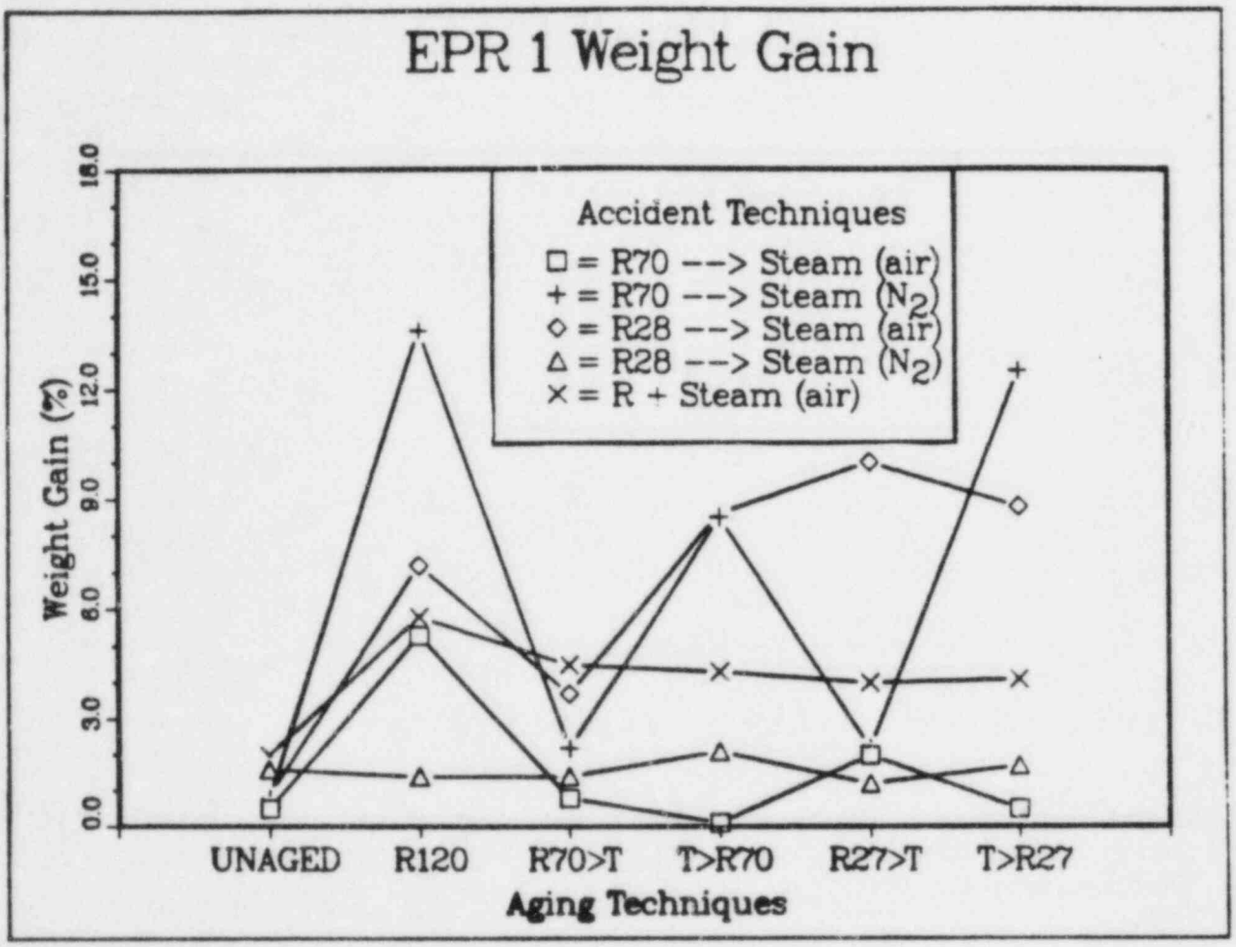

Figure 5.12: EPR 1 Weight Gain for Several Aging and Accident Simulation Techniques

e_{aging}/e_o values between 0.4 and 0.5. By completion of the accident exposure, the EPR 2 e/e_o variation was much larger, ranging from 0.03 to 0.34 (excluding the unaged samples from consideration). Figure 5.13 illustrates the e/e_o values at completion of the accident exposure. Figure 5.14 presents e/e_{aging} data. The least degrading accident exposure was the R + steam(N_2) simulation. The most degrading exposures were the R70→steam(air) and R + steam(air) simulations.

Moisture absorption data for EPR 2 is shown in Figure 5.15. The R120 aging technique generally enhances EPR 2's weight gain.

5.1.5 XLPO 1

At completion of aging XLPO 1's tensile elongation and tensile strength did not have a substantial dependence on the aging technique. Variations in results of less than 20% were noted. Figures 5.16-5.19 present tensile and weight gain data for XLPO 1. Degradation of the ultimate tensile elongation strongly depended on the accident exposure. The more severe accident exposures were the R28→steam (air), R28→steam (N_2), R + steam (N_2), and R70→steam (air). The less severe accident exposures were the R70→steam (N_2), and R + steam (air) exposures. Degradation of the ultimate tensile strength also strongly depended on the accident exposure. The most severe accident exposures were the R70→steam (air), R + steam (air), R70→steam (N_2). The least severe accident exposure was R + steam (N_2). Hence, those accident exposures which most degraded the ultimate tensile elongation were least degrading to the tensile strength and vice versa.

XLPO 1 did not absorb significant amounts of moisture during the LOCA simulation exposures (see Figure 5.19).

5.1.6 XLPO 2

At completion of aging XLPO 2's tensile elongation and tensile strength did not have a substantial dependence on the aging technique. Variations of less than 30% were observed. During accident simulations, the most degraded state for XLPO 2's ultimate tensile elongation was at the completion of the R28 and R70 accident irradiations prior to the sequential accident thermodynamic exposures (see the Appendix data for XLPO 2). Subsequent or concurrent thermodynamic exposures improved the elongation values. After the thermodynamic exposures (Figures 5.20 and 5.21), the R70→steam(air) and R28→steam(air) exposures were most severe; the R70→steam(N_2) and R28→steam(N_2) were intermediate in severity; the R + steam(N_2) and R + steam(air) were least severe. Moisture absorption data for XLPO 2 is shown in Figure 5.22.

5.1.7 TEFZEL 1

Figure 5.23 presents weight gain information for TEFZEL 1 samples. During the accident irradiations and steam exposures, TEFZEL 1 lost mass (i.e., it experienced a negative weight gain.)

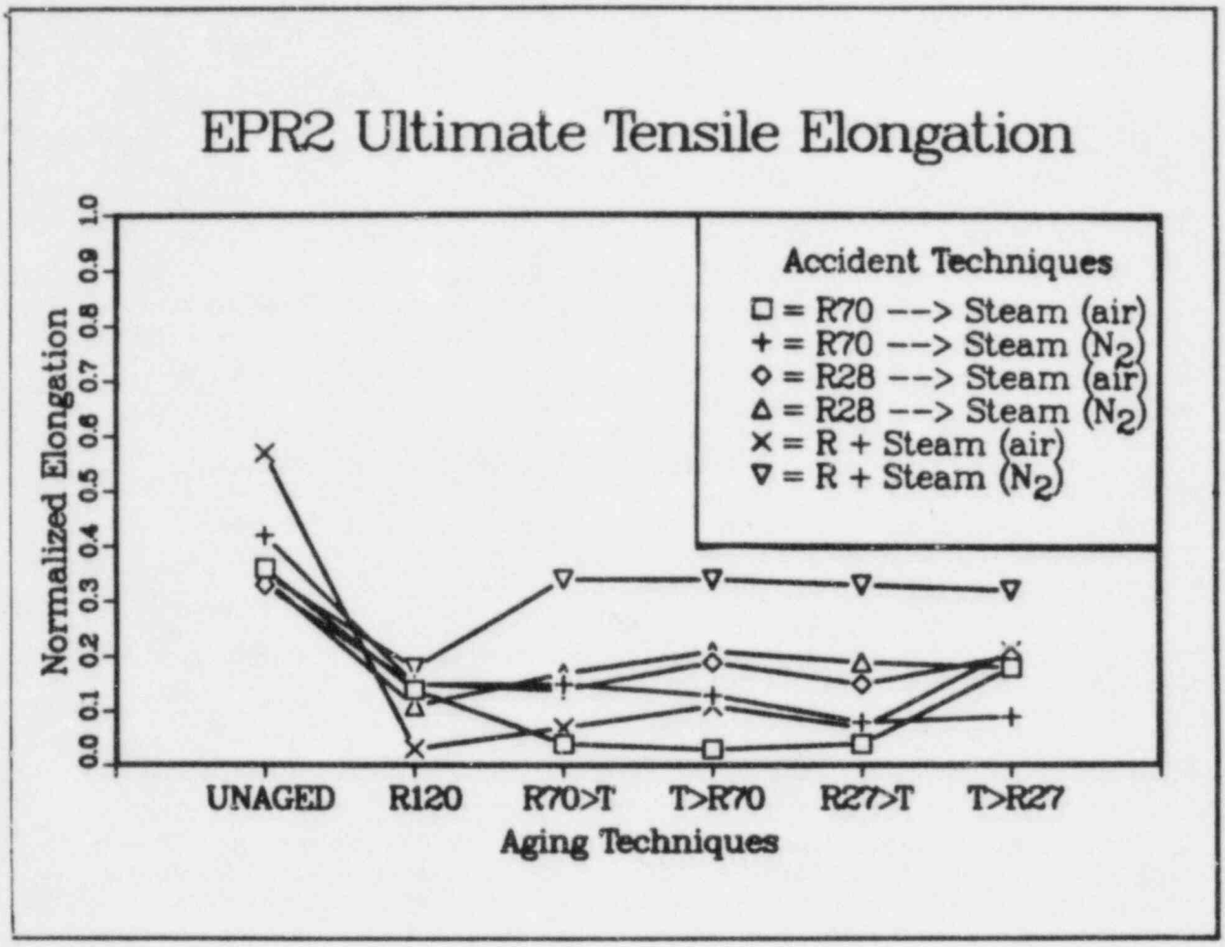

Figure 5.13: Ultimate Tensile Elongation of EPR 2 at Completion of the Accident Exposure. Sample tensile elongation divided by the initial (unaged) elongation is plotted for several aging and accident simulation techniques.

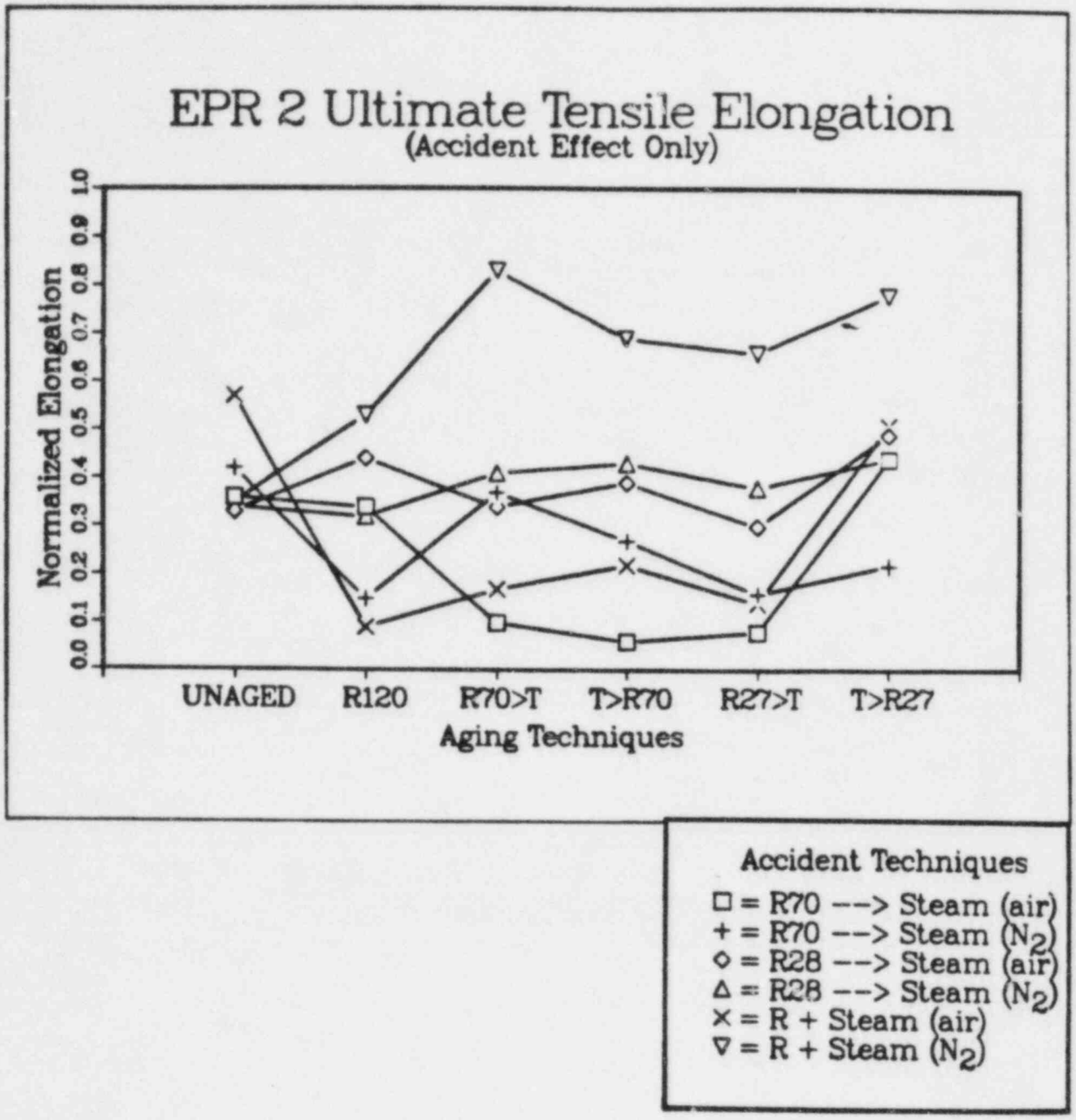

Figure 5.14: Ultimate Tensile Elongation of EPR 2 at Completion of the Accident Exposure. Sample tensile elongation divided by the after aging elongation is plotted for several aging and accident simulation techniques.

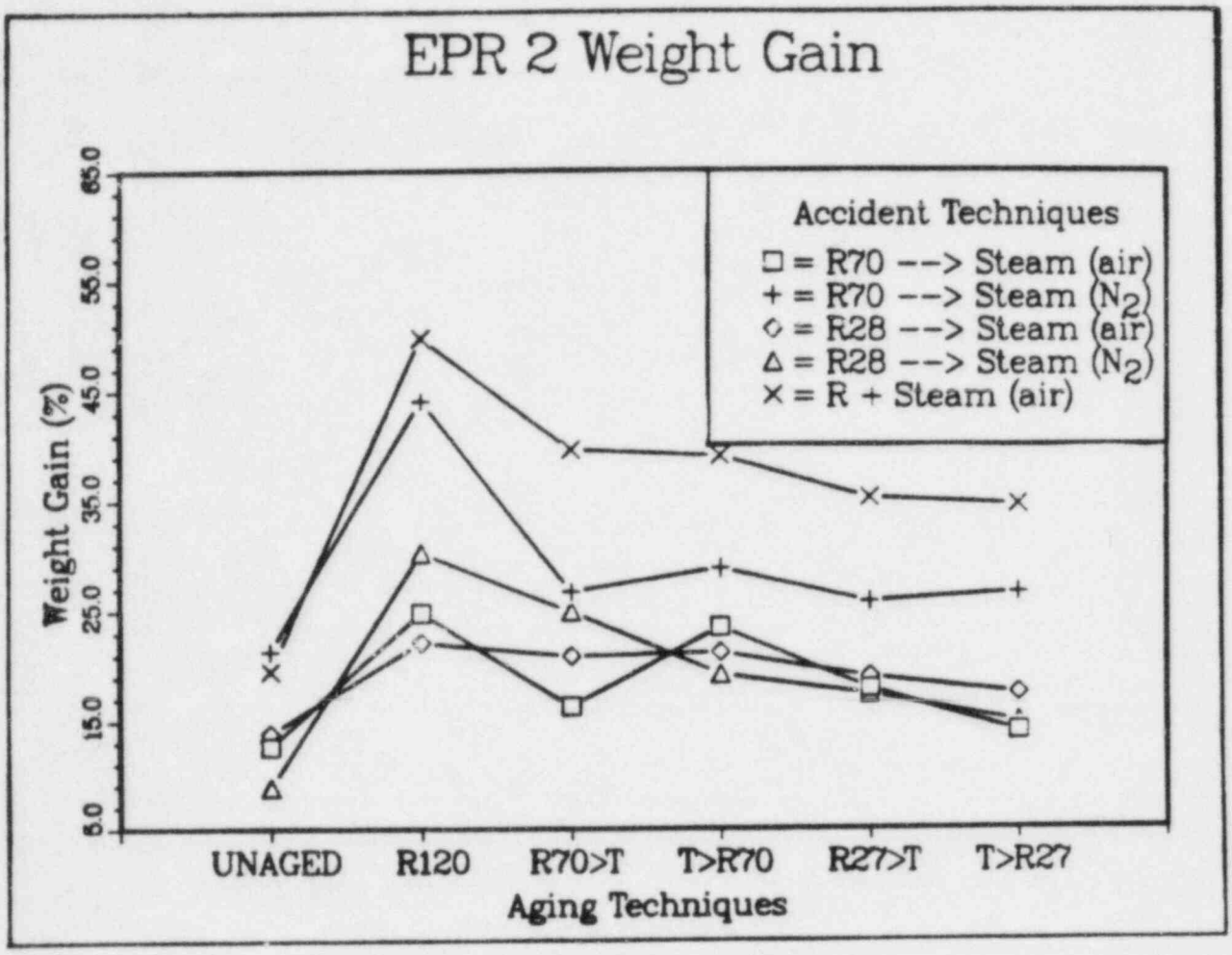

Figure 5.15: EPR 2 Weight Gain for Several Aging and Accident Simulation Techniques

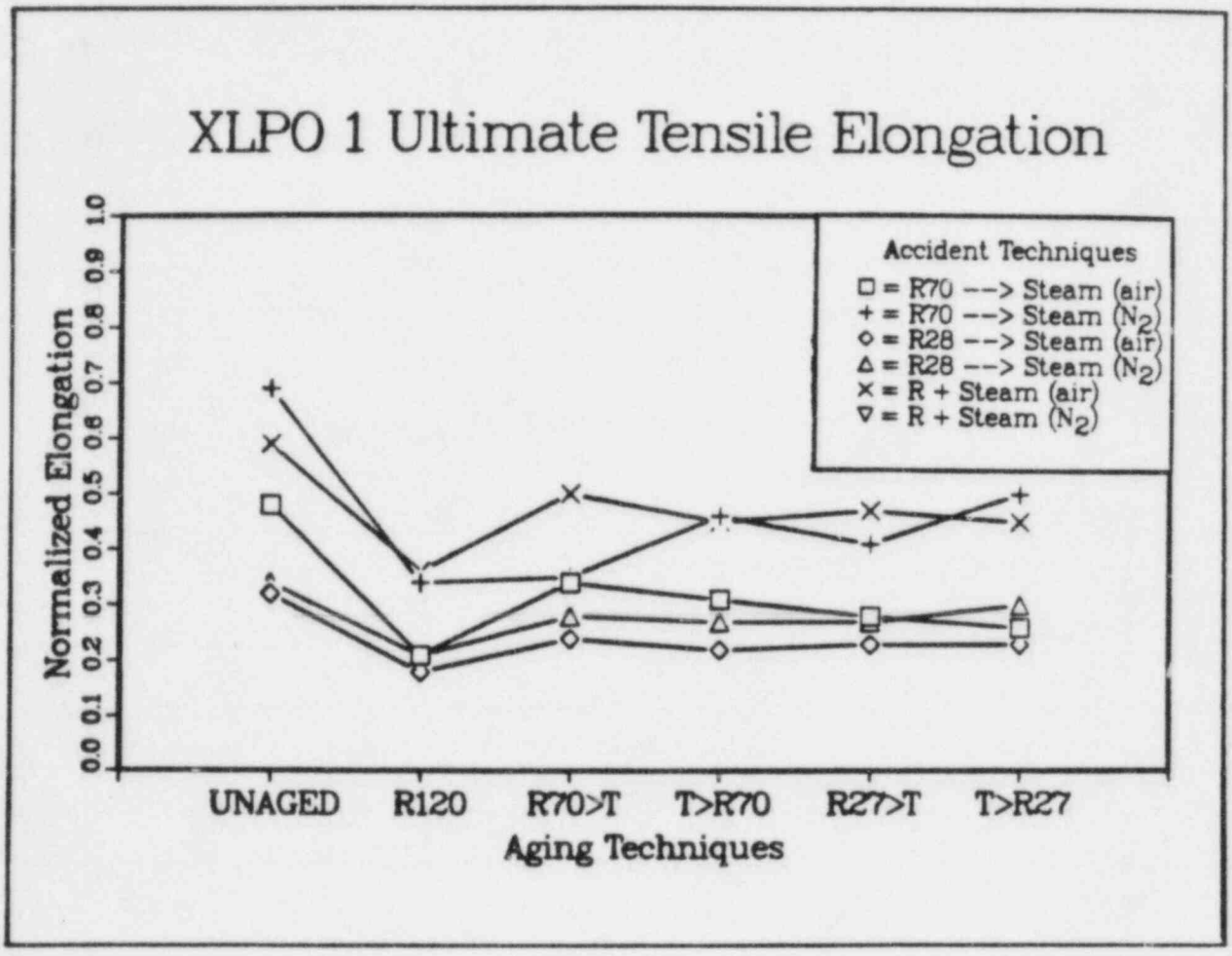

Figure 5.16: Ultimate Tensile Elongation of XLPO 1 at Completion of the Accident Exposure. Sample tensile elongation divided by the initial (unaged) elongation is plotted for several aging and accident simulation techniques.

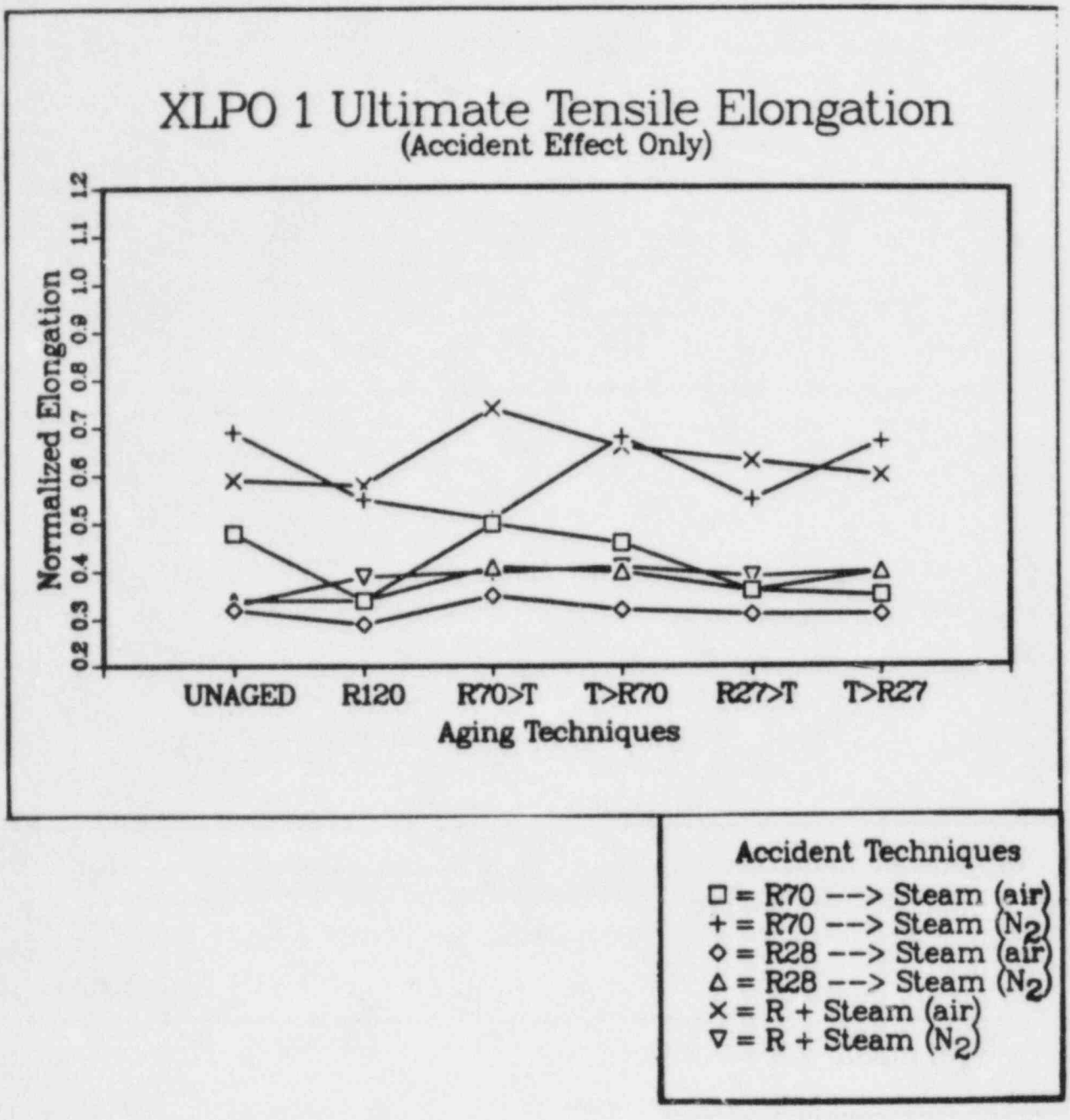

Figure 5.17: Ultimate Tensile Elongation of XLPO 1 at Completion of the Accident Exposure. Sample tensile elongation divided by the after aging elongation is plotted for several aging and accident simulation techniques.

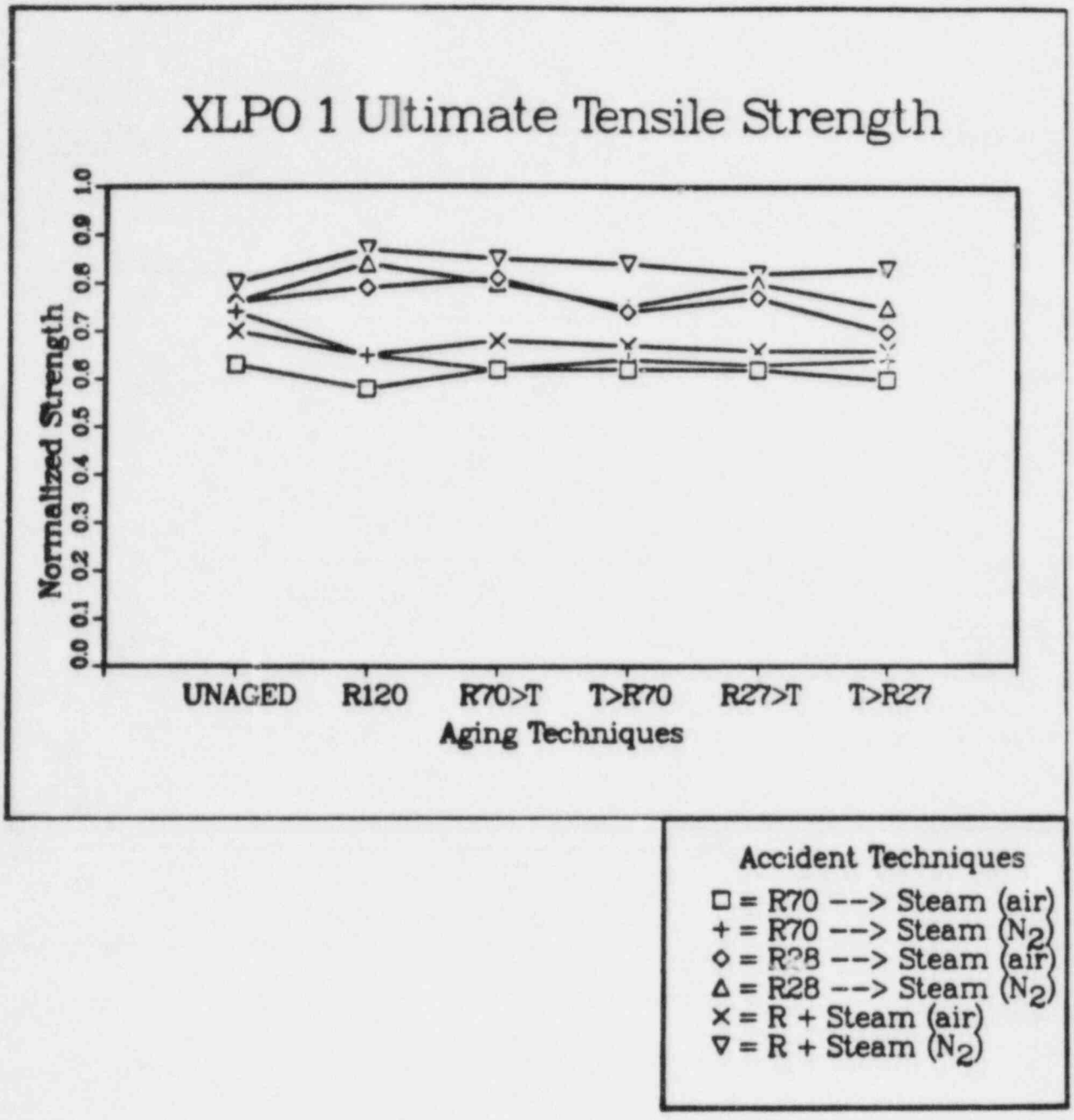

Figure 5.18: Ultimate Tensile Strength of XLPO 1 at Completion of the Accident Exposure. Sample tensile strength divided by initial (unaged) strength is plotted for several aging and accident simulation techniques.

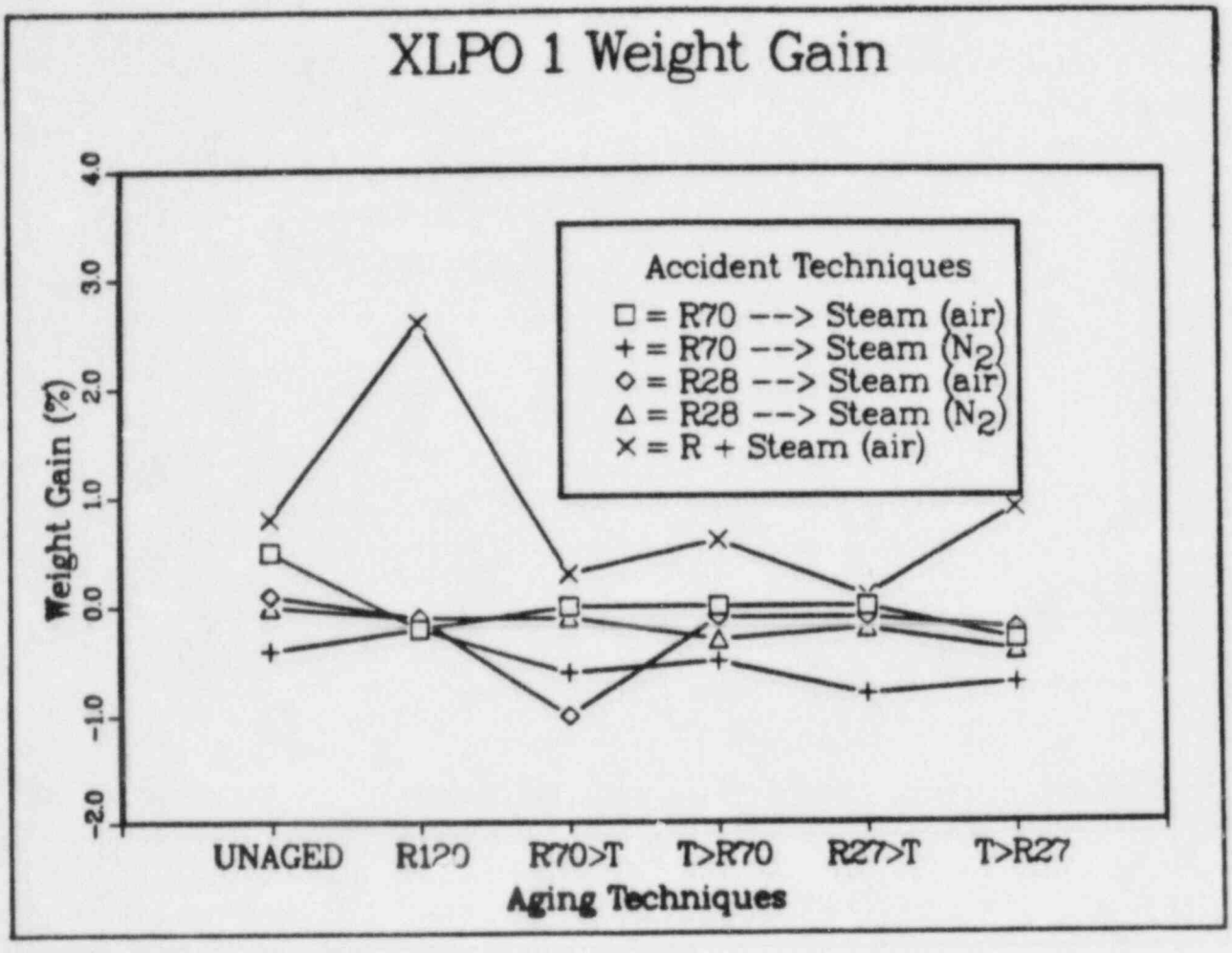

Figure 5.19: XLPO 1 Weight Gain for Several Aging and Accident Simulation Techniques

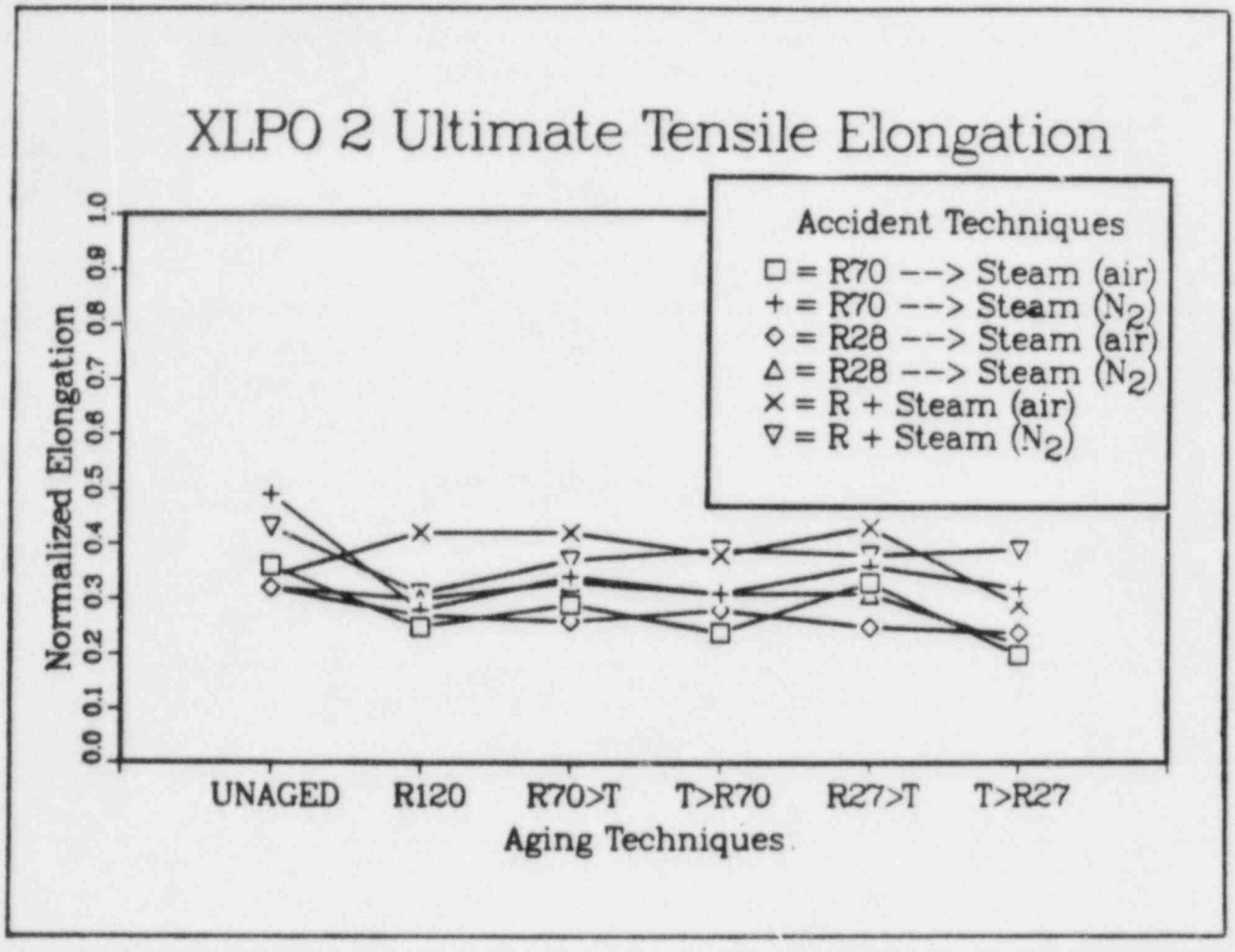

Figure 5.20: Ultimate Tensile Elongation of XLPO 2 at Completion of the Accident Exposure. Sample tensile elongation divided by the initial (unaged) elongation is plotted for several aging and accident simulation techniques.

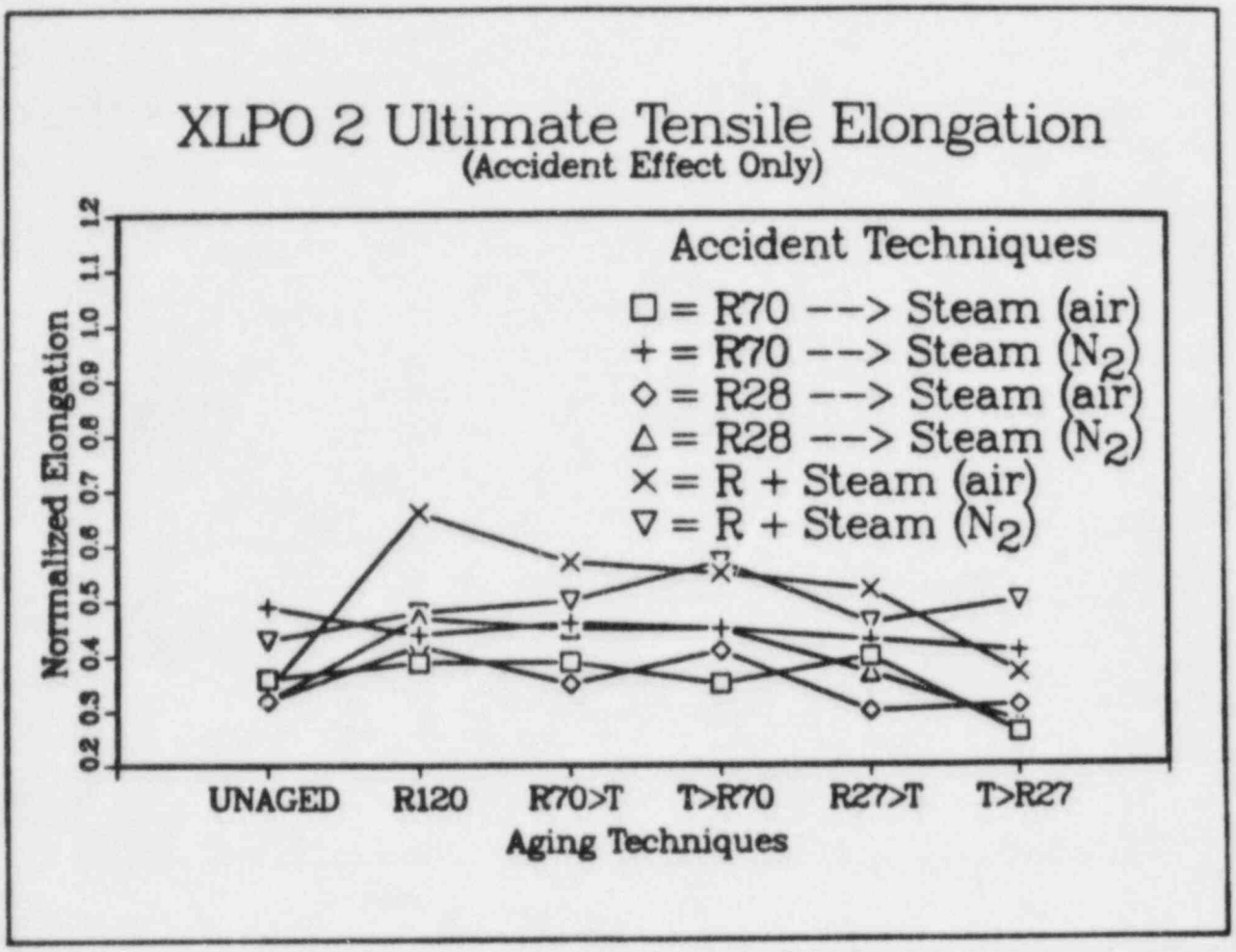

Figure 5.21: Ultimate Tensile Elongation of XLPO 2 at Completion of the Accident Exposure. Sample tensile elongation divided by the after aging elongation is plotted for several aging and accident simulation techniques.

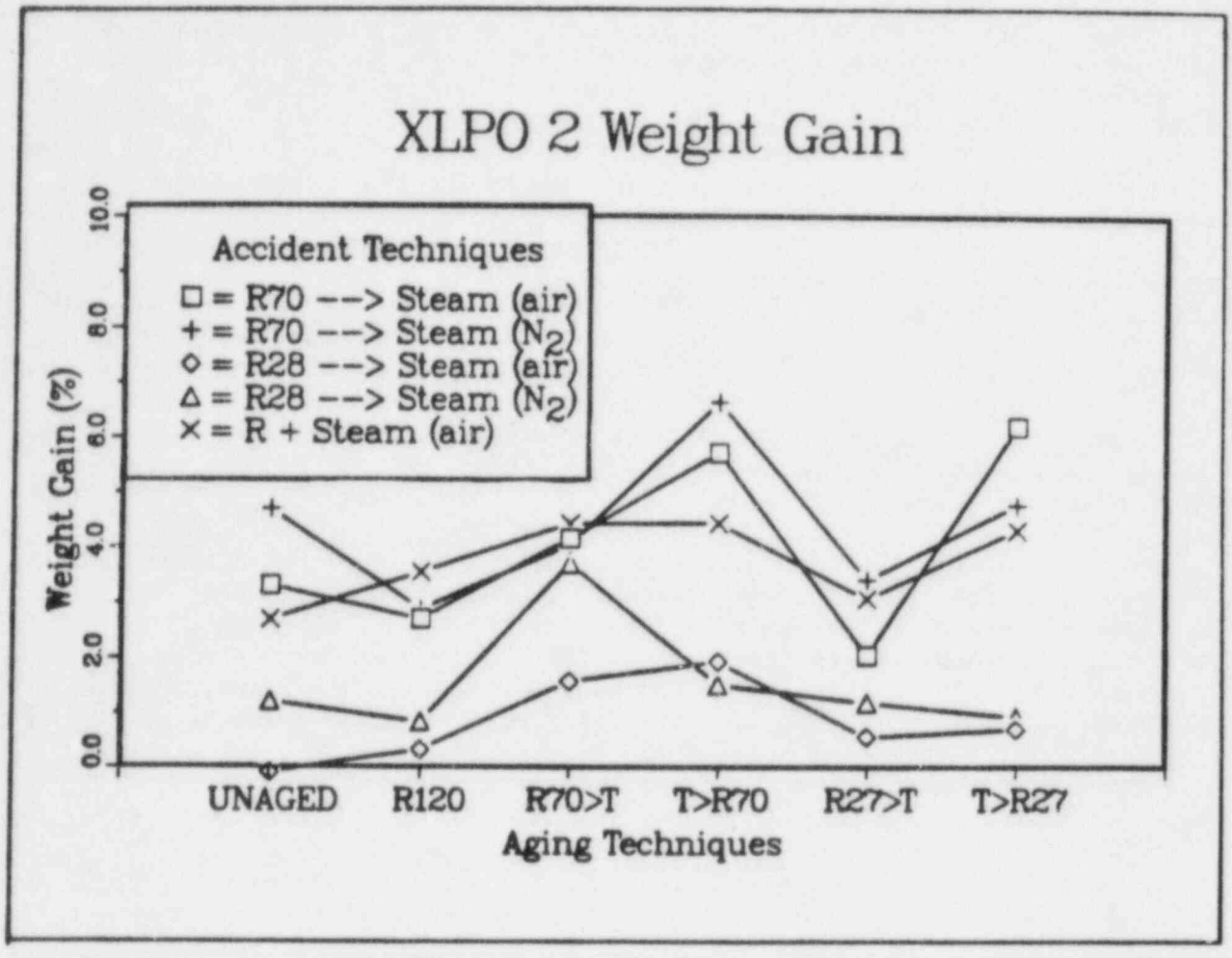

Figure 5.22: XLPO 2 Weight Gains for Several Aging and Accident Simulation Techniques

For each combination of aging and accident simulations, four TEFZEL 1 samples were successively wrapped around tubes of smaller diameter until insulation cracking or breakage was visually observed. Bend radii between 75 and 6 times the radii of the TEFZEL specimens were employed. Insulation cracking and breakage was observed to occur for a spread of bend radii. Table 5.1 illustrates the bend radii for which cracking or breakage was first observed (i.e., the largest diameter at which at least one specimen cracked.) Table 5.2 illustrates the bend radii by which all four specimens had cracked or broken. The results indicate that those accident exposures with a high temperature irradiation in an air environment more severely degraded TEFZEL 1 than did accident simulations with ambient temperature or nitrogen irradiations (i.e., R + steam (air), R70→steam (N_2), and R70→steam (air)) were more severe than R28 → steam (air), R28→steam (N_2), and R + steam (N_2).

We previously have reported evidence suggesting that the T→R aging sequences are more severe than the R→T aging sequences for TEFZEL 1 (see Reference 1). This previous conclusion is confirmed for the R + steam (N_2) accident simulations but is not generic for all accident simulation techniques.

5.1.8 TEFZEL 2

Figure 5.24 presents weight gain information for TEFZEL 2 samples. During the accident irradiations and steam exposures, TEFZEL 2 lost mass (i.e., it experienced a negative weight gain.)

For each combination of aging and accident simulations, four TEFZEL 2 samples were successively wrapped around tubes of smaller diameter until insulation cracking or breakage was visually observed. Bend radii between 75 and 6 times the radii of the TEFZEL specimens were employed. Insulation cracking and breakage was observed to occur for a spread of bend radii. Table 5.3 indicates the bend radii for which cracking or breakage was first observed (i.e., the largest diameter at which at least one specimen cracked.) Table 5.4 indicates the bend radii by which all four specimens had cracked or broken.

For TEFZEL 2, the R + steam (air) accident exposure caused all TEFZEL 2 samples (both aged and unaged) to crack when subjected to a 75x bend test. For other accident exposure techniques, the TEFZEL 2 degradation depended on the aging technique. The R120, R70→120, and the 120→R70 aging techniques were generally more severe than the R27→120 and the 120→R27 sequences.

5.1.9 U.S. Compression Set Tests

Our compression set tests employed compression samples with thicknesses ~.18 cm. As mentioned in Section 3.3.3.1, this thickness represents actual use conditions but produces large uncertainties in the

value of compression set, C:

$$C = \frac{t_o - t_i}{t_o - t_n}$$

where t_o = original thickness

t_i = final thickness

t_n = compressed thickness.

We predict our absolute uncertainties for C to exceed .10.

Tables 5.5 - 5.9 present our compression set test results. After aging data from Reference 1 is also provided. Aging and accident exposures substantially increase the compression set. Because of our absolute uncertainty of $\pm$ .10, we do not note meaningful differences between alternative aging and accident simulations.

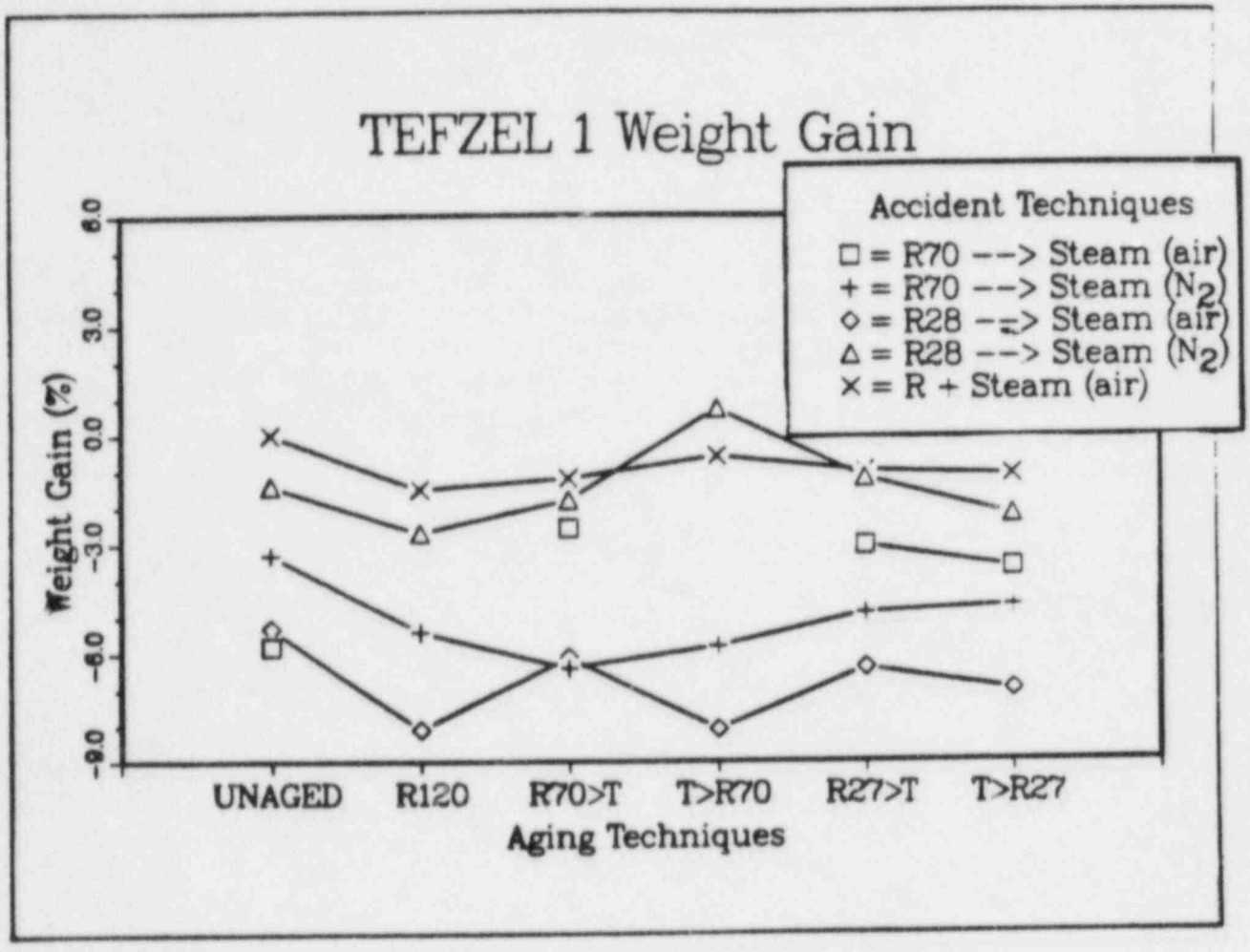

Figure 5.23: TEFZEL 1 Weight Gain for Several Aging and Accident Simulation Techniques

Table 5.1

TEFZEL 1: Largest Bend Radii At Which One Sample Cracked. Table entries are expressed as multiples of the TEFZEL 1 sample radius.

	ACCIDENT SIMULATIONS					
	R70→ST(AIR)	R70→ST(N_2)	R28→ST(AIR)	R28→ST(N_2)	R + ST(AIR)	R + ST(N_2)
UNAGED	75.00	75.00	44.00	11.00	75.00	
R120	75.00	75.00	75.00		75.00	75.00
R70→120	75.00	75.00	75.00	75.00	75.00	50.00
120→R70	75.00	75.00	56.00	50.00	75.00	75.00
R27→120	75.00	75.00	75.00	75.00	75.00	31.00
120→R27	75.00	75.00	75.00	75.00	75.00	75.00

Table 5.2

TEFZEL 1: Bend Radii By Which All Samples Cracked. Table entries are expressed as multiples of the TEFZEL 1 sample radius.

	ACCIDENT SIMULATIONS					
	R70→ST(AIR)	R70→ST(N_2)	R28→ST(AIR)	R28→ST(N_2)	R + ST(AIR)	R + ST(N_2)
UNAGED	69.00	75.00	11.00	6.00	69.00	
R120	75.00	75.00	75.00		75.00	75.00
R70→120	75.00	75.00	69.00	50.00	75.00	44.00
120→R70	75.00	75.00	44.00	31.00	75.00	69.00
R27→120	75.00	75.00	44.00	75.00	75.00	22.00
120→R27	75.00	75.00	75.00	75.00	75.00	56.00

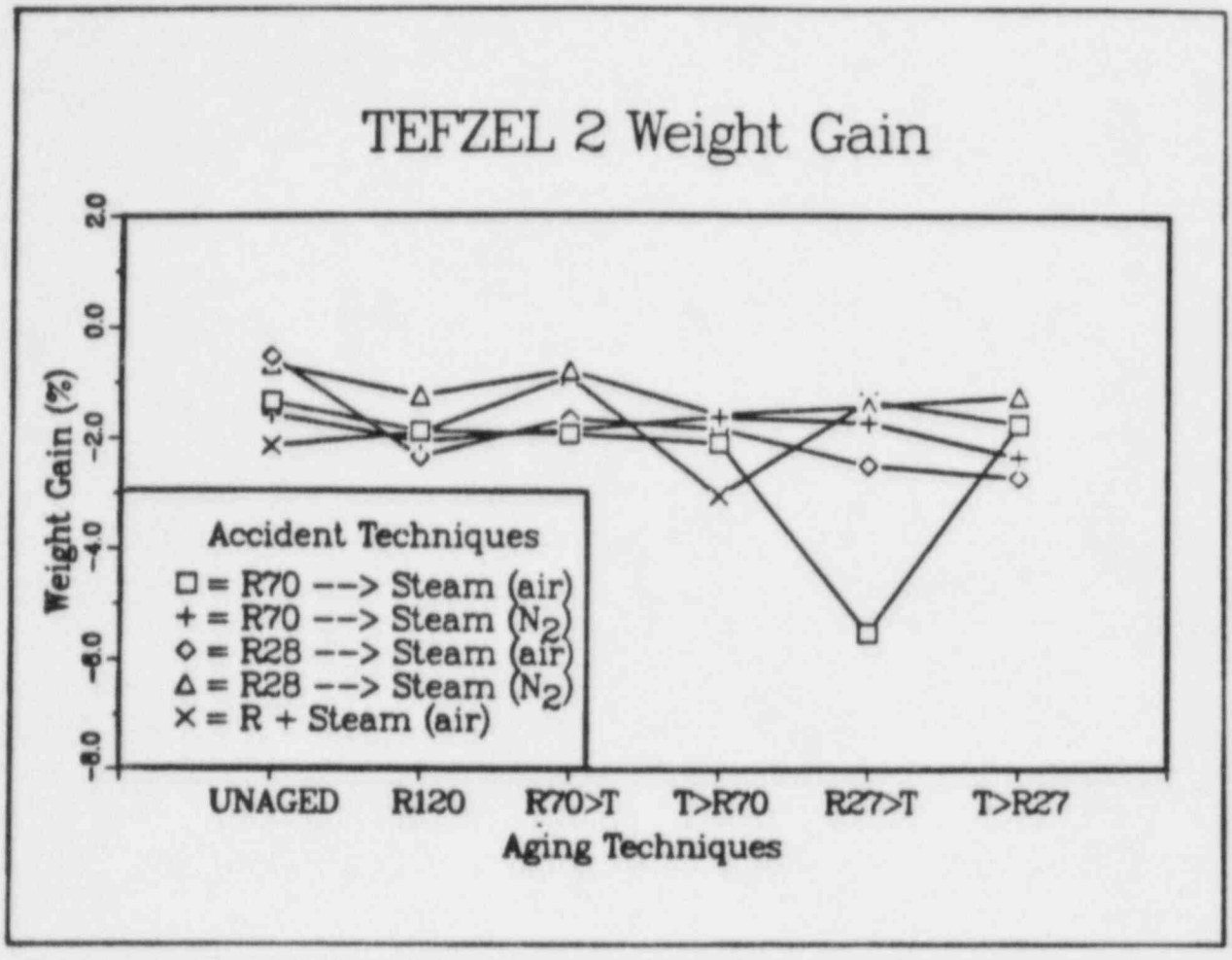

Figure 5.24: TEFZEL 2 Weight Gain for Several Aging and Accident Simulation Techniques

Table 5.3

TEFZEL 2: Largest Bend Radii At Which One Sample Cracked. Table entries are expressed as multiples of the TEFZEL 2 sample radius.

	ACCIDENT SIMULATIONS					
	R70→ST(AIR)	R70→ST(N_2)	R28→ST(AIR)	R28→ST(N_2)	R + ST(AIR)	R + ST(N_2)
UNAGED	11.00	6.00			75.00	
R120	75.00	75.00	75.00	75.00	75.00	75.00
R70→120	75.00	75.00	75.00	75.00	75.00	75.00
120→R70	75.00	75.00	75.00	75.00	75.00	75.00
R27→120	22.00	44.00	22.00	22.00	75.00	44.00
120→R27	75.00	31.00	22.00	31.00	75.00	69.00

Table 5.4

TEFZEL 2: **Bend Radii By Which All Samples Cracked.** Table entries are expressed as multiples of the TEFZEL 2 sample radius.

	ACCIDENT SIMULATIONS					
	R70→ST(AIR)	R70→ST(N_2)	R28→ST(AIR)	R28→ST(N_2)	R + ST(AIR)	R + ST(N_2)
UNAGED	6.00	6.00			75.00	
R120	75.00	75.00	75.00	75.00	75.00	75.00
R70→120	75.00	75.00	44.00	75.00	75.00	56.00
120→R70	22.00	75.00	75.00	56.00	75.00	75.00
R27→120	11.00	11.00	11.00	11.00	75.00	22.00
120→R27	22.00	11.00	11.00	22.00	75.00	44.00

Table 5.5

Permanent Set After Compression, c, for U.S. EPR A
Errors reflect ± σ for four samples. Absolute error is ± .10

	Aging Technique			
	R27→120	120→R27	R120	Unaged
After Aging (Data from Ref 1)	#13 = .67±.02 #14 = .67±.03	#20 = .68±.04 #50 = .79±.06	#32 = .74±.03	#38 = .09±.01
After Accident Exposures L7: R27	#3 = .86±.01		#29 = .92±.01	#25 = .79±.03
L7: R27→ Steam(air)	#4 = .88±.01	#18 = .88±.01	#30 = .94±.01	#26 = .80±.02
L9: R + Steam(air)	#9 = .80±.01	#19 = .82±.02		#16 = .75±.04
L10: R + Steam (N_2)				#15 = .73±.03
No Accident Exposure (Measured with Accident Specimens				#28 = .08±.02 #39 = .10±.02 #40 = .09±.03 #46 = .07±.03

Table 5.6

Permanent Set After Compression, c, for U.S. EPR B
Errors reflect ± σ for four samples. Absolute error is ± .10

	Aging Technique			
	R27→120	120→R27	R120	Unaged
After Aging (Data from Ref 1)	#13 = .96±.03 #14 = .98±.03	#20 = .91±.02 #50 = .95±.01	#32 = 1.0	#38 = .11±.02
After Accident Exposures L7: R27	#3 = .86±.01		#29 = 1.02±.01	#25 = .95±.01
L7: R27→ Steam(air)	#4 = 1.02±.02	#18 = 1.01±.01	#30 = 1.05±.01	#26 = .98±.01
L9: R + Steam(air)	#9 = 1.02±.01	#19 = 1.01±.02		#16 = 1.00±.01
L10: R + Steam (N_2)				#15 = .96±.01
No Accident Exposure (Measured with Accident Specimens				#28 = .15±.02 #39 = .12±.02 #40 = .13±.01 #46 = .11±.02

Table 5.7

Permanent Set After Compression, c, for U.S. BUNA N
Errors reflect ± σ for four samples. Absolute error is ± .10

	Aging Technique			
	R27→120	120→R27	R120	Unaged
After Aging (Data from Ref 1)	#13 = .63±.01 #14 = .59±.02	#20 = .68±.02 #50 = .71±.02	#32 = .68±.01	#38 = .07±.01
After Accident Exposures L7: R27	#3 = .82±.02		#29 = .88±.01	#25 = .62±.02
L7: R27→ Steam(air)	#4 = .87±.01	#18 = .88±.01	#30 = .88±.01	#26 = .79±.02
L9: R + Steam(air)	#9 = .81±.05	#19 = .85±.01		#16 = .72±.01
L10: R + Steam (N_2)				#15 = .71±.01
No Accident Exposure (Measured with Accident Specimens				#28 = .11±.02 #39 = .09±.01 #40 = .11±.01 #46 = .10±.01

Table 5.8

Permanent Set After Compression, c, for U.S. SILICONE
Errors reflect ± σ for four samples. Absolute error is ± .10

	Aging Technique			
	R27→120	120→R27	R120	Unaged
After Aging (Data from Ref 1)	#13 = .83±.03 #14 = .86±.01	#20 = .72±.01 #50 = .81±.01	#32 = 1.0	#38 = .07±.03
After Accident Exposures L7: R27	#3 = .95±.01		#29 = 1.04±.02	#25 = .90±.01
L7: R27→ Steam(air)	#4 = 1.01±.02	#18 = .99±.01	#30 = 1.05±.02	#26 = 1.02±.02
L9: R + Steam(air)	#9 = .98±.02	#19 = .98±.01		#16 = .96±.02
L10: R + Steam (N_2)				#15 = .92±.01
No Accident Exposure (Measured with Accident Specimens				#28 = .11±.01 #39 = .09±.02 #40 = .11±.02 #46 = .08±.01

Table 5.9

Permanent Set After Compression, c, for U.S. VITON
Errors reflect ± σ for four samples. Absolute error is ± .10

	Aging Technique			
	R27→120	120→R27	R120	Unaged
After Aging (Data from Ref 1)	#13 = .88±.01 #14 = .89±.01	#20 = .80±.01 #50 = .83±.02	#32 = .97±.02	#38 = .17±.01
After Accident Exposures L7: R27	#3 = .97±.01		#29 = 1.02±.01	#25 = .96±.02
L7: R27→ Steam(air)	#4 = 1.00±.01	#18 = .95±.01	#30 = 1.02±.01	#26 = .96±.02
L9: R + Steam(air)	#9 = 1.01±.03	#19 = .96±.01		#16 = .96±.01
L10: R + Steam (N_2)				#15 = .92±.01
No Accident Exposure (Measured with Accident Specimens				#28 = .18±.01 #39 = .18±.01 #40 = .18±.02 #46 = .14±.01

5.2 French Samples

5.2.1 PRC (82I1)

At completion of aging, PRC's tensile properties depended on the aging sequence. The two R→T aging sequences resulted in a 90% decrease in the ultimate tensile elongation. In contrast, the two T→R aging sequences produced only a 28% decrease in ultimate tensile elongation. Figure 5.25 illustrates these aging results; ultimate tensile elongation data at completion of various phases of the accident simulations is also presented. No matter which aging simulation method was used, the simultaneous accident simulation (R + LOCA(air)) consistently yielded severe degradation. (The tabular presentation of the data in the Appendix allows for additional resolution of the data.) For the unaged samples corresponding to the start of reactor operation, the LOCA→R70 accident simulation technique was least degrading.

Figure 5.26 presents the influence of the accident exposure on the after aging elongation values; i.e., the e/e_{aging} values are plotted. The effect of the R70→LOCA(air) and the R28→LOCA(air) accident simulations was more pronounced for those samples least degraded at completion of aging (i.e., the T→R aging sequences) and less pronounced for those samples most degraded at the completion of aging. Hence for PRC, the R→LOCA(air) accident simulations partially compensated for sequencing effects originally observed at completion of aging.

5.2.2 EPDM (82I2)

At the completion of aging, the two R→T aging simulation techniques had caused significantly more degradation than did the two T→R aging techniques. The ultimate tensile elongation at completion of the R→T aging simulations was no more than 1% of the value for a nonaged sample, whereas after the T→R70 and T→R27 aging simulations the elongation value was still 34% and 49% of the initial unaged value. These results are illustrated in Figure 5.27; the effect of various phases of the accident simulations is also illustrated. Figure 5.28 presents the influence of the accident exposure on the after aging elongation values; i.e., the e/e_{aging} values are plotted. In Figure 5.28 results are only plotted for the two T→R aging sequences since at completion of the R→T aging sequences the elongation was sufficiently deteriorated for it to be impossible to judge the effects of the various phases of the accident simulation.

For unaged and samples aged by T→R techniques, the LOCA→R70 accident simulation results in elongation degradation less significant than that caused by the other accident simulations. The R + LOCA(air) and R70→LOCA(air) accident simulations caused severe degradation of the EPDM samples, regardless of the aging simulation technique.

The degradation of these EPDM materials also depended on the accident irradiation temperature. Both unaged and samples aged by the T→R70 technique experienced more degradation during the R70→LOCA(air)

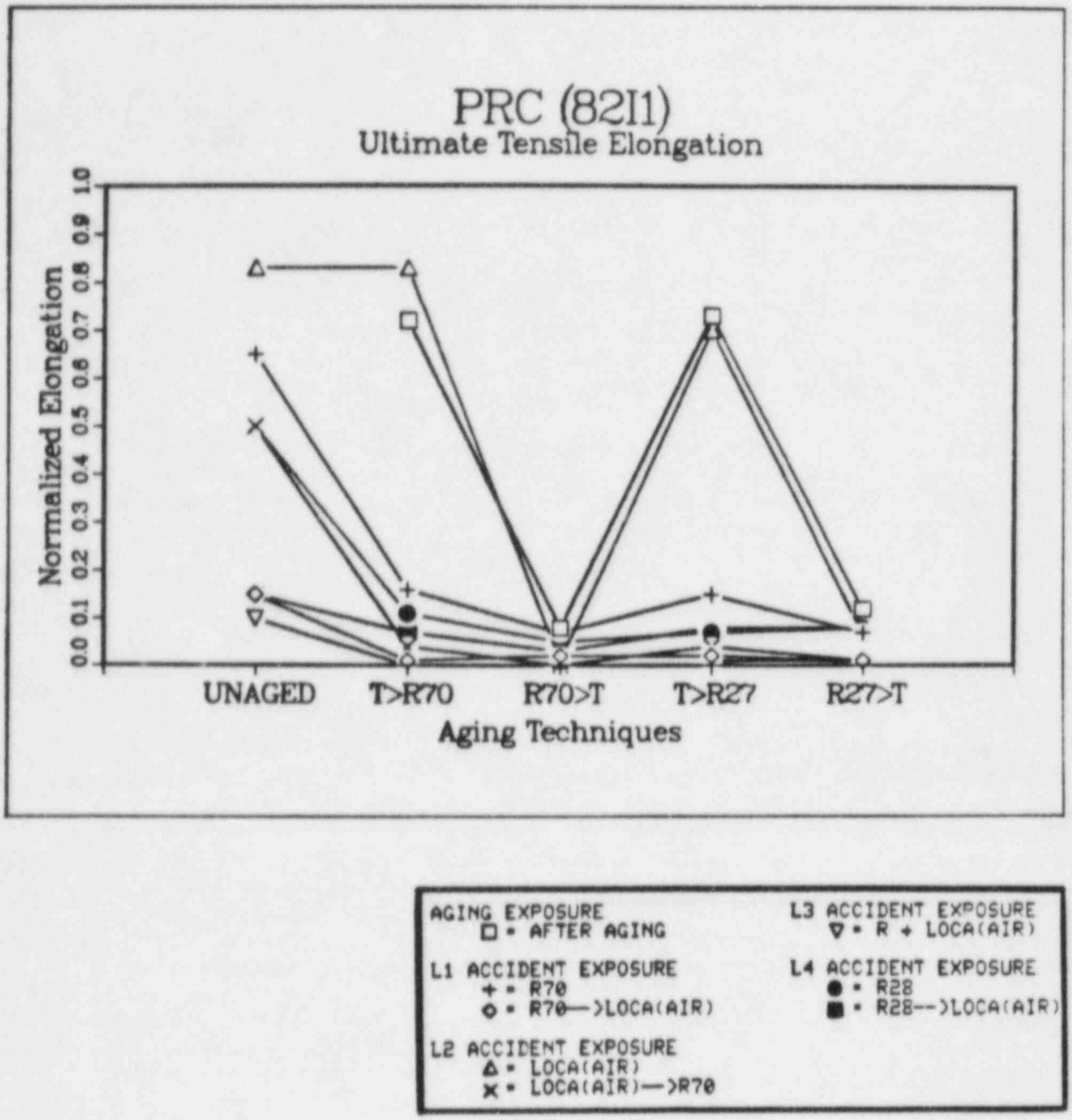

Figure 5.25: Ultimate Tensile Elongation of PRC (82I1) at Completion of Various Phases of the Accident Exposure. Sample tensile elongation divided by the initial (unaged) elongation is plotted for several aging and accident simulation techniques.

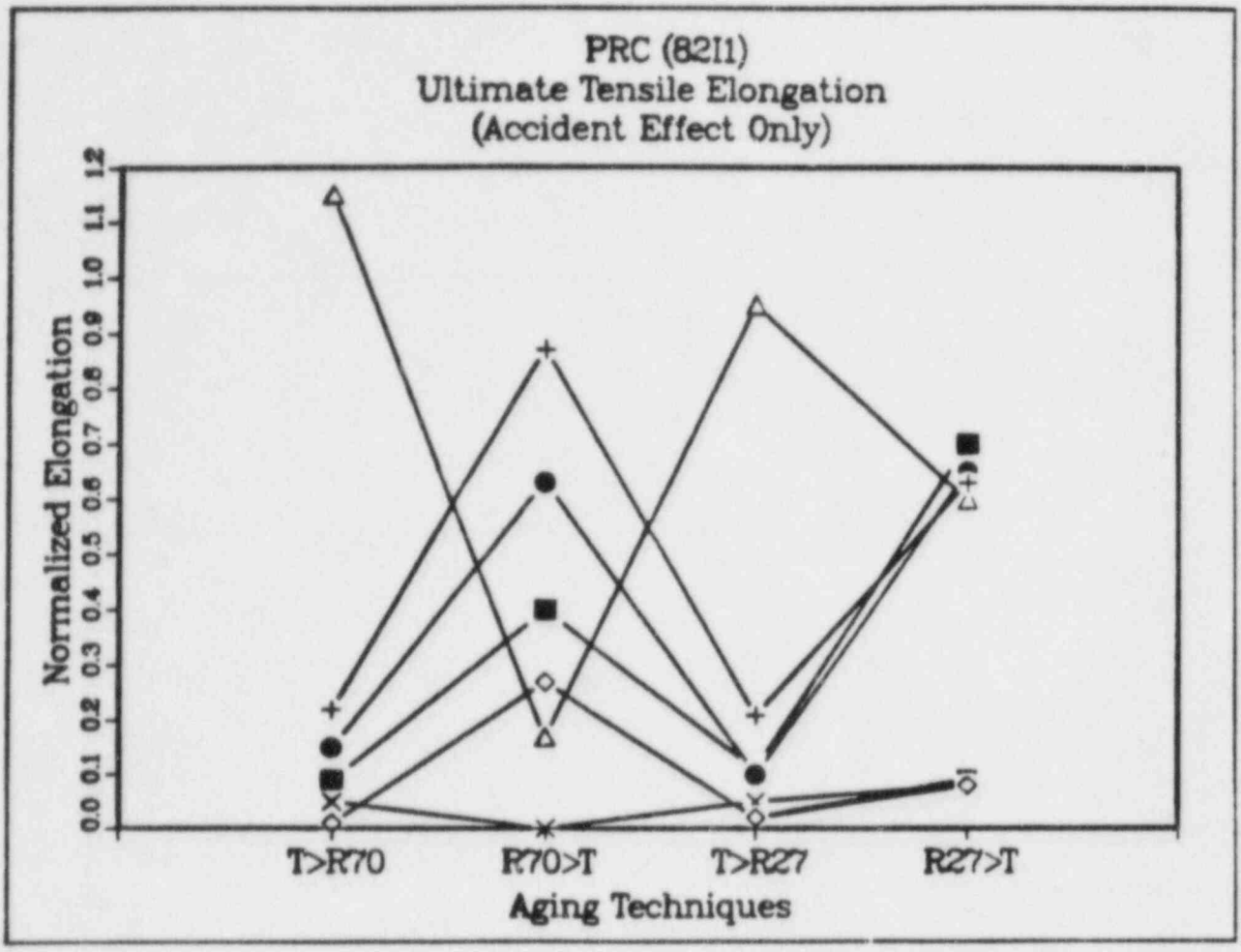

Figure 5.26: Ultimate Tensile Elongation of PRC (8211) at Completion of Various Phases of the Accident Exposure. Sample tensile elongation divided by the after aging elongation is plotted for several aging and accident simulation techniques.

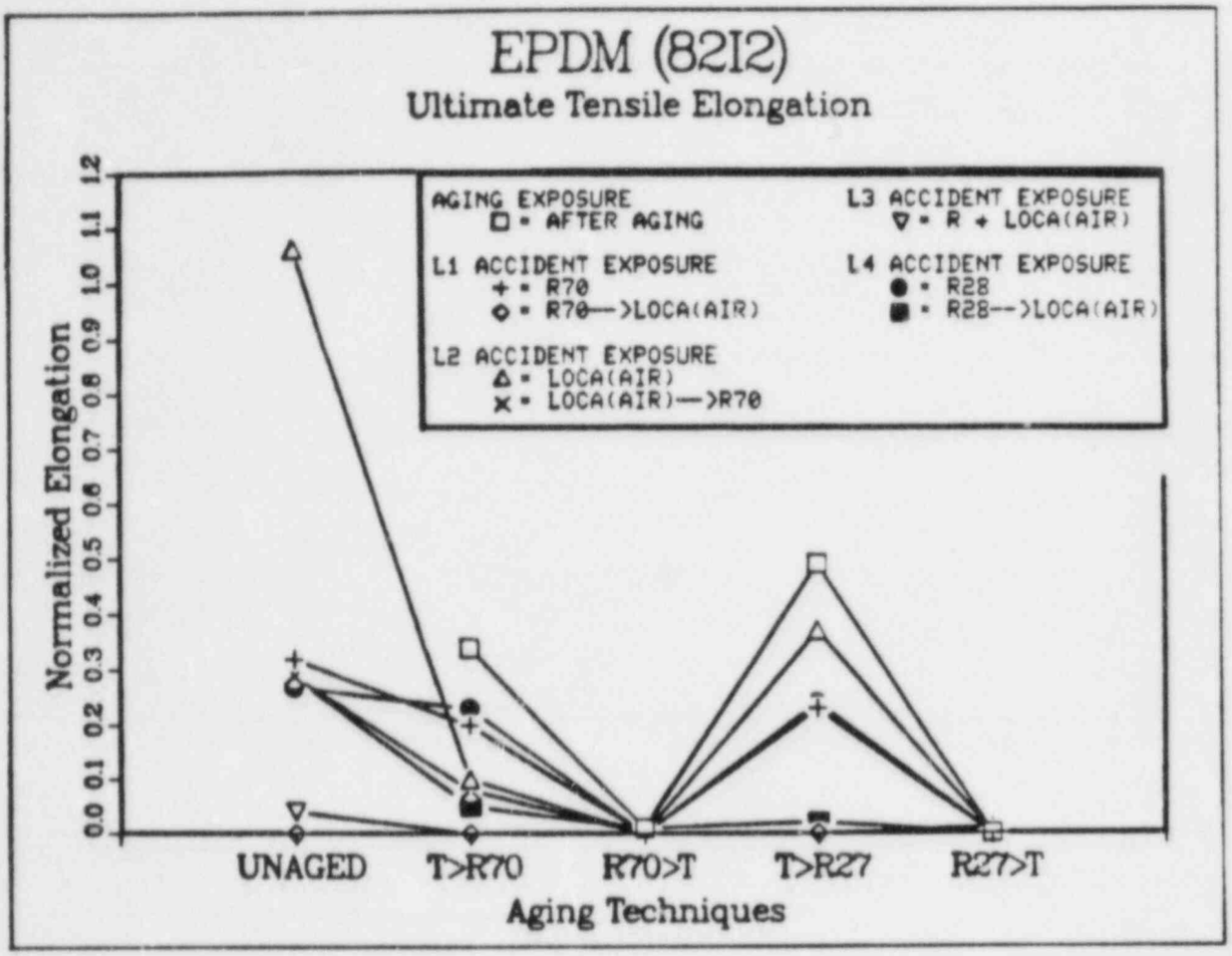

Figure 5.27: Ultimate Tensile Elongation of EPDM (8212) at Completion of Various Phases of the Accident Exposure. Sample tensile elongation divided by the initial (unaged) elongation is plotted for several aging and accident simulation techniques.

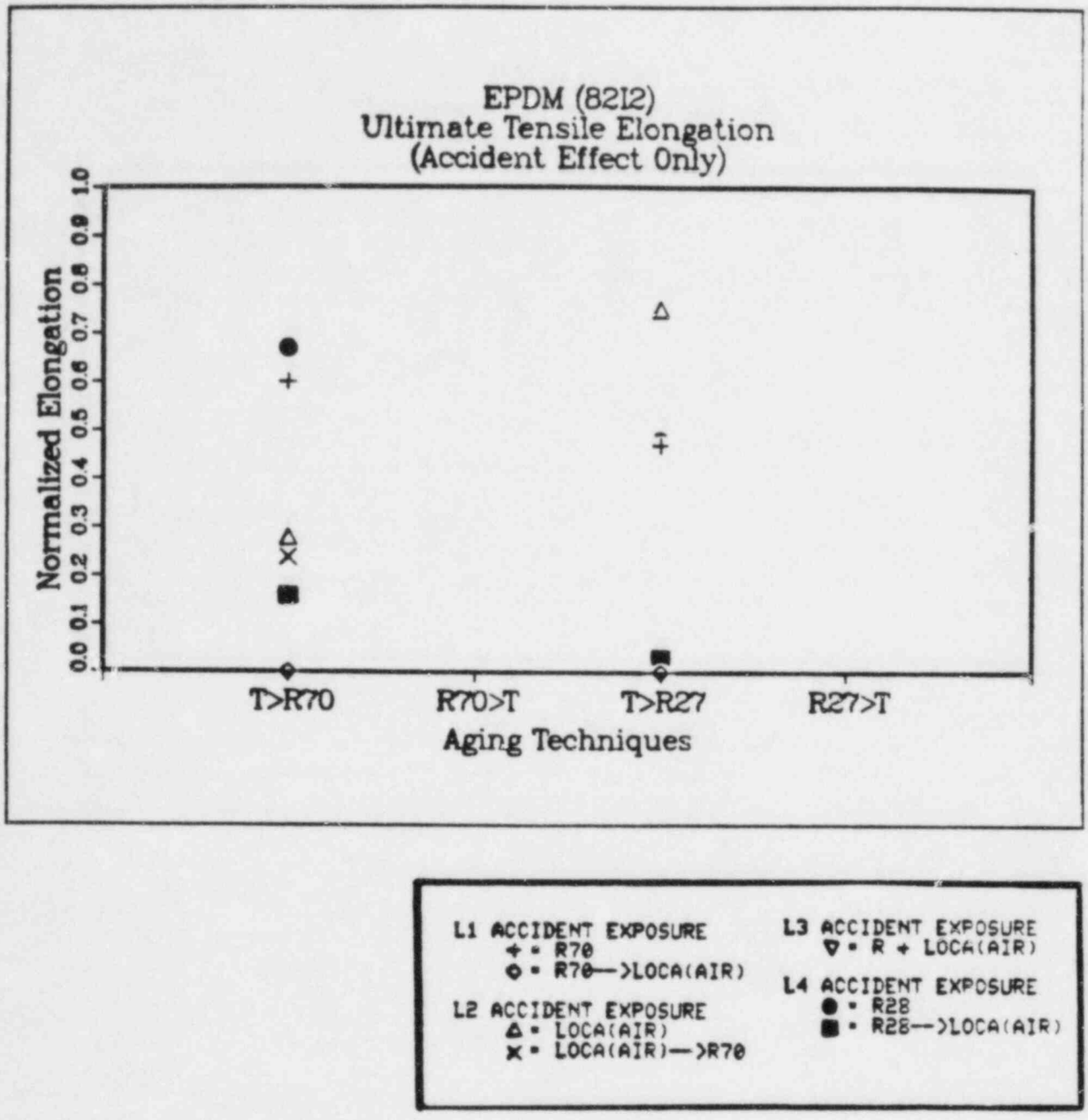

Figure 5.28: Ultimate Tensile Elongation of EPDM (82I2) at Completion of Various Phases of the Accident Exposure. Sample tensile elongation divided by the after aging elongation is plotted for several aging and accident simulation techniques.

accident simulation than they did during the R28→LOCA(air) accident simulation. The effect of accident irradiation temperature was less pronounced for samples preconditioned by the T→R28 aging technique.

5.2.3 Fire-proof EPDM (82I9)

At completion of aging, the R→T aging techniques had decreased the tensile properties of fire-proof EPDM more than had the reverse order techniques, i.e., T→R. After the T→R aging simulations the ultimate tensile elongation was still 34% of its initial unaged value, whereas, after the R→T aging simulations this property was only 13% of its initial unaged value. These results are illustrated in Figure 5.29; the effect of various phases of the accident simulations is also illustrated. Figure 5.30 presents the influence of the accident exposure on the after aging elongation values; i.e., the e/e_{aging} values are plotted.

Tensile elongation data for fire-proof EPDM indicates that the less severe accident simulations were the LOCA(air)→R70 and the R28→LOCA(air) techniques. The most severe technique was the simultaneous accident exposure (R + LOCA(air)). After this accident simulation, the elastomer samples were very hard and brittle. Figure 5.30 clearly shows that the R70→LOCA(air) simulation was more severe than the LOCA(air)→R70 simulation. Figure 5.30 also demonstrates that the accident irradiation temperature influenced tensile properties. The R70→LOCA(air) simulation was more severe than the R28→LOCA(air) simulation.

5.2.4 VAMAC (82H3 and 82J3)

VAMAC was tested both as tensile dumbbells and as O-rings. Hence we report both ultimate tensile properties and values for permanent set after compression. Ultimate tensile elongation results are plotted in Figures 5.31 and 5.32; permanent set after compression values are presented in Figure 5.33. As for all materials, the Appendix provides additional information on ultimate tensile strength.

Variation of aging techniques did not significantly modify the after aging elongation of VAMAC. The most significant reduction in ultimate tensile elongation (to 66% of the initial value) was observed after the T→R27 aging simulation; the least significant (to 78% of the initial value) occurred during the T→R70 aging simulation. At completion of aging, the permanent set values ranged from 0.56 to 0.76.

At completion of the accident exposures, VAMAC's ultimate tensile elongation had only been slightly degraded by the simultaneous accident simulation (R + LOCA(air)). The most significant degradation occurred during the R28→LOCA(air) accident simulation. Varying the order of the accident sequence (R70→LOCA(air) compared to LOCA(air)→R70 did not have a large effect on VAMAC's tensile strength nor on its tensile elongation. The largest effect was noted for initially unaged samples; here the LOCA(air)→R70 accident simulation reduced the elongation by 40% while the R70→LOCA(air) simulation yielded a 20% reduction in the elongation.

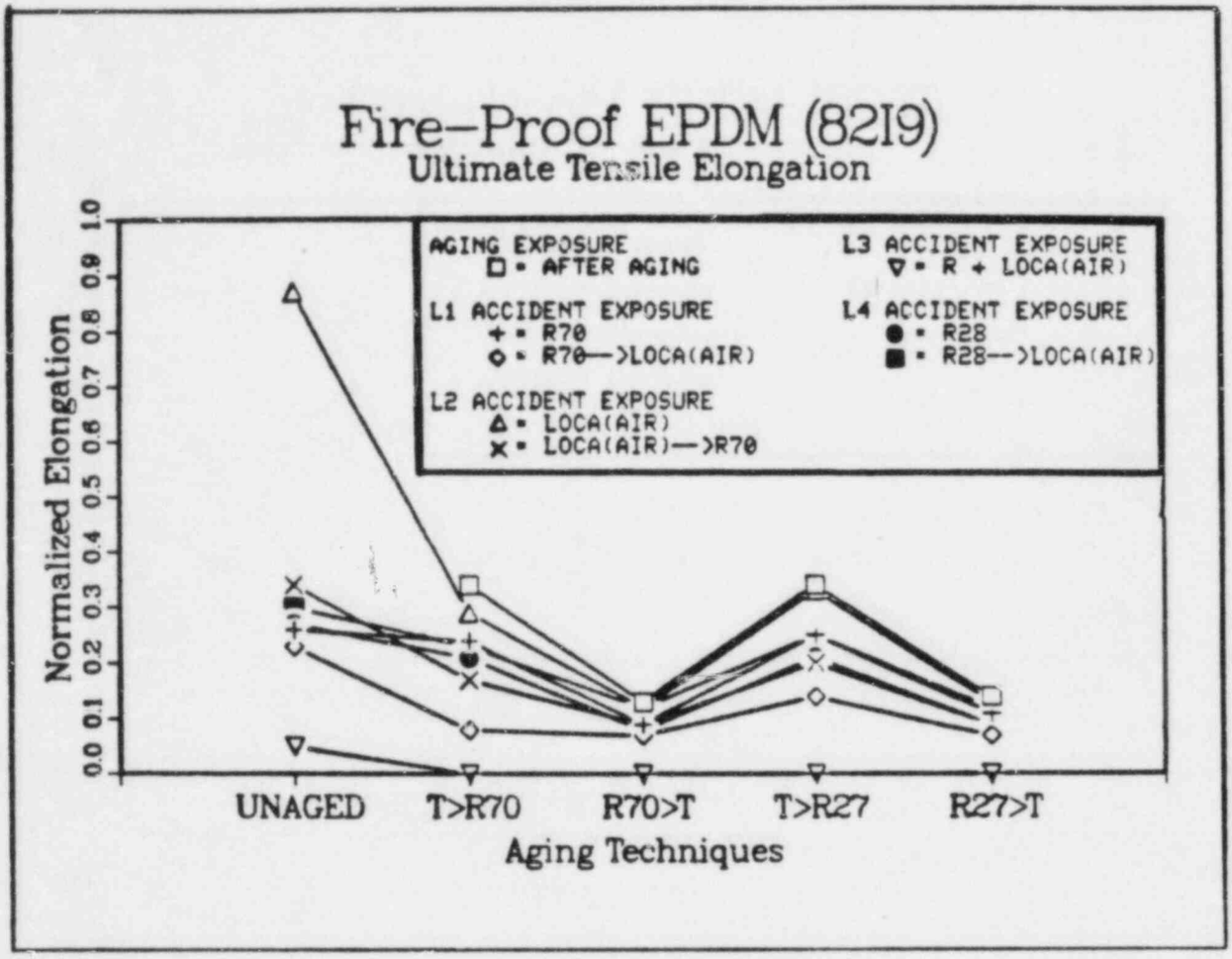

Figure 5.29: Ultimate Tensile Elongation of Fire-proof EPDM (8219) at Completion of Various Phases of the Accident Exposure. Sample tensile elongation divided by the initial (unaged) elongation is plotted for several aging and accident simulation techniques.

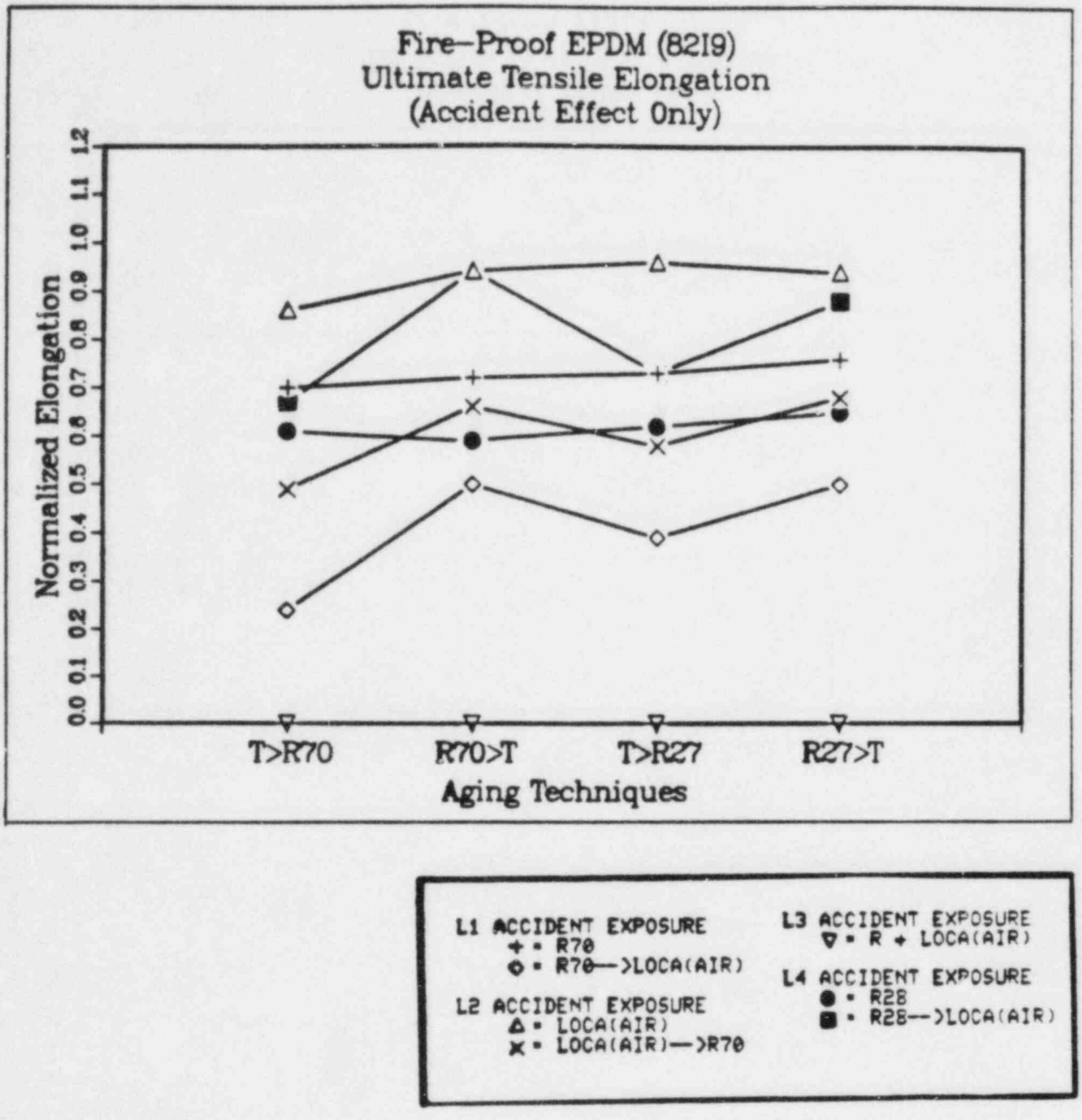

Figure 5.30: Ultimate Tensile Elongation of Fire-proof EPDM (8219) at Completion of Various Phases of the Accident Exposure. Sample tensile elongation divided by the after aging elongation is plotted for several aging and accident simulation techniques.

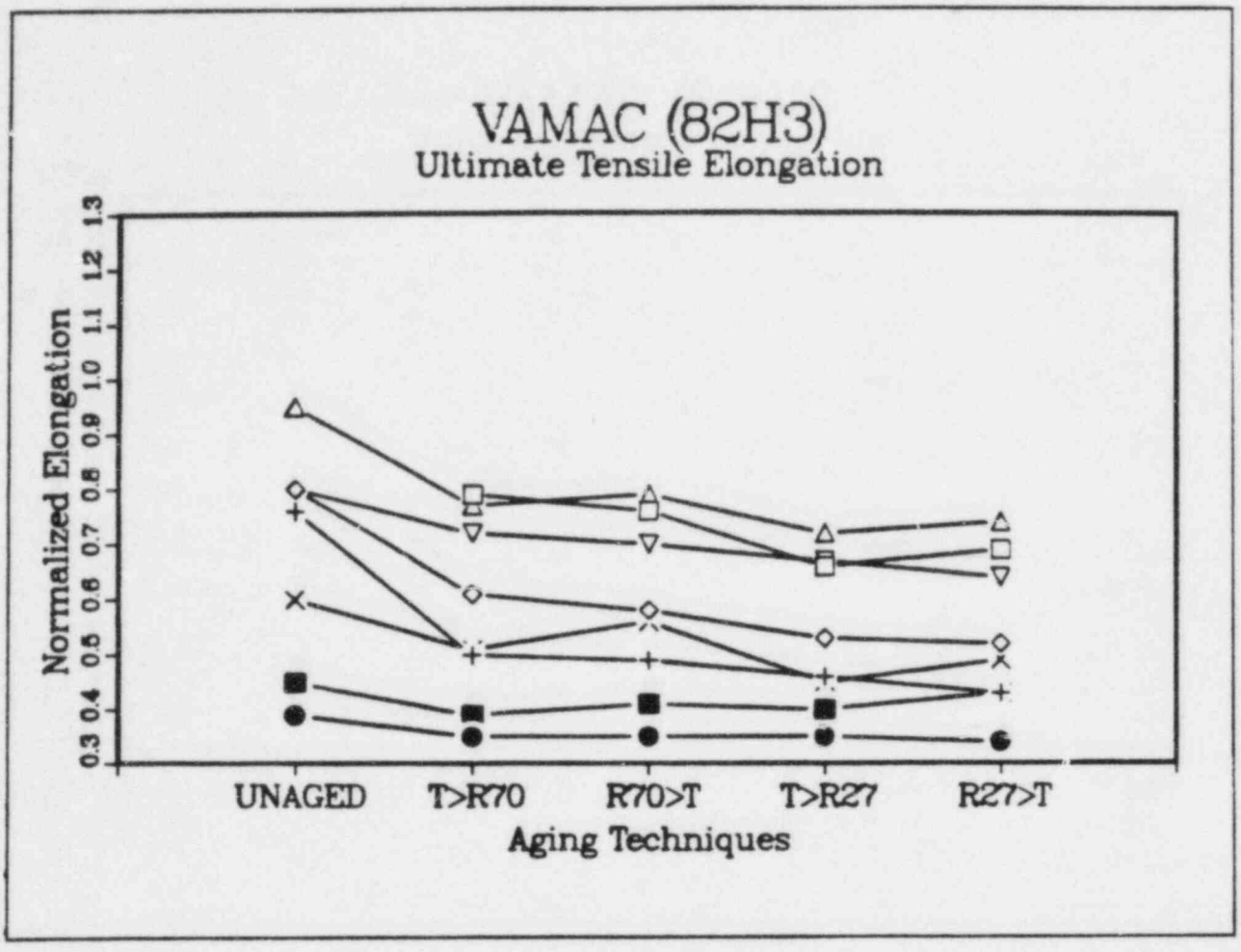

AGING EXPOSURE
□ = AFTER AGING

L1 ACCIDENT EXPOSURE
+ = R70
◇ = R70—>LOCA(AIR)

L2 ACCIDENT EXPOSURE
△ = LOCA(AIR)
× = LOCA(AIR)—>R70

L3 ACCIDENT EXPOSURE
▽ = R + LOCA(AIR)

L4 ACCIDENT EXPOSURE
● = R28
■ = R28-->LOCA(AIR)

Figure 5.31: Ultimate Tensile Elongation of VAMAC (82H3) at Completion of Various Phases of the Accident Exposure. Sample tensile elongation divided by the initial (unaged) elongation is plotted for several aging and accident simulation techniques.

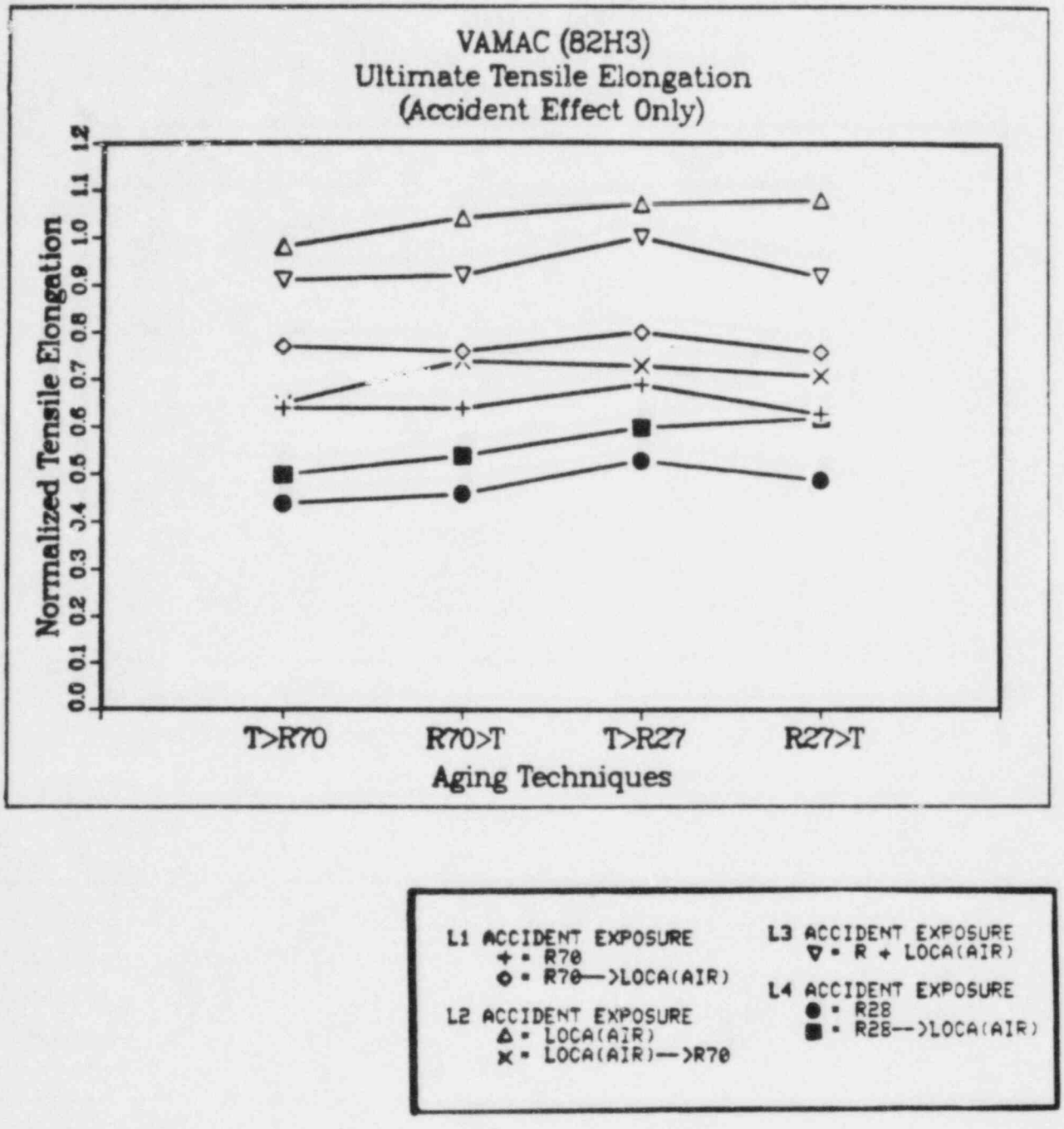

Figure 5.32: Ultimate Tensile Elongation of VAMAC (82H3) at Completion of Various Phases of the Accident Exposure. Sample tensile elongation divided by the after aging elongation is plotted for several aging and accident simulation techniques.

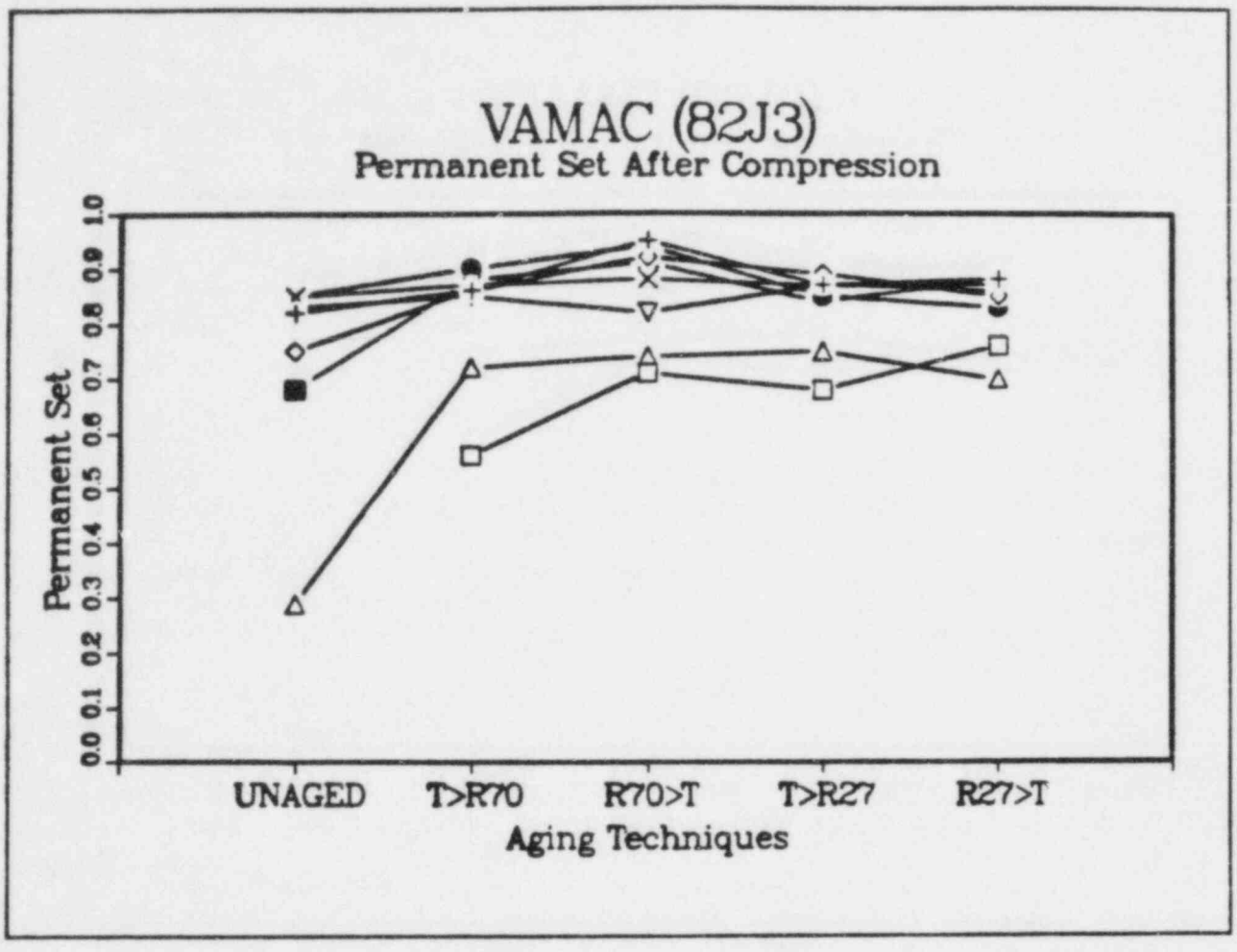

AGING EXPOSURE
□ • AFTER AGING

L1 ACCIDENT EXPOSURE
+ • R70
◇ • R70—>LOCA(AIR)

L2 ACCIDENT EXPOSURE
△ • LOCA(AIR)
× • LOCA(AIR)—>R70

L3 ACCIDENT EXPOSURE
▽ • R + LOCA(AIR)

L4 ACCIDENT EXPOSURE
● • R28
■ • R28—>LOCA(AIR)

Figure 5.33: Permanent Set After Compression of VAMAC (82J3) at Completion of Various Phases of the Accident Exposure

VAMAC's ultimate tensile elongation was affected by the accident irradiation temperature. The elongation was more degraded by the R28→LOCA(air) simulation than by the R70→LOCA(air) simulation. The ultimate tensile strength was unaffected by changes in accident irradiation temperature.

Figure 5.33 illustrates VAMAC's compression properties at completion of various phases of the aging and accident simulations. When VAMAC was enclosed in a sealed metal groove as an O-ring, the permanent set after compression was independent of the accident simulation technique. (The only exception in Figure 5.33 is the LOCA(air) simulation, but this represents only the first phase of a complete accident simulation. It was followed by an R70 irradiation.) At completion of these exposures, the O-rings had high compression set values, ~.9, and hence were near the limits of this use.

5.2.5 EPR (82H4 and 82J4)

EPR was tested both as tensile dumbbells and as O-rings. Hence we report both ultimate tensile properties and values for permanent set after compression. Ultimate tensile elongation results are plotted in Figures 5.34 and 5.35; permanent set after compression values are presented in Figure 5.36. As for all materials, the Appendix provides additional information on ultimate tensile strength.

By completion of aging, EPR's tensile properties were not significantly affected by variations in the aging techniques. The R→T aging techniques did cause slightly more degradation of the ultimate tensile elongation (to 46% and 42% of the initial value) than did the T→R aging techniques (to 57% and 53% of the initial value).

For EPR (82H4)'s ultimate tensile elongation the R + LOCA(air) accident simulation technique was less severe than the sequential accident simulations. It reduced the after aging elongation values by approximately 30%; the sequential techniques produced a 50% reduction of the after aging elongation values (see Figure 5.35). In contrast, the ultimate tensile strength (see the Appendix) was most degraded by the simultaneous simulation (R + LOCA(air)) and the R70→LOCA(air) sequential sequence.

The accident irradiation temperature did influence EPR (82H4)'s tensile strength. The R70→LOCA(air) simulation was more degrading than the R28→LOCA(air) simulation. The ultimate tensile elongation was not affected by the accident irradiation temperature.

The permanent set after compression properties for EPR are similar to those of VAMAC. At completion of the accident simulations, the O-rings were at the limits of use and differences between various aging and accident simulation methods were not noted.

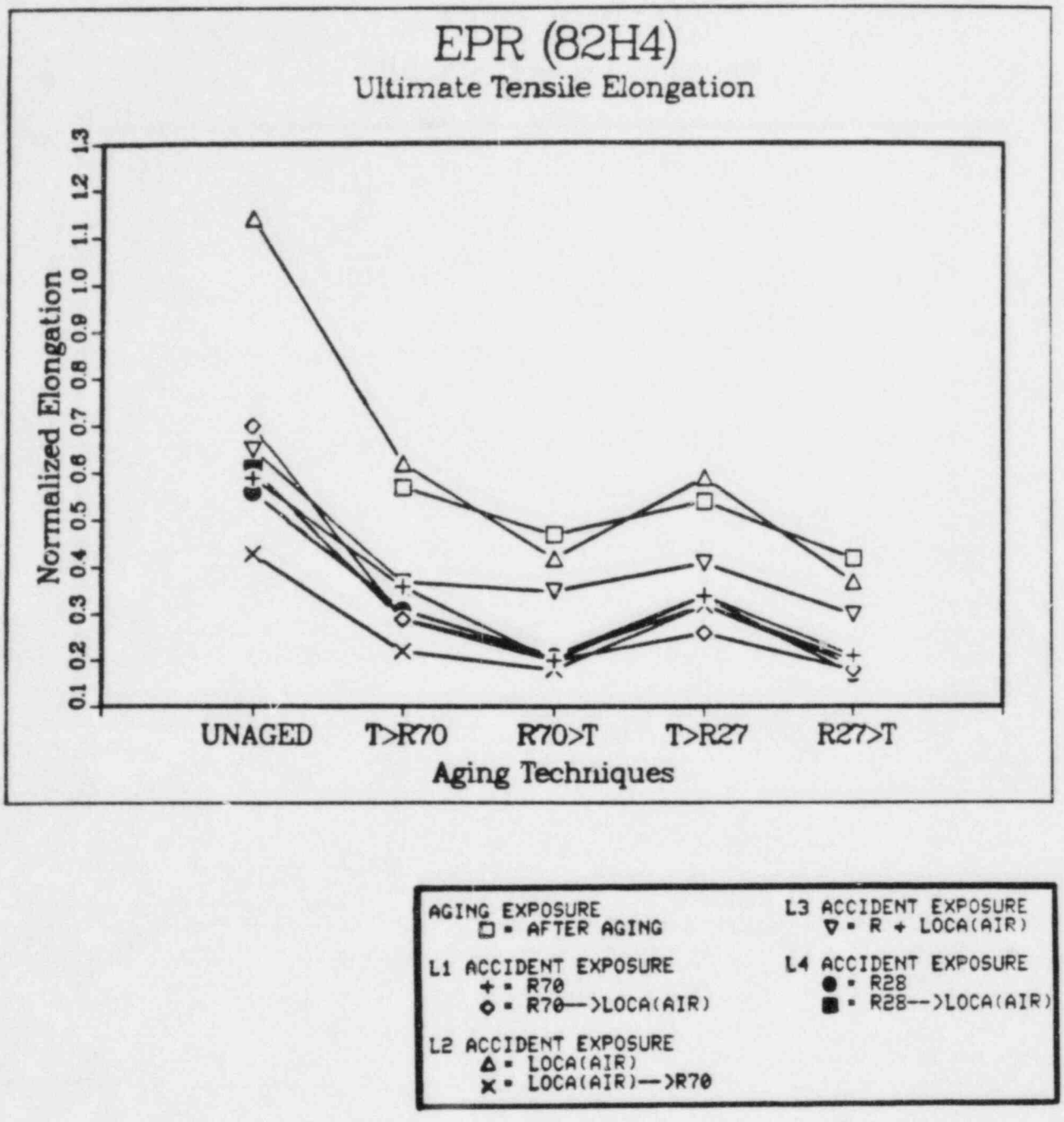

Figure 5.34: Ultimate Tensile Elongation of EPR (82H4) at Completion of Various Phases of the Accident Exposure. Sample tensile elongation divided by the initial (unaged) elongation is plotted for several aging and accident simulation techniques.

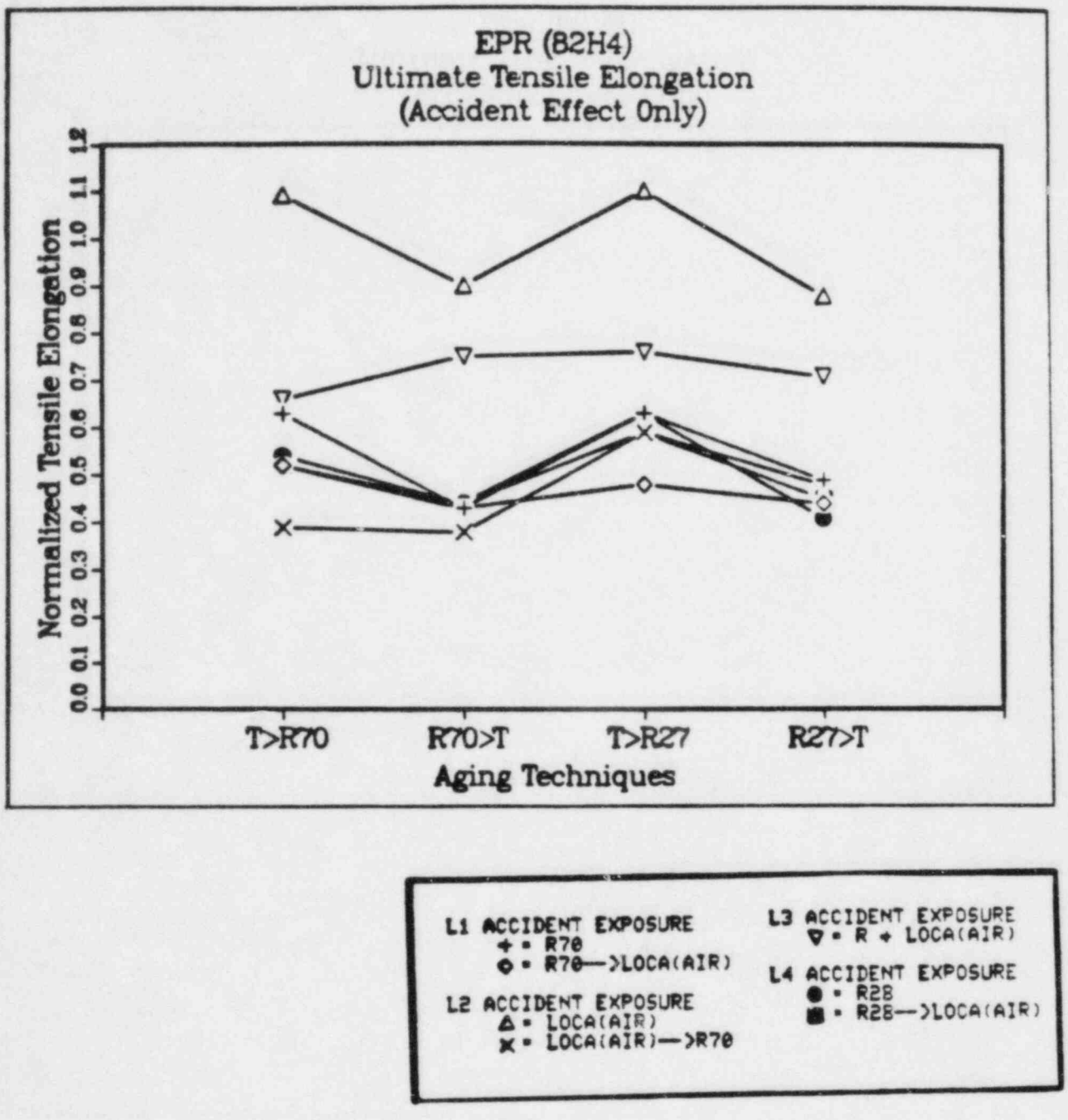

Figure 5.35: Ultimate Tensile Elongation of EPR (82H4) at Completion of Various Phases of the Accident Exposure. Sample tensile elongation divided by the after aging elongation is plotted for several aging and accident simulation techniques.

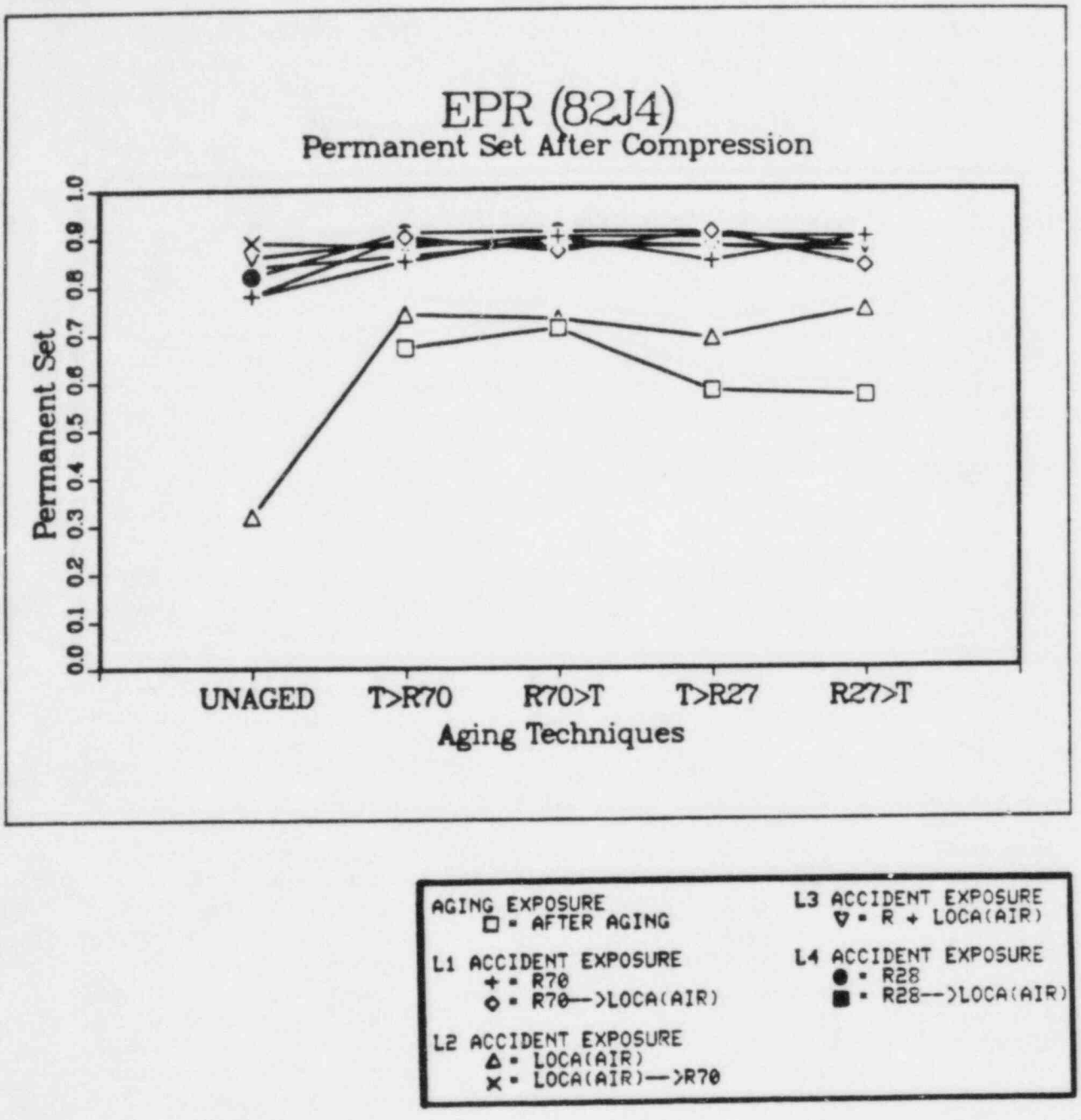

Figure 5.36: Permanent Set After Compression of EPR (82J4) at Completion of Various Phases of the Accident Exposure

5.2.6 Polydiallylphtalate (82H5)

Ultimate tensile strength data for polydiallylphtalate is presented in Figures 5.37 and 5.38. The tensile strength increased by less than 10% during the aging simulations. The sequential accident irradiations (R70 and R28) caused a 40-50% increase in tensile strength. Subsequent thermodynamic exposures (steam and chemical spray) reduced the tensile strength. The R70→LOCA(air) exposure was most severe for polydiallylphtalate; the LOCA(air)→R70 exposure least severe. For all accident exposures, the tensile strength degraded less than 40% compared to its initial unaged values.

5.2.7 PPS (82H6)

Ultimate tensile strength data for PPS is presented in Figures 5.39 and 5.40. At completion of the aging simulations the tensile strength was approximately 90% of its initial value. There was minimal influence caused by variations in the aging technique. The sequential accident irradiations caused an increase in tensile strength. Subsequent thermodynamic exposures reduced the tensile strength to approximately 60% of its initial unaged value. The tensile strength of PPS is similar after each of the accident simulations.

5.2.8 HYPALON (82G10)

Ultimate tensile elongation data for HYPALON is presented in Figures 5.41 and 5.42. Ultimate tensile strength data is provided in Figure 5.43. At completion of the aging exposures, HYPALON retains approximately 50% of its ultimate tensile elongation and more than 70% of its strength. In contrast to some of the other materials we have tested (for example, PRC (82I1), EPDM (82I2), and fire-proof EPDM (82I9)), HYPALON withstood well our aging simulations of normal environments in French PWRs.

Examination of Figure 5.43 indicates that HYPALON's tensile strength is only slightly decreased beyond its after aging values by the LOCA(air)→R70 accident simulation. This accident simulation, however, substantially reduced the ultimate tensile elongation (Figures 5.41 and 5.42). The opposite effect is observed during the simultaneous accident simulation (R + LOCA(air)). When compared to other accident simulations, this accident simulation technique produced the lowest strength values but the highest elongation values. (The LOCA(air) elongation data in Figure 5.41 does not represent a completed accident simulation; to complete the accident simulation its exposure was followed by a R70 exposure.) The tensile strength of HYPALON was more degraded by the accident sequence that started with irradiation (R70→LOCA(air)) than by the accident sequence that began with the thermodynamic exposure (LOCA(air)→R70).

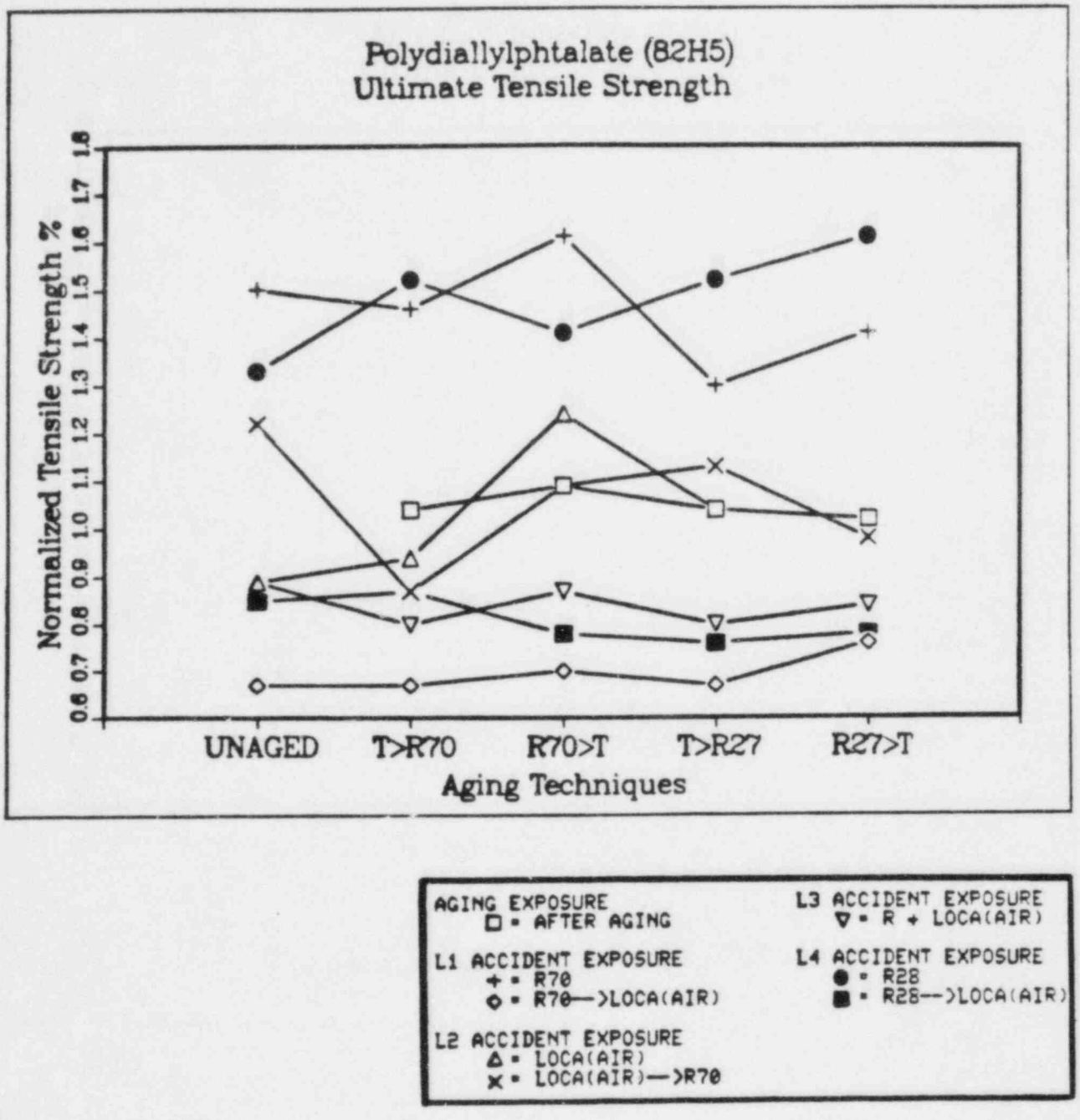

Figure 5.37: Ultimate Tensile Strength of Polydiallylphtalate (82H5) at Completion of Various Phases of the Accident Exposure. Sample tensile elongation divided by the initial (unaged) elongation is plotted for several aging and accident simulation techniques.

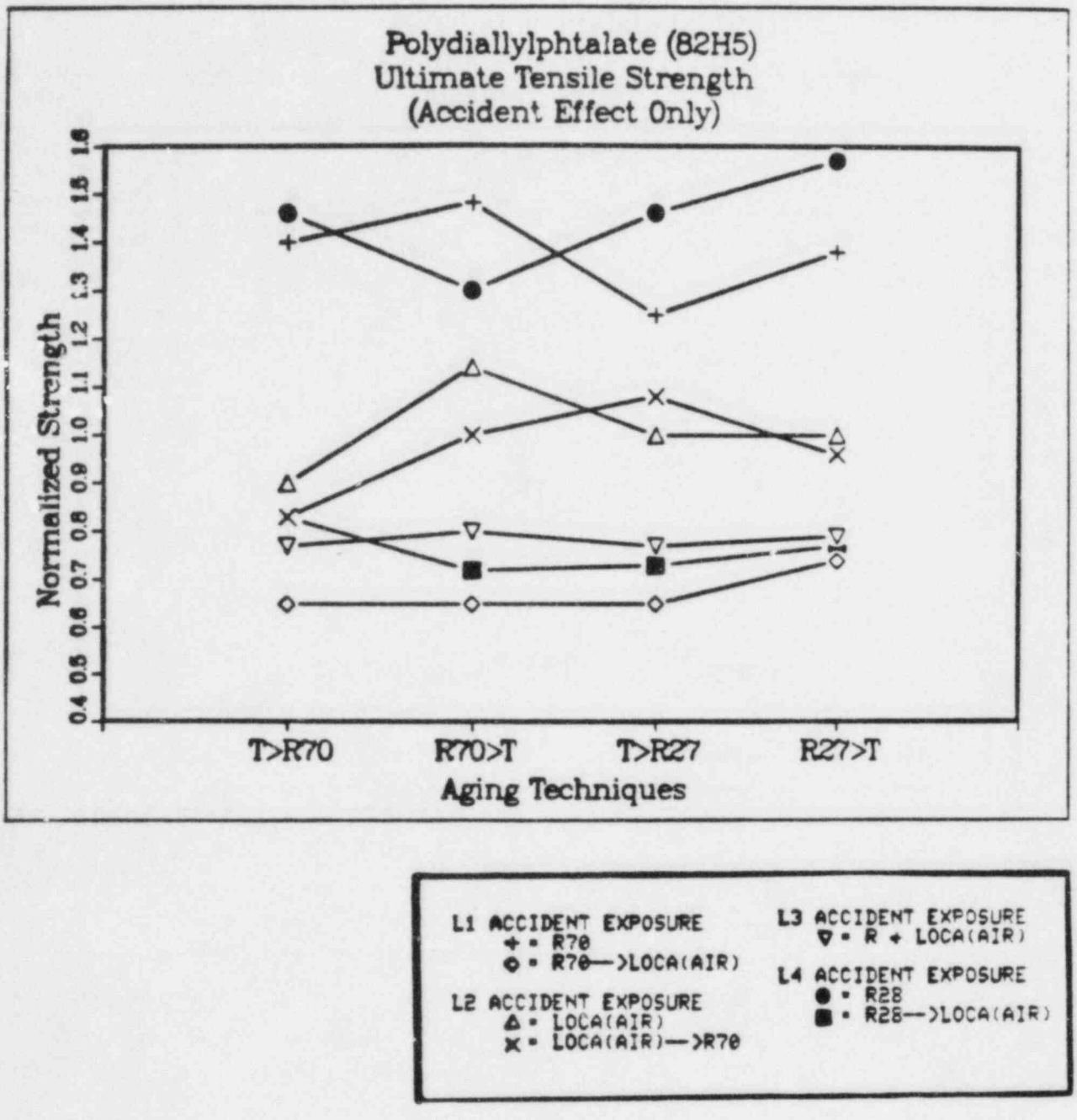

Figure 5.38: Ultimate Tensile Strength of Polydiallylphtalate (82H5) at Completion of Various Phases of the Accident Exposure. Sample tensile elongation divided by the after aging elongation is plotted for several aging and accident simulation techniques.

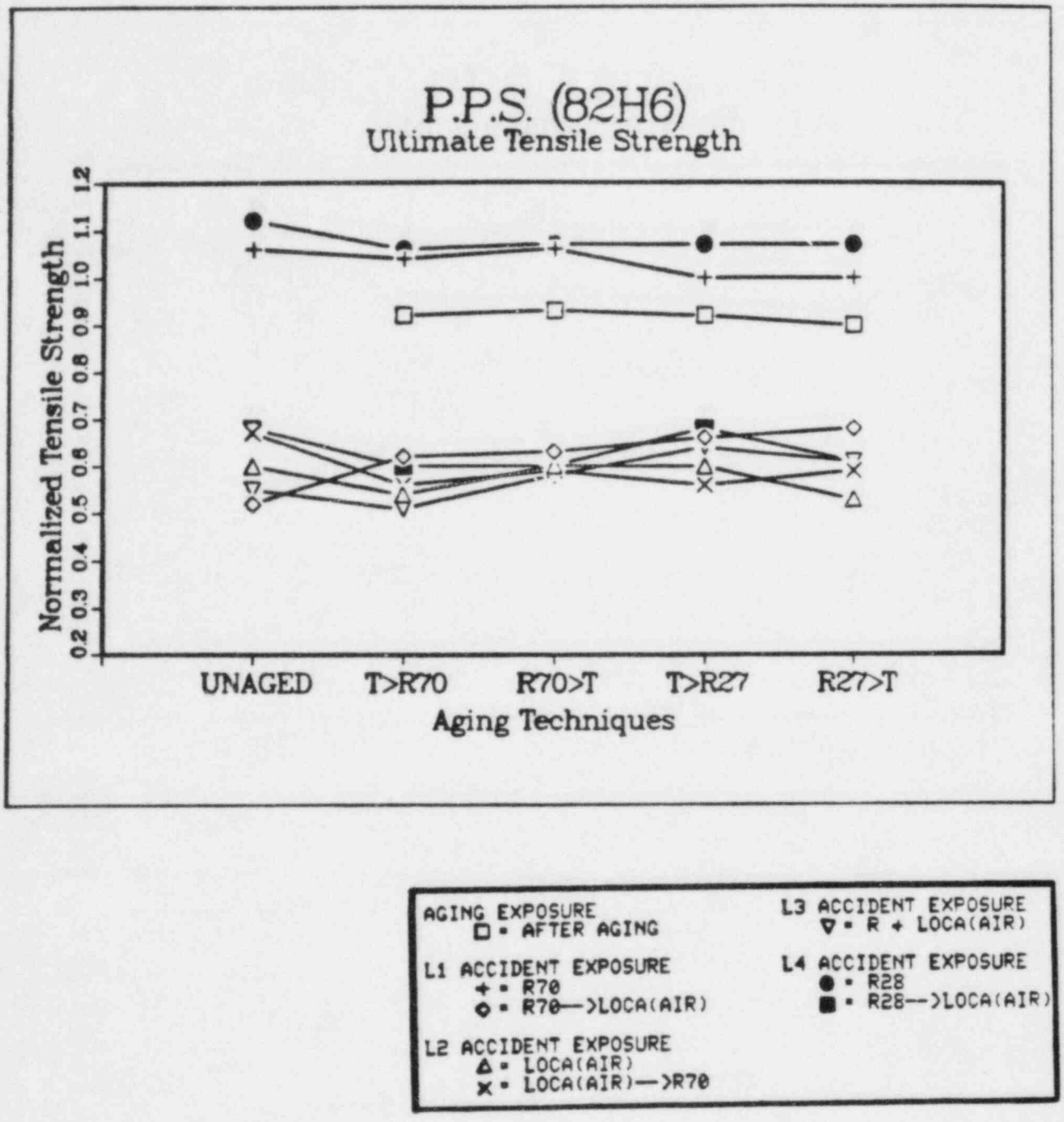

Figure 5.39: Ultimate Tensile Strength of PPS (82H6) at Completion of Various Phases of the Accident Exposure. Sample tensile strength divided by the initial (unaged) strength is plotted for several aging and accident simulation techniques.

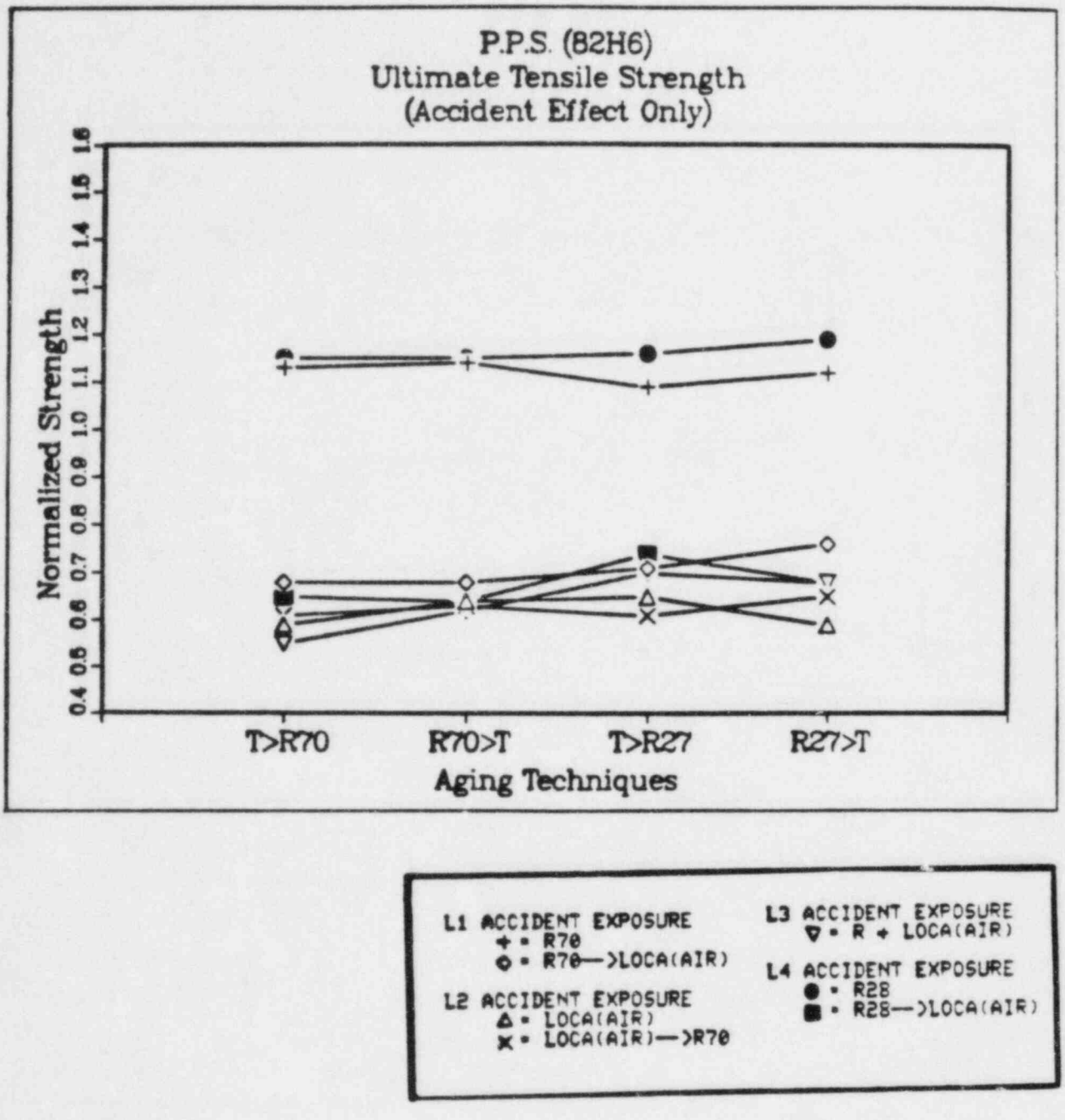

Figure 5.40: Ultimate Tensile Strength of PPS (82H6) at Completion of Various Phases of the Accident Exposure. Sample tensile strength divided by the after aging strength is plotted for several aging and accident simulation techniques.

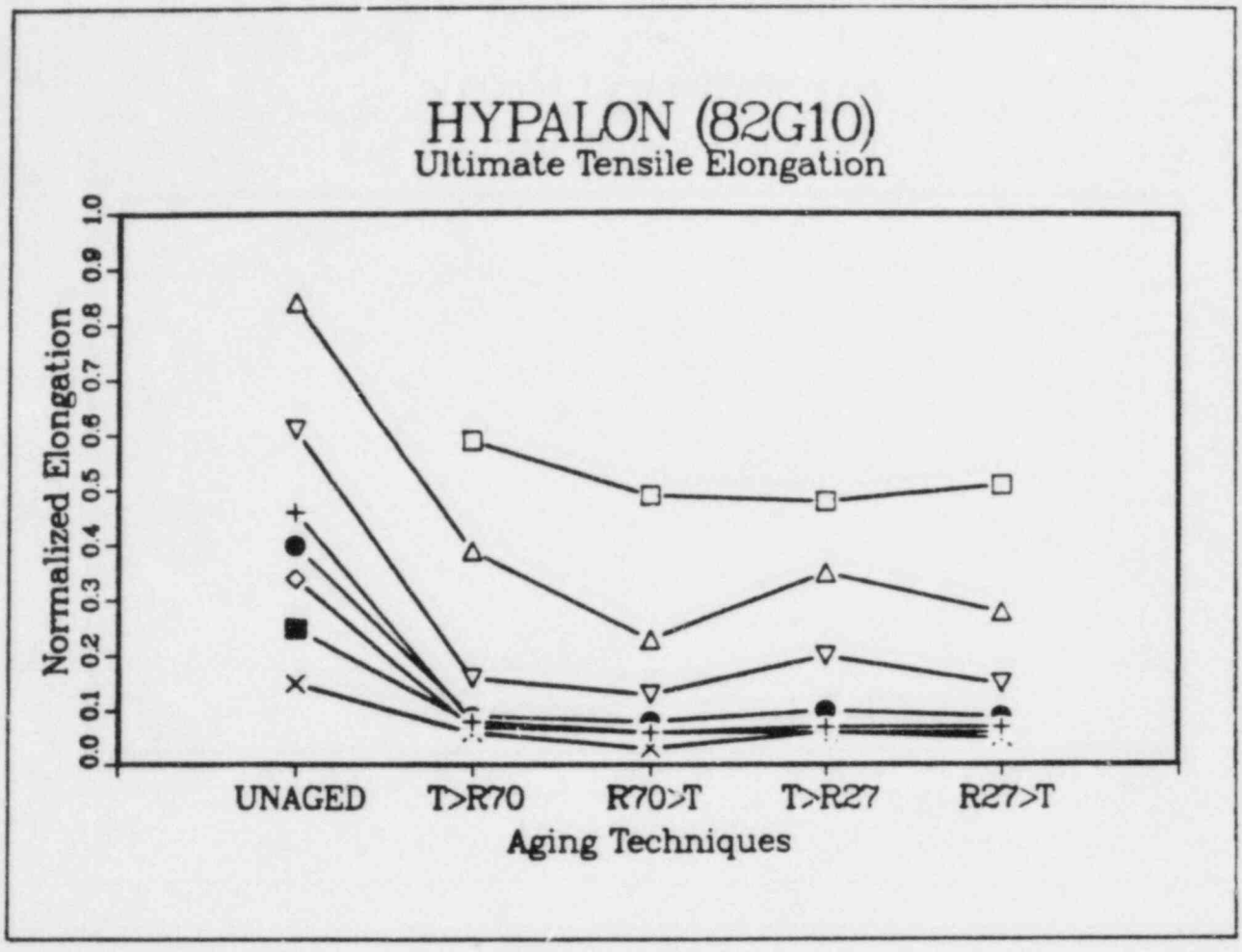

AGING EXPOSURE
□ = AFTER AGING

L1 ACCIDENT EXPOSURE
+ = R70
◇ = R70—>LOCA(AIR)

L2 ACCIDENT EXPOSURE
△ = LOCA(AIR)
× = LOCA(AIR)—>R70

L3 ACCIDENT EXPOSURE
▽ = R + LOCA(AIR)

L4 ACCIDENT EXPOSURE
● = R28
■ = R28—>LOCA(AIR)

Figure 5.41: Ultimate Tensile Elongation of HYPALON (82G10) at Completion of Various Phases of the Accident Exposure. Sample tensile elongation divided by the initial (unaged) elongation is plotted for several aging and accident simulation techniques.

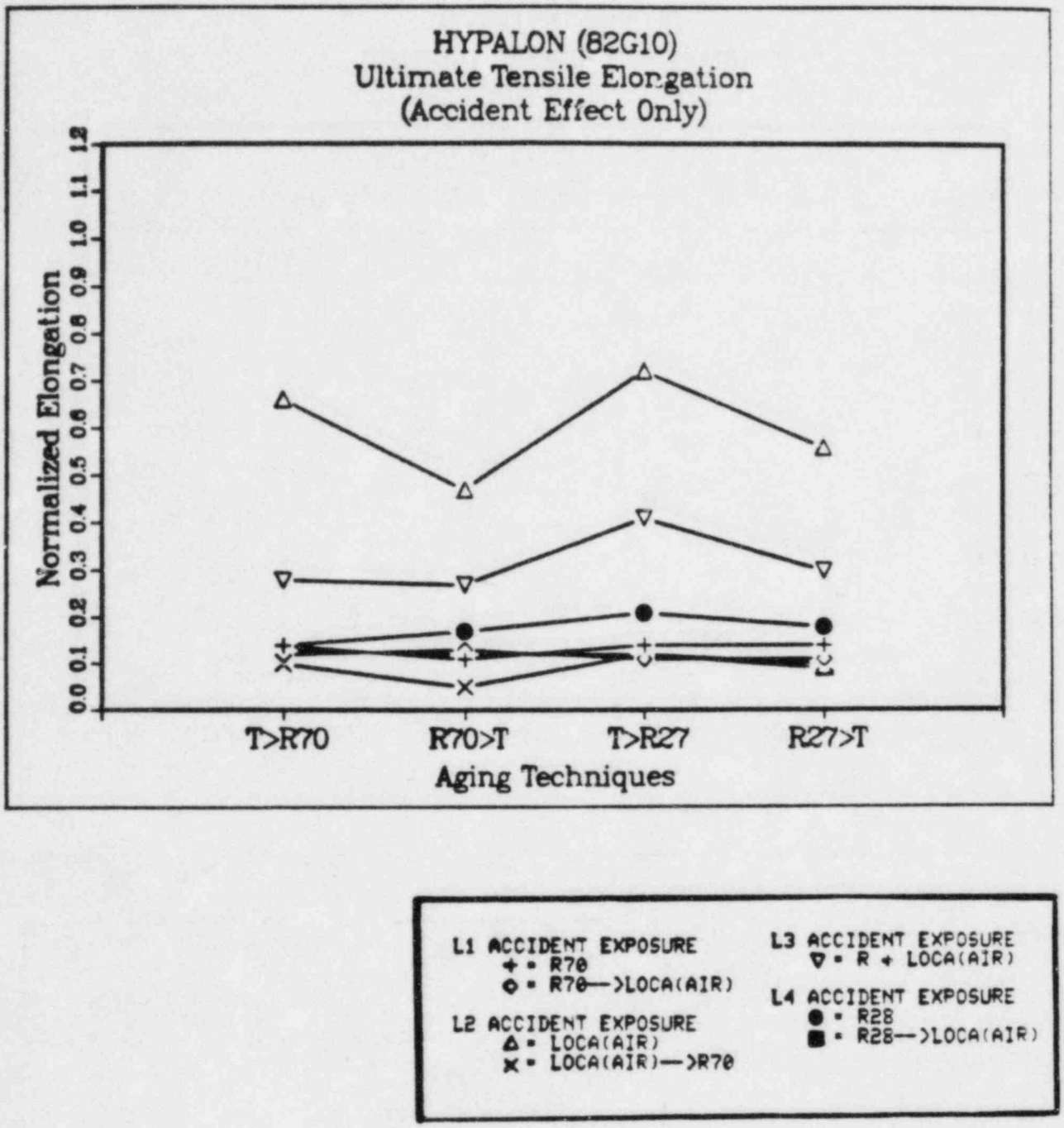

Figure 5.42: Ultimate Tensile Elongation of HYPALON (82G10) at Completion of Various Phases of the Accident Exposure. Sample tensile elongation divided by the after aging elongation is plotted for several aging and accident simulation techniques.

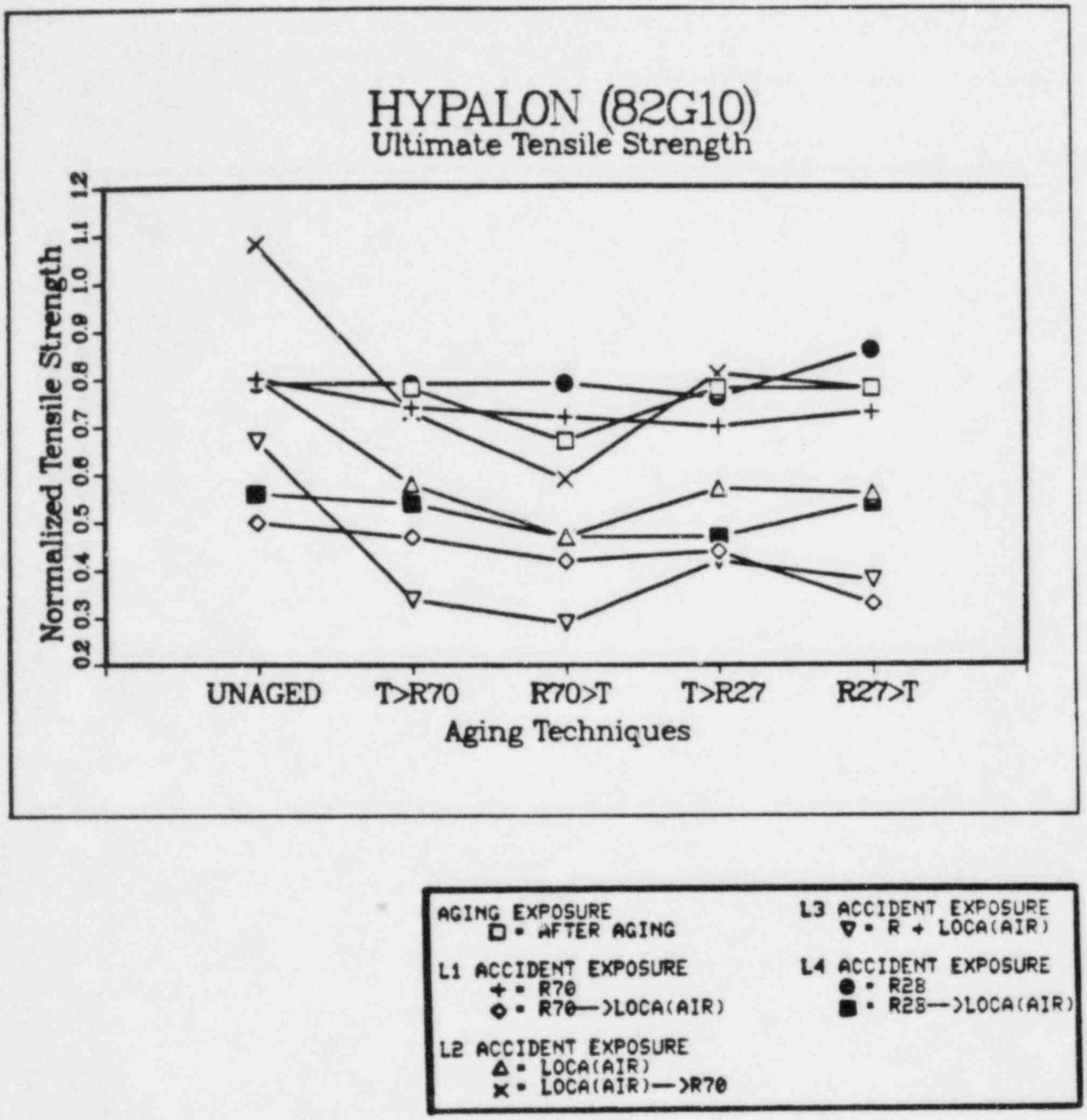

Figure 5.43: Ultimate Tensile Strength of HYPALON (82G10) at Completion of Various Phases of the Accident Exposure. Sample tensile strength divided by the initial (unaged) tensile elongation is plotted for several aging and accident simulation techniques.

HYPALON's ultimate tensile properties were typically independent of the accident irradiation temperature. One exception was noted. For HYPALON aged with 27°C irradiation, the subsequent accident exposure R70→LOCA(air) was more stressful to HYPALON's strength than was the accident exposure R28→LOCA(air).

6.0 DISCUSSION

Section 5.0 and the Appendix provide a substantial data base concerning the effect of alternative aging and accident simulations on polymer properties. Twenty-one different materials were tested; twenty-three different sample sets were employed (i.e., two materials were tested both for tensile properties and for permanent set after compression.) We combined qualification accident and aging research into one comprehensive test program; both aging and accident test parameters were varied in order to assess the relative importance of each parameter.

Some general trends were observable during our experiments. For example, ultimate tensile elongation for both U.S. EPR materials was more degraded by the accident simulations with air than with nitrogen (i.e., without air). The opposite effect was noted for both of the U.S. XLPO materials. (Note, the French materials were not tested in a nitrogen environment). We also noted that TEFZEL's mechanical properties were substantially reduced by our simulations, especially if high temperature irradiations or accident simulations with air were employed.

Other researchers have also tested EPR, XLPO, and TEFZEL materials (sometimes of different composition and different processing condition). Y. Kusama, et al.,[6] report for two EPR and one XLPE materials the effect of air during PWR simulations. For all three materials the most degraded state for mechanical properties occurred for simultaneous accident simulations that included air. K. Gillen, et al.,[5] also report on the importance of oxygen in LOCA simulation tests. They noted a pronounced dependence on the oxygen concentration during simulations for EPR mechanical properties. Greater degradation was observed at higher oxygen concentrations Both a XLPE and a XLPO material were tested by Gillen, et al. They did not observe significant effects of oxygen concentration during LOCA simulations. For TEFZEL, Gillen, et al., noted important radiation dose rate effects (samples aged at low dose rates experienced substantial mechanical degradation) but did not observe effects due to the oxygen concentration during LOCA simulations. Bustard[16] has also exposed TEFZEL cables to a simultaneous accident simulation that was preceded by a simultaneous thermal and radiation aging exposure. He observed substantial cracking of the TEFZEL jacket but continued integrity of the underlying TEFZEL insulation. (This insulation material was concurrently tested as TEFZEL 1 in this U.S.-French program). Cable manufacturers report successful qualification of TEFZEL products for thermal aging conditions and radiation doses in excess of those employed during our tests.

For example, BIW Cable Systems[17] performed a 100 Mrd irradiation, followed by a seven-day, 150°C thermal exposure and then a 100-day LOCA exposure. The cable passed a 5x bend test and a 2200 Vac withstand test. Okonite[18] exposed both single conductor and multiconductor TEFZEL cables to 180°C for seven days, did a 200 Mrd gamma irradiation, followed by a 30-day LOCA steam simulation. The cables passed a 40x bend test and an 80 Vac/mil withstand test.

We also noted substantial variability in test results because of differences in either the chemical composition or processing of test samples. For example, the response of the French cross-linked polyolefin material to alternative simulation techniques is different than the response of the two U.S. cross-linked polyolefin materials. Similar variability was noted both within and between other classes of materials.

Our overall research goal was to determine whether some combinations of aging and accident simulations are better suited for qualification activities than other alternative simulation techniques. To answer this question we looked for combinations of aging and accident simulation techniques that produced degradation similar to the worst degradation obtained during our simultaneous R + LOCA(air) tests. (Degradation variability for a given material during the R + LOCA(air) simulation is caused by differences in the aging simulations that preceded the accident exposure.) We consider the simultaneous R + LOCA(air) accident simulation to most reasonably reflect a design basis event accident scenario (except for inerted Boiling Water Reactor containments).

We also examined for that aging technique that is most conservative (i.e., produces the most degradation) when followed by the R + LOCA(air) accident simulation.

Cross-linked Polyolefins: Our experimental program included three cross-linked polyolefin materials, namely the U.S. XLPO 1 and XLPO 2 samples and the French PRC samples. The U.S. materials were irradiation cross-linked, while the French material was chemically cross-linked.

The effect of alternative simulation techniques on the two U.S. materials is vastly different than for the French material. For both U.S. materials, the R + steam(air) accident simulation produces less degradation of the ultimate tensile elongation than the other accident simulations. Since this is the most realistic accident simulation, any of the sequential accident simulation techniques would be appropriate. For neither of the U.S. cross-linked polyolefin materials was degradation strongly dependent on the aging technique.

The French material (PRC (82I1)), in contrast, was most severely degraded by the R + LOCA(air) accident exposure. The sequential accident technique best suited to simulate the simultaneous exposure results is the R70→LOCA(air) accident simulation. The choice of aging simulation technique is less important than the choice of accident simulation technique.

Ethylene Propylene Rubbers: Our experimental program included five ethylene propylene rubber materials, namely the U.S. fire-proof EPRs: EPR 1 and EPR 2; and the French EPDM (82I2), fire-proof EPDM (82I9), and EPR (82H4). In addition, EPR compression set materials were tested but we discuss them with the other compression set materials VAMAC, SILICONE, BUNA N, and VITON.

The French EPR materials 82I2 and 82I9 were most degraded by the R + LOCA(air) accident simulation. For 82I2, similar degradation is possible (for any accident simulation technique), provided a radiation followed by thermal (R→T) aging technique is employed. For 82I9, performing the R→T aging technique will enhance the conservatism of the qualification process, but no sequential accident technique is as degrading as the R + LOCA(air) technique. The R70→LOCA(air) simulation most approaches the R + LOCA(air) results.

For the French 82H4 EPR material, the R + LOCA(air) accident technique is least degrading. Any combination of sequential aging and accident simulation techniques is more degrading than this simultaneous accident exposure.

For the U.S. EPR 2, the simultaneous R + steam(air) accident exposure is most conservatively simulated by the R70→steam(air) technique. The R28→steam(air or N_2) and the R + steam(N_2) techniques are less conservative. The R120 and T→R27 aging techniques would be less conservative than the other three aging techniques. For the U.S. EPR 1 material, an appropriate aging and accident sequential qualification technique would be R(27 or 70)→T followed by R70→steam(air).

TEFZEL: Our experimental program included two TEFZEL materials, namely the U.S. TEFZEL 1 and TEFZEL 2 samples. Test results at completion of the accident exposures are presented in Tables 5.1 and 5.4.. For each combination of aging and accident simulations, we tested four specimens. The tables provide the largest bend radii for which at least one of the four samples had cracked as well as the radii by which all four samples had cracked. Both materials were more degraded when oxygen was present during simultaneous LOCA simulations (R + steam). If sequential qualification procedures are employed, then performing the aging and accident irradiations at elevated temperatures (i.e., 70°C) is desirable for TEFZEL. The aging sequence should be R70→T for TEFZEL 2. Any accident simulation consistent with these constraints is acceptable.

Chlorosulfonated Polyethylene (HYPALON): Two chlorosulfonated polyethylene materials were included in the data base, namely the U.S. CSPE and the French HYPALON (82G10). For the French material the R + LOCA(air) exposure was less degrading than all the sequential aging and accident techniques. Hence any sequential qualification procedure is appropriate. For the U.S. CSPE, all accident techniques produced similar degradation, the R70→T and R120 aging techniques produced more degradation than other techniques. A sequential qualification procedure appropriate for the U.S. CSPE would start with a R70→T aging simulation followed by any convenient accident simulation technique.

O-ring Materials: Seven O-ring or gasket materials were included in the test program; namely, the French VAMAC (82J3), EPR (82J4), and the U.S. EPR A, EPR B, BUNA N, SILICONE, and VITON materials. By the end of all accident simulations significant differences (within our estimated errors) between alternative aging and accident simulation procedures were not noted.

Connector Materials: Two connector materials were included in our test program, namely the thermosetting material polydiallylphtalate (82H5) and the thermoplastic material PPS (82H6). For both materials we monitored ultimate tensile strength behavior. For neither material were differences between alternative aging techniques important. For PPS (82H6) there also was little difference caused by alternative accident techniques. For polydiallylphtalate (82H5), the R28→LOCA(air) accident simulation most closely matches the degradation achieved by the R + LOCA(air) technique. The R70→LOCA(air) simulation is more conservative and might also be employed for qualification purposes.

VAMAC: One VAMAC sheet material was tested; namely, the French VAMAC (82H3). The R + LOCA(air) accident simulation technique was least degrading and therefore any sequential accident simulation technique would be appropriate. Any aging technique would provide appropriate preconditioning for a sequential accident exposure.

CPE: One chlorinated polyethylene jacket material was tested; namely, the U.S. CPE. For this material, the choice of accident technique is relatively unimportant; the R70→T aging exposure is most conservative.

Table 6.1 summarizes our qualitative conclusions for each material. Examination of Table 6.1 indicates that the R70→T aging technique followed by the R70→LOCA(air) accident technique could be employed for most of our materials.

In addition to the evaluation summarized in Table 6.1, we have performed an alternative evaluation to identify those aging and accident simulation techniques that most degrade polymer material properties. Tables 6.2 through 6.5 illustrate our evaluation technique and its results. Each table contains a location for each of the aging and accident simulation combinations employed during our test program. (Separate tables are employed for the U.S. and French materials). For each table location, we list all applicable materials whose mechanical properties were degraded by that combination of aging and accident simulations to values below or equal to a specified threshhold value. For example, in Table 6.2, we list for each aging and accident technique combination those U.S. materials whose normalized elongation (i.e., e/e_o) was reduced to .05 or less. (For the TEFZEL materials, we listed those aging and accident combinations that caused all four samples of a sample group to crack at bend radii greater than or equal to 44 times the sample radii). Only materials that were exposed to all possible combinatios of aging and accident simulations were considered during this evaluation. Hence the U.S. compression materials were not included in the Table 6.2 evaluation.

A qualitative examination of Table 6.2 indicates which aging and accident combinations affect the most number of U.S. materials. For example, six U.S. materials (out of eight) experienced substantial mechanical degradation when subjected to a R70→120 aging exposure followed by a R70→Steam(air) accident exposure. In contrast, only one U.S. material is listed for the 120→R27 aging exposure followed by the R28→Steam(N_2) accident exposure combination. Similar information for the French materials is provided in Table 6.3. (Note the French compression materials were not evaluated in Table 6.3 since material properties were near the end of use conditions and hence variations between alternative aging and accident simulations were not meaningful). Tables 6.4 and 6.5 repeat the analysis using a higher mechanical degradation threshhold value.

Some materials are more sensitive to the choice of aging and accident simulation combination than are other materials. For example, in Table 6.2 EPR 2 is listed in 5 of the 30 table locations. In contrast, TEFZEL 1 is listed 27 times. Clearly the choice of qualification methodology is more significant for EPR 1 than for TEFZEL 1. To account for this difference, each table entry is provided a weight according to the number of times that material appears in the table. A low weight is given to each table entry if the material's degradation is insensitive to the choice of aging and accident simulation techniques. A high weight is provided if the material's degradation is very sensitive to the choice of aging and accident simulation techniques. For example, EPR 2 which is listed 5 times is given a weight of .200, while TEFZEL 1 which is listed 27 times is given a weight of .037. These weights are also evaluated for Tables 6.3 through 6.5. We sum across each row of each table to evaluate the relative importance of each aging technique. (The aging technique with the largest sum is most significant). Simiarly, summing down the column of each table provides a means to evaluate the relative importance of each accident simulation technique.

Table 6.1

Qualitative Conclusions for Each Material

Material	Appropriate Sequential Qualification Procedures
Cross-linked Polyolefins	
XLPO 1	Any sequential simulation
XLPO 2	Any sequential simulation
PRC (82I1)	Any aging simulation followed by the R70→LOCA(air) accident simulation.
Ethylene Propylene Rubbers	
EPDM (82I2)	A R→T aging sequence followed by any accident simulation
EPDM(82I9)	A R→T aging sequence followed by a R70→LOCA(air) accident simulation
EPR (82H4)	Any sequential simulation
EPR 1	A R→T aging sequence followed by a R70→LOCA(air) accident simulation
EPR 2	A R70→T, R27→T, or T→R70 aging sequence followed by R70→LOCA(air) accident simulation
TEFZEL	
TEFZEL 1	Elevated temperature irradiations for sequential aging and accident exposures
TEFZEL 2	R70→T aging sequence followed by an accident simulation
Chlorosulfonated Polyethylene	
HYPALON (82G10)	Any sequential simulation
CSPE	R70→T aging sequence followed by any accident simulation.
O-ring Materials	Any sequential simulation

Table 6.1
(continued)

Qualitative Conclusions for Each Material

Material	Appropriate Sequential Qualification Procedures
Connector Materials	
PPS (82H6)	Any sequential simulation
Polydiallylphtalate (82H5)	Any aging simulation followed by the R28→LOCA(air) or R70→LOCA(air) accident simulations
VAMAC	Any sequential simulation
CPE	R70→T aging technique followed by any accident simulation

Examination of Tables 6.2 through 6.5 provide insights concerning those aging and accident simulation techniques that most degrade polymer material properties. Note that only six U.S. materials contributed to Tables 6.2 and 6.4 (two U.S. materials did not exhibit sufficient degradation to be included) and only four French materials contributed to Tables 6.3 and 6.5 (four French materials did not exhibit sufficient degradation to be included and the two O-ring materials were not evaluated because they were at their end of use condition.) Hence our data base is small. The insights are:

1. Both Tables 6.2 and 6.3 suggest the possible importance of R→T aging techniques. In both tables the R→T aging techniques (at a given irradiation temperature) contribute more to degradation than do the corresponding T→R aging techniques at the same temperature.

2. Table 6.2 suggests that oxygen presence during LOCA exposures enhances degradation. The R + Steam(air) exposure was more degrading than the R + Steam(N_2)) exposure. Likewise, the R70→Steam(air) exposure was more degrading than the R70→Steam(N_2).

3. Tables 6.4 and 6.5 suggest that as the degradation threshold is raised, differences between alternative aging and accident simulations decrease.

Table 6.2

Aging and Accident Combinations That Resulted in Degradation for U.S. Samples of Ultimate Tensile Elongation to Less Than 5% of Initial Values. (For TEFZEL, failure to pass a 44X bend test (all samples) was the selection criteria). The numbers in the table refer to weighting averages as discussed in the text.

Aging Environment \ Accident Environment	R70→ST(AIR)	R70→ST(N_2)	R28→ST(AIR)	R28→ST(N_2)	R + ST(AIR)	R + ST(N_2)	Totals
R120	EPR1=.143 TEFZEL1=.037 TEFZEL2=.050	EPR2=.200 TEFZEL1=.037 TEFZEL2=.050	CSPE=.125 TEFZEL1=.037 TEFZEL2=.050	CSPE=.125 TEFZEL2=.050	EPR1=.143 EPR2=.200 TEFZEL1=.037 TEFZEL2=.050	TEFZEL1=.037 TEFZEL2=.050	1.421
R70 → 120	EPR1=.143 EPR2=.200 CSPE=.125 CPE=.167 TEFZEL1=.037 TEFZEL2=.050	CPSE=.125 TEFZEL1=.037 TEFZEL2=.050	CSPE=.125 CPE=.167 TEFZEL1=.037 TEFZEL2=.050	CSPE=.125 CPE=.167 TEFZEL1=.037 TEFZEL2=.050	CSPE=.125 CPE=.167 TEFZEL1=.037 TEFZEL2=.050	CSPE=.125 TEFZEL1=.037 TEFZEL2=.050	2.283
120 → R70	EPR2=.200 TEFZEL1=.037	TEFZEL1=.037 TEFZEL2=.050	TEFZEL1=.037 TEFZEL2=.050	CPE=.167 TEFZEL2=.050	EPR1=.143 TEFZEL1=.037 TEFZEL2=.050	TEFZEL1=.037 TEFZEL2=.050	.945
R27 → 120	EPR1=.143 EPR2=.200 TEFZEL1=.037	TEFZEL1=.037	CPE=.167 TEFZEL1=.037	TEFZEL1=.037	TEFZEL1=.037 TEFZEL2=.050		.745
120 → R27	EPR1=.143 TEFZEL1=.037	TEFZEL1=.037	TEFZEL1=.037	TEFZEL1=.037	EPR1=.143 TEFZEL1=.037 TEFZEL2=.050	TEFZEL1=.037 TEFZEL2=.050	.608
Totals	1.749	.660	.919	.845	1.356	.473	6.002

Table 6.3

Aging and Accident Combinations That Resulted in Degradation for French Samples of Mechanical Properties to Less Than 5% of Initial Values. The numbers in the table refer to weighting averages as discussed in the text.

Aging Environment \ Accident Environment	R70+LOCA(AIR)	LOCA(AIR)+R70	R + LOCA(AIR)	R28+LOCA(AIR)	Totals
T + R70	EPDM = 0.071 PRC = 0.077	PRC = 0.077	FP-EPDM = 0.25 EPDM = 0.071 PRC = 0.077	EPDM = 0.071	0.694
R70 + T	EPDM = 0.071 PRC = 0.077	HYPALON = 0.333 EPDM = 0.071 PRC = 0.077	FP-EPDM = 0.25 EPDM = 0.071 PRC = 0.077	EPDM = 0.071 PRC = 0.077	1.175
T + R27	EPDM = 0.071 PRC = 0.077	PRC = 0.077	FP-EPDM = 0.25 EPDM = 0.071 PRC = 0.077	EPDM = 0.071	0.694
R27 + T	EPDM = 0.071 PRC = 0.077	HYPALON = 0.3333 EPDM = 0.071 PRC = 0.077	FP-EPDM = 0.25 EPDM = 0.071 PRC = 0.077	HYPALON = 0.333 EPDM = 0.071	1.431
Totals	0.592	1.116	1.592	0.694	3.99 3.99

Table 6.4

Aging and Accident Combinations That Resulted in Degradation for U.S. Samples of Ultimate Tensile Elongation to Less Than 10% of Initial Values. (For TEFZEL, failure to pass a 22X bend test (all samples) was the selection criteria). The numbers in the table refer to weighting averages as discussed in the text.

Aging Environment \ Accident Environment	R70→ST(AIR)	R70→ST(N_2)	R28→ST(AIR)	R28→ST(N_2)	R + ST(AIR)	R + ST(N_2)	Totals
R120	EPR1=.100 CSPE=.053 CPE=.040 TEFZEL1=.034 TEFZEL2=.042	EPR2=.125 CSPE=.053 CPE=.040 TEFZEL1=.034 TEFZEL2=.042	CSPE=.053 CPE=.040 TEFZEL1=.034 TEFZEL2=.042	CSPE=.053 CPE=.040 TEFZEL2=.042	EPR1=.100 EPR2=.125 CSPE=.053 TEFZEL1=.034 TEFZEL2=.042	CSPE=.053 TEFZEL1=.034 TEFZEL2=.042	1.350
R70 → 120	EPR1=.100 EPR2=.125 CSPE=.053 CPE=.040 TEFZEL1=.034 TEFZEL2=.042	CPSE=.053 CPE=.040 TEFZEL1=.034 TEFZEL2=.042	CSPE=.053 CPE=.040 TEFZEL1=.034 TEFZEL2=.042	CSPE=.053 CPE=.040 TEFZEL1=.034 TEFZEL2=.042	EPR2=.125 CSPE=.053 CPE=.040 TEFZEL1=.034 TEFZEL2=.042	CSPE=.053 TEFZEL1=.034 TEFZEL2=.042	1.324
120 → R70	EPR2=.125 CSPE=.053 CPE=.040 TEFZEL1=.034 TEFZEL2=.042	CPE=.040 TEFZEL1=.034 TEFZEL2=.042	CSPE=.053 CPE=.040 TEFZEL1=.034 TEFZEL2=.042	CPE=.040 TEFZEL1=.034 TEFZEL2=.042	EPR1=.100 CPE=.040 TEFZEL1=.034 TEFZEL2=.042	TEFZEL1=.034 TEFZEL2=.042	.987
R27 → 120	EPR1=.100 EPR2=.125 CSPE=.053 CPE=.040 TEFZEL1=.034	CSPE=.053 CPE=.040 TEFZEL1=.034	CSPE=.053 CPE=.040 TEFZEL1=.034	CSPE=.053 CPE=.040 TEFZEL1=.034	EPR2=.125 CSPE=.053 CPE=.040 TEFZEL1=.034 TEFZEL2=.042	CPE=.040 TEFZEL1=.034 TEFZEL2=.042	1.143
120 → R27	EPR1=.100 CPE=.040 TEFZEL1=.034 TEFZEL2=.042	EPR1=.100 EPR2=.125 CPE=.040 TEFZEL1=.034	EPR1=.100 CPE=.040 TEFZEL1=.034	EPR1=.100 CPE=.040 TEFZEL1=.034 TEFZEL2=.042	EPR1=.100 CPE=.040 TEFZEL1=.034 TEFZEL2=.042	TEFZEL1=.034 TEFZEL2=.042	1.197
Totals	1.525	1.005	.808	.763	1.374	.526	6.001

Table 6.5

Aging and Accident Combinations That Resulted in Degradation for French Samples of Mechanical Properties to Less Than 10% of Initial Values. The numbers in the table refer to weighting averages as discussed in the text.

Aging Environment \ Accident Environment	R70→LOCA(AIR)	LOCA(AIR)→R70	R + LOCA(AIR)	R28→LOCA(AIR)	Totals
T → R70	HYPALON = 0.083 FP-EPDM = 0.111 EPDM = 0.067 PRC = 0.067	HYPALON = 0.083 EPDM = 0.067 PRC = 0.067	FP-EPDM = 0.111 EPDM = 0.067 PRC = 0.067	HYPALON = 0.083 EPDM = 0.067 PRC = 0.067	1.007
R70 → T	HYPALON = 0.083 FP-EPDM = 0.111 EPDM = 0.067 PRC = 0.067	HYPALON = 0.083 FP-EPDM = 0.111 EPDM = 0.067 PRC = 0.067	FP-EPDM = 0.111 EPDM = 0.067	HYPALON = 0.083 EPDM = 0.067 PRC = 0.067	1.051
T → R27	HYPALON = 0.083 EPDM = 0.067 PRC = 0.067	HYPALON = 0.083 PRC = 0.067	FP-EPDM = 0.111 EPDM = 0.067 PRC = 0.067	HYPALON = 0.083 EPDM = 0.067 PRC = 0.067	0.829
R27 → T	HYPALON = 0.083 FP-EPDM = 0.111 EPDM = 0.067 PRC = 0.067	HYPALON = 0.083 FP-EPDM = 0.111 EPDM = 0.067 PRC = 0.067	FP-EPDM = 0.111 EPDM = 0.067 PRC = 0.067	HYPALON = 0.083 EPDM = 0.067 PRC = 0.067	1.118
Totals	1.201	1.023	0.913	0.868	4.005

4. The tables present conflicting data concerning the importance of elevated temperature irradiations (R70 versus R28). Table 6.2 suggests that an elevated temperature aging irradiation is important for the U.S. materials. It also indicates than an elevated temperature accident irradiation is more important when followed by a steam exposure with air. This conclusion is not confirmed in Table 6.3 which presents results for the French materials.

CONCLUSION

We have experimentally evaluated a number of polymer materials to determine the effect of alternative sequential and simultaneous aging and accident simulation procedures on material properties. Our overall research goal was to determine which aging and accident simulation technique most closely match anticipated real simultaneous conditions and therefore are better suited for qualification activities.

Some general conclusions have been identified from our experimental base. Results in Tables 6.2 - 6.5 indicate that radiation followed by a thermal exposure is a more conservative choice for an aging sequence than would a thermal followed by radiation exposure aging sequence. We also note that the presence or absence of air during accident simulations can influence the degree of degradation in some materials. The U.S. EPR and TEFZEL materials are examples where degradation is enhanced when air (oxygen) is present during accident simulations; the U.S. XLPO materials are examples where degradation is reduced by the presence of air. Hence, since most reactor containments are not inerted, a conservative accident simulation for qualifying materials would include air in the LOCA test chamber.

We noted substantial variability in test results because of differences in either the chemical composition or processing of test samples. For example, the response of the French cross-linked polyolefin material to alternative simulation techniques is different than the response of the two U.S. cross-linked polyolefin materials. Similar variability was noted both within and between other classes of materials.

We are encouraged that our empirically-based conclusions agree well with the findings of numerous research programs. Research reports have stressed the need to consider R→T aging simulations [1,2,7,13] and have recognized the importance to polymer degradation of oxygen during LOCA exposures [5,6].

We encourage the development of a larger data base. This will enable our preliminary insights to either be solidified or appropriately modified. In closing we would like to stress some of the limitations of our work. We monitored only mechanical properties of our polymer materials. Mechanical failure is an important but not the sole method by which polymers can contribute to functional degradation of Class 1E equipment. We also have tested a limited number of materials. Many important classes of polymers were not included in our study. Our

conclusions, representing simply the dominant trends, may not apply to all materials. For some materials alternative aging and accident simulation techniques may be equally appropriate. Finally, we chose experimental test conditions (radiation dose, steam temperature and pressure profiles, etc.) that may not be applicable to all nuclear utilities. These limitations should be considered prior to incorporating our "preliminary" insights into a qualification program for Class 1E equipment.

References

1. L.D. Bustard, E. Minor, J. Chenion, F. Carlin, C. Alba, G. Gaussens, and M. LeMeur, "The Effect of Thermal and Irradiation Aging Simulation Procedures on Polymer Properties," NUREG/CR-3629, SAND83-2651, Sandia National Laboratories, April 1984.

2. R.L. Clough, K.T. Gillen, J.L. Campan, G. Gaussens, H. Schonbacher, T. Seguchi, H. Wilski, and S. Machi, "Accelerated-Aging Tests for Predicting Radiation Degradation of Organic Material," NUCLEAR SAFETY, 25, 238 (March-April 1984)

3. L.D. Bustard, "The Effect of LOCA Simulation Procedures on Ethylene Propylene Rubber's Mechanical and Electrical Properties," NUREG/CR-3538, SAND83-1258, Sandia National Laboratories, October 1983.

4. L.D. Bustard, "The Effect OF LOCA Simulation Procedures on Cross-linked Polyolefin Cable's Performance," NUREG/CR-3588, SAND83-2406, Sandia National Laboratories, April 1984

5. K.T. Gillen, R.L. Clough, G. Ganouna-Cohen, J. Chenion, and G. Delmas, "The Importance of Oxygen in LOCA Simulation Tests," NUCLEAR ENGINEERING AND DESIGN, 74, 271 (1982)

6. Y. Kusama, S. Okada, M. Yoshikawa, M. Ito, T. Yagi, Y. Nakase, T. Seguchi, and K. Yoshida, "Methodology Study for Qualification Testing of Wire and Cable at LOCA Conditions," NUREG/CP-0041, Proceedings of the U.S. Nuclear Regulatory Commission Tenth Water Reactor Safety Research Information Meeting, Vol 5, p 330.

7. K. Yoshida, T. Seguchi, S. Okada, M. Ito, Y Kusama, T. Yagi, and M. Yoshikawa, "Progress on Qualification Testing Methodology Study of Electric Cables," NUREG/CP-0048, Proceedings of the U.S. Nuclear Regulatory Commission Eleventh Reactor Safety Research Information Meeting, Vol 5, p 283.

8. C. Alba, F. Carlin, J. Chenion, G. Gaussens, M. Le Meur, and M. Petitjean, "Synergetic Effects in Accident Simulation," Proceedings of the Colloque International 'Vieillissement Dans Les Essais De Materiel De Surete Pour Centrales Nucleaires', Paris, France, May 15-16, 1984.

9. T. H. Ling and W. F. Morrison, "Qualification of Power and Control Cable for Class 1E Applications," presented at the IEEE Power Engineering Society Winter Meeting, New York, NY, January 27-February 1, 1974, Conference Paper C744045-1.

10. F. V. Thome, "Preliminary Data Report: Testing to Evaluate Synergistic Effects from LOCA Environments, Test IX, Simultaneous Mode, Cables, Splice Assemblies, and Electrical Insulation Samples," SAND78-0718, April 1978.

11. K. Yoshida, Y. Nakase, S. Okada, M. Ito, Y. Kusama, S. Tanaka, Y. Kasahara, S. Machi, "Methodology Study for Qualification Testing of Wire and Cable at LOCA Condition," presented at 8th Water Reactor Safety Research Information Meeting, U.S. Nuclear Regulatory Commission, October 1980.

12. R. L. Clough, K. T. Gillen, and C. A. Quintana, "Heterogeneous Oxidative Degradation in Irradiated Polymers," Sandia National Laboratories, SAND83-2493, NUREG/CR-3643, April 1984.

13. R. L. Clough and K. T. Gillen, "Combined Environment Aging Effects: Radiation-Thermal Degradation of Polyvinyl Chloride and Polyethylene, J. Polym. Sci., Polym. Chem. Ed., 19(8): 2041-2051, August 1981.

14. L. Bonzon, R. L. Clough, K. T. Gillen, E. A. Salazar, "Qualification Testing Evaluation Program Light-Water Reactor Safety Research Quarterly Report, April-June 1979, Sandia National Laboratories, SAND80-0276, NUREG/CR-1343, April 1980.

15. ASTM D 395-78, An American National Standard: "Standard Test Methods for Rubber Property-Compression Set."

16. L. Bustard, private communication.

17. BIW Cable Systems, Report 74H017, dated December 16, 1976. This report sent to L. Bustard from J. Pirrong (BIW) on May 21, 1982.

18. Okonite, Report No. K-0-1, September 1979.

APPENDIX

In this appendix we report in tabular form our measurement results for each of the U.S. and French samples tested as part of the Joint French-U.S. Cooperative Research Program. Where appropriate, weight gains, ultimate tensile properties, bend test, and permanent set after compression (i.e., compression set) values are reported. Information is provided for all combinations of accident and aging simulation techniques.

Several of the tables employ the aging letter code described in Sections 4.1.1 and 4.1.2 of the report. For clarity, the letter code descriptions are repeated here. They are:

U.S. Samples:

A = R70→120°C: A 16-day irradiation at ~65 krd/h and 70°C followed by a 16-day thermal exposure at 120°C.

B = R27→120°C: A 16-day irradiation at ~65 krd/h and ambient temperatures (~27°C) followed by a 16-day thermal exposure at 120°C.

C = 120°C→R70: A 16-day thermal exposure at 120°C followed by 16-day irradiation at ~65 krd/h and 70°C.

D = 120°C→R27: A 16-day thermal exposure at 120°C followed by a 16-day irradiation at ~65 krd/h and ambient temperatures (~27°C).

E = R120: A 16-day simultaneous exposure to 120°C thermal and ~65 krd/h irradiation environments.

F = Unaged.

French Samples:

A = T→R70: A 10-day thermal exposure followed by a 9- or 10-day irradiation at ~115 krd/h and 70°C.

B = R70→T: A 9- or 10-day irradiation at ~115 krd/h and 70°C followed by a 10-day thermal exposure.

C = T→R27: A 10-day thermal exposure followed by a 9- or 10-day irradiation at ~115 krd/h and ambient temperatures (~27°C).

D = R27→T: A 9- or 10-day irradiation at ~115 krd/h and ambient temperatures (~27°C) followed by a 10-day thermal exposure.

U = Unaged.

The 10-day thermal exposure temperature depended on the French specimen material. The VAMAC dumbbell and O-ring samples (82H3 and 82J3) were thermally aged at 120°C. The PRC, EPDM, EPR and HYPALON samples (82I1, 82I2, 82I9, 82H4, 82J4, and 82G10) were thermally aged at 140°C. A 160°C thermal aging exposure was employed for the PPS and Polydiallylphtalate samples (82H6 and 82H5).

Many of our samples were either insulation "tubes" or jacket strips removed from actual cable. For insulation tubes, we calculated a typical cross-sectional area by subtracting the stranded copper cross-sectional area from the overall insulated conductor cross-sectional area. This typical cross-sectional value was used to calculate the tensile strength after we measured the force necessary to cause tensile failure. For jacket strips, we calculated the average cross-sectional area for several specimens and used it as a basis for evaluating the tensile strength. We express tensile strength in units of $daN.mm^{-2}$ = 10 MPa.

The measurement accuracy for the French samples is discussed in Section 3.3.3.2. For the U.S. samples, we report in this Appendix $\pm$ one standard deviation ($\pm \sigma$). This was evaluated using a population of four samples at each data location. Large variations in σ are observed during our measurements and are reflected in the tables. Other sources of error are contributed by dimensional uncertainties and tensile measurement accuracy. These generally were smaller than the larger values of σ reported in the tables.

TEFZEL 1: Weight Gains (%)

ACCIDENT SIMULATIONS

	R70→ST(AIR)	R70→ST(N2)	R28→ST(AIR)	R28→ST(N2)	R+ST(AIR)
UNAGED	-5.79	-3.35	-5.31	-1.44	-0.08
R120		-5.41	-8.13	-2.75	-1.52
R70→120	-2.57	-6.48	-6.13	-1.83	-1.25
120→R70		-5.88	-8.18	0.74	-0.69
R27→120	-3.05	-4.99	-6.42	-1.23	-1.04
120→R27	-3.64	-4.73	-7.05	-2.24	-1.16

TEFZEL 1: Largest Bend Radii At Which One Sample Cracked. Table entries are expressed as multiples of the TEFZEL 1 sample radius (i.e., 75x)

ACCIDENT SIMULATIONS

	R70→ST(AIR)	R70→ST(N2)	R28→ST(AIR)	R28→ST(N2)	R+ST(AIR)	R+ST(N2)
UNAGED	75.00	75.00	44.00	11.00	75.00	
R120	75.00	75.00	75.00		75.00	75.00
R70→120	75.00	75.00	75.00	75.00	75.00	50.00
120→R70	75.00	75.00	56.00	50.00	75.00	75.00
R27→120	75.00	75.00	75.00	75.00	75.00	31.00
120→R27	75.00	75.00	75.00	75.00	75.00	75.00

TEFZEL 1: Bend Radii By Which All Samples Cracked. Table entries are expressed as multiples of the TEFZEL 1 sample radius (i.e., 75x)

ACCIDENT SIMULATIONS

	R70→ST(AIR)	R70→ST(N2)	R28→ST(AIR)	R28→ST(N2)	R+ST(AIR)	R+ST(N2)
UNAGED	69.00	75.00	11.00	6.00	69.00	
R120	75.00	75.00	75.00		75.00	75.00
R70→120	75.00	75.00	69.00	50.00	75.00	44.00
120→R70	75.00	75.00	44.00	31.00	75.00	69.00
R27→120	75.00	75.00	44.00	75.00	75.00	22.00
120→R27	75.00	75.00	75.00	75.00	75.00	56.00

TEFZEL 2: Weight Gains (%)

ACCIDENT SIMULATIONS

	R70→ST(AIR)	R70→ST(N2)	R28→ST(AIR)	R28→ST(N2)	R+ST(AIR)
UNAGED	-1.34	-1.57	-0.53	-0.67	-2.14
R120	-1.88	-2.06	-2.34	-1.24	-1.91
R70→120	-1.93	-1.86	-1.66	-0.79	-0.90
120→R70	-2.09	-1.62	-1.83	-1.58	-0.03
R27→120	-5.50	-1.72	-2.49	-1.43	-0.01
120→R27	-1.75	-2.34	-2.71	-1.24	-0.02

TEFZEL 2: Largest Bend Radii At Which One Sample Cracked. Table entries are expressed as multiples of the TEFZEL 2 sample radius (i.e., 75x)

ACCIDENT SIMULATIONS

	R70→ST(AIR)	R70→ST(N2)	R28→ST(AIR)	R28→ST(N2)	R+ST(AIR)	R+ST(N2)
UNAGED	11.00	6.00			75.00	
R120	75.00	75.00	75.00	75.00	75.00	75.00
R70→120	75.00	75.00	75.00	75.00	75.00	75.00
120→R70	75.00	75.00	75.00	75.00	75.00	75.00
R27→120	22.00	44.00	22.00	22.00	75.00	44.00
120→R27	75.00	31.00	22.00	31.00	75.00	69.00

TEFZEL 2: Bend Radii By Which All Samples Cracked. Table entries are expressed as multiples of the TEFZEL 2 sample radius (i.e., 75x)

ACCIDENT SIMULATIONS

	R70→ST(AIR)	R70→ST(N2)	R28→ST(AIR)	R28→ST(N2)	R+ST(AIR)	R+ST(N2)
UNAGED	6.00	6.00			75.00	
R120	75.00	75.00	75.00	75.00	75.00	75.00
R70→120	75.00	75.00	44.00	75.00	75.00	56.00
120→R70	22.00	75.00	75.00	56.00	75.00	75.00
R27→120	11.00	11.00	11.00	11.00	75.00	22.00
120→R27	22.00	11.00	11.00	22.00	75.00	44.00

XLPO 1: Weight Gains (%)

ACCIDENT SIMULATIONS

	R70→ST(AIR)	R70→ST(N2)	R28→ST(AIR)	R+ST(AIR)	R28→ST(N2)
UNAGED	0.50	-0.49	0.18	-0.02	0.88
R120	-0.21	-0.25	-0.14	-0.18	2.68
R70→120	0.00	-0.65	-1.06	-0.19	0.37
120→R70	0.00	-0.56	-0.19	-0.34	0.64
R27→120	0.00	-0.80	-0.12	-0.23	0.19
120→R27	-0.34	-0.72	-0.21	-0.40	0.93

XLPO 1: Ultimate Tensile Properties

T = Ultimate tensile strength (Units = 10 MPa)
E = Ultimate tensile elongation (Units = %)

Aging / Accident	Tests	A	B	C	D	E	F
R70	T	1.31 ± .06	1.40 ± .07	1.39 ± .05	1.37 ± .02	1.42 ± .02	1.51 ± .06
	E	129 ± 15	165 ± 5	157 ± 9	130 ± 6	139 ± 5	253 ± 2
L5: R70+steam(air)	T	1.15 ± .03	1.15 ± .04	1.15 ± .02	1.11 ± .05	1.08 ± .08	1.17 ± .05
	E	133 ± 12	107 ± 13	120 ± 2	100 ± 18	81 ± 8	186 ± 14
L6: R70+steam(N_2)	T	1.14 ± .01	1.18 ± .03	1.19 ± .04	1.20 ± .03	1.21 ± .01	1.38 ± .01
	E	137 ± 6	159 ± 3	178 ± 15	193 ± 10	133 ± 8	270 ± 15
R28	T	1.59 ± .05	1.62 ± .04	1.57 ± .05	1.58 ± .06	1.71 ± .12	1.45 ± .03
	E	95 ± 4	91 ± 3	121 ± 7	123 ± 6	66 ± 8	129 ± 15
L7: R28+steam(air)	T	1.51 ± .01	1.44 ± .03	1.37 ± .02	1.29 ± .03	1.47 ± .03	1.40 ± .07
	E	93 ± 3	89 ± 5	87 ± 3	90 ± 7	72 ± 2	125 ± 4
L8: R28+steam(N_2)	T	1.48 ± .06	1.48 ± .03	1.39 ± .06	1.39 ± .06	1.57 ± .01	1.42 ± .07
	E	109 ± 9	106 ± 4	106 ± 8	118 ± 22	82 ± 4	130 ± 7
L9: R+steam(air)	T	1.27 ± .04	1.22 ± .06	1.24 ± .02	1.22 ± .03	1.20 ± .02	1.29 ± .03
	E	194 ± 11	183 ± 25	176 ± 18	174 ± 18	139 ± 10	228 ± 10
L10: R28+steam(N_2)	T	1.59 ± .06	1.52 ± .04	1.56 ± .07	1.54 ± .05	1.62 ± .02	1.49 ± .01
	E	105 ± 7	111 ± 2	108 ± 11	118 ± 10	93 ± 5	128 ± 8

T_o (units = 10 MPa) = 1.86 ± .04
E_o (units = %) = 389 ± 8

XLPO 2: Weight Gains (%)

ACCIDENT SIMULATIONS

	R70→ST(AIR)	R70→ST(N2)	R28→ST(AIR)	R28→ST(N2)	R+ST(AIR)
UNAGED	3.31	4.70	-0.11	1.21	2.69
R120	2.71	2.88	0.32	0.84	3.55
R70→120	4.16	4.04	1.58		4.43
120→R70	5.72	6.64	1.94	1.52	4.44
R27→120	2.06	3.42	0.56	1.19	3.08
120→R27	6.21	4.78	0.70	0.93	4.32

XLPO 2: Ultimate Tensile Properties

T = Ultimate tensile strength (Units = 10 MPa)
E = Ultimate tensile elongation (Units = %)

Aging / Accident	Tests	A	B	C	D	E	F
R70	T	1.56 ± .02	1.49 ± .03	1.48 ± .02	1.39 ± .03	1.69 ± .03	1.36 ± .03
	E	59 ± 7	71 ± 2	53 ± 5	40 ± 4	77 ± 4	140 ± 7
L5: R70+steam(air)	T	1.38 ± .04	1.29 ± .05	1.32 ± .06	1.15 ± .02	1.39 ± .03	1.28 ± .05
	E	98 ± 9	111 ± 13	82 ± 8	67 ± 9	85 ± 13	120 ± 20
L6: R70+steam(N_2)	T	1.51 ± .09	1.49 ± .10	1.48 ± .16	1.29 ± .08	1.57 ± .17	1.33 ± .02
	E	114 ± 10	121 ± 10	103 ± 17	106 ± 13	95 ± 10	164 ± 11
R28	T	1.43 ± .03	1.36 ± .01	1.43 ± .01	1.36 ± .08	1.62 ± .02	1.24 ± .02
	E	59 ± 7	66 ± 10	26 ± 6	8 ± 1	78 ± 9	19 ± 13
L7: R28+steam(air)	T	1.37 ± .04	1.28 ± .05	1.37 ± .03	1.20 ± .02	1.41 ± .06	1.19 ± .03
	E	87 ± 10	85 ± 12	93 ± 7	81 ± 11	89 ± 2	107 ± 11
L8: R28+steam(N_2)	T	1.50 ± .02	1.36 ± .05	1.43 ± .04	1.23 ± .02	1.61 ± .10	1.18 ± .02
	E	111 ± 9	105 ± 6	105 ± 9	75 ± 7	102 ± 10	107 ± 8
L9: R+steam(air)	T	1.72 ± .06	1.62 ± .05	1.49 ± .04	1.41 ± .03	1.73 ± .02	1.42 ± .03
	E	140 ± 7	144 ± 6	129 ± 4	96 ± 5	142 ± 2	113 ± 27
L10: R28+steam(N_2)	T	1.81 ± .10	1.69 ± .10	1.89 ± .06	1.74 ± .04	1.68 ± .17	1.63 ± .12
	E	123 ± 6	128 ± 11	132 ± 12	131 ± 8	104 ± 10	143 ± 12

T_o (units = 10 MPa) = 1.46 ± .04
E_o (units = %) = 336 ± 15

EPR 1: Weight Gains (%)

ACCIDENT SIMULATIONS

	R70→ST(AIR)	R70→ST(N2)	R28→ST(AIR)	R28→ST(N2)	R+ST(AIR)
UNAGED	0.56	0.82	0.98	1.64	2.08
R120	5.39	13.63	7.24	1.42	5.81
R70→120	0.86	2.25	3.79	1.42	4.55
120→R70	0.19	8.52	8.68	2.19	4.36
R27→120	2.08	2.22	10.03	1.27	4.04
120→R27	0.52	12.53	8.89	1.75	4.13

EPR 1: Ultimate Tensile Properties

T = Ultimate tensile strength (Units = 10 MPa)
E = Ultimate tensile elongation (Units = %)

Aging / Accident	Tests	A	B	C	D	E	F
R70	T	.87 ± .01	.86 ± .01	.86 ± .04	.91 ± .01	.82 ± .02	.99 ± .06
	E	90 ± 5	91 ± 6	82 ± 11	90 ± 1	55 ± 5	138 ± 6
L5: R70+steam(air)	T	.67 ± .04	.54 ± .06	.73 ± .01	.65 ± .02	.66 ± .04	.72 ± .01
	E	22 ± 10	10 ± 1	63 ± 8	22 ± 10	21 ± 14	61 ± 14
L6: R70+steam(N_2)	T	.81 ± .02	.78 ± .01	.75 ± .03	.70 ± .02	.83 ± .01	.73 ± .03
	E	96 ± 11	70 ± 1	53 ± 1	28 ± 3	148 ± 3	25 ± 4
R28	T	1.04 ± .03	1.03 ± .04	1.03 ± .03	.99 ± .01	1.10 ± .01	.98 ± .01
	E	111 ± 12	69 ± 5	87 ± 6	62 ± 3	70 ± 7	96 ± 5
L7: R28+steam(air)	T	.85 ± .06	.85 ± .04	.83 ± .02	.75 ± .05	.85 ± .01	.91 ± .04
	E	78 ± 5	58 ± 6	53 ± 9	43 ± 10	72 ± 4	108 ± 15
L8: R28+steam(N_2)	T	.93 ± .02	.91 ± .02	.92 ± .03	.88 ± .01	.96 ± .02	1.01 ± .06
	E	107 ± 11	66 ± 5	61 ± 8	41 ± 2	117 ± 8	83 ± 9
L9: R+steam(air)	T	.66 ± .01	.72 ± .02	.58 ± .08	.56 ± .01	.64 ± .02	.71 ± .01
	E	56 ± 6	61 ± 12	20 ± 11	8 ± 1	30 ± 10	66 ± 18
L10: R28+steam(N_2)	T	1.15 ± .03	1.19 ± .07	1.15 ± .05	1.14 ± .05	1.12 ± .08	1.14 ± .07
	E	111 ± 1	110 ± 8	107 ± 8	108 ± 9	99 ± 10	133 ± 12

T_o (units = 10 MPa) = 1.36 ± .03
E_o (units = %) = 419 ± 13

EPR 2: Weight Gains

ACCIDENT SIMULATIONS

	R70→ST(AIR)	R70→ST(N2)	R28→ST(AIR)	R28→ST(N2)	R+ST(AIR)
UNAGED	12.71	21.43	13.90	8.90	19.63
R120	24.93	44.13	22.20	30.35	49.81
R70→120	16.40	26.88	21.00	25.02	39.72
120→R70	23.61	28.91	21.30	19.32	39.14
R27→120	18.08	25.96	19.10	17.59	35.38
120→R27	14.19	26.73	17.60	15.06	34.77

EPR 2: Ultimate Tensile Properties

T = Ultimate tensile strength (Units = 10 MPa)
E = Ultimate tensile elongation (Units = %)

Aging / Accident	Tests	A	B	C	D	E	F
R70	T	1.11 ± .11	1.16 ± .03	1.12 ± .06	1.23 ± .01	1.09 ± .01	1.34 ± .03
	E	54 ± 17	59 ± 1	51 ± 8	71 ± 2	30 ± 7	83 ± 9.
L5: R70+steam(air)	T	.86 ± .01	.87 ± .03	.80 ± .06	.88 ± .05	.50 ± .16	1.13 ± .03
	E	8 ± 1	9 ± 2	8 ± 1	40 ± 13	10	81 ± 13
L6: R70+steam(N_2)	T	.45 ± .03	.95 ± .02	.91 ± .02	.92 ± .02	.81 ± .01	1.20 ± .02
	E	34 ± 9	18 ± 4	29 ± 8	20 ± 8	11 ± 1	93 ± 4
R28	T	1.00 ± .01	1.54 ± .08	1.37 ± .18	1.61 ± .06	1.30 ± .03	1.47 ± .05
	E	10 ± 1	45 ± 7	41 ± 8	53 ± 5	29 ± 1	61 ± 2
L7: R28+steam(air)	T	.87 ± .04	.91 ± .03	.98 ± .05	1.08 ± .07	.95 ± .03	1.26 ± .07
	E	31 ± 2	32 ± 2	43 ± 1	44 ± 1	33 ± 2	73 ± 2
L8: R28+steam(N_2)	T	1.18 ± .07	1.23 ± .04	1.17 ± .03	1.20 ± .07	.91 ± .04	1.43 ± .14
	E	38 ± 6	41 ± 2	47 ± 5	40 ± 8	24 ± 4	75 ± 10
L9: R+steam(air)	T	.75 ± .04	.78 ± .02	.80 ± .01	.85 ± .01	.76 ± .06	1.41 ± .08
	E	15 ± 7	16 ± 6	25 ± 6	47 ± 6	7 ± 2	126 ± 5
L10: R28+steam(N_2)	T	1.52 ± .06	1.61 ± .08	1.60 ± .08	1.53 ± .09	1.07 ± .12	1.62 ± .10
	E	77 ± 6	73 ± 1	76 ± 5	71 ± 2	41 ± 10	79 ± 6

T_O (units = 10 MPa) = 1.40 ± .06
E_O (units = %) = 223 ± 13

CSPE: Weight Gains (%)

ACCIDENT SIMULATIONS

	R70→ST(AIR)	R70→ST(N2)	R28→ST(AIR)	R28→ST(N2)	R+ST(AIR)
UNAGED	13.13	28.37	6.97	2.03	2.15
R120	1.88	5.26	-0.41	1.69	14.31
R70→120	8.02	13.94	-4.83	10.24	25.21
120→R70	14.93	27.00	9.66	21.07	30.82
R27→120	9.85	24.08	9.63	12.06	36.83
120→R27	11.39	11.61	5.69	10.73	16.81

CSPE: Ultimate Tensile Properties

T = Ultimate tensile strength (Units = 10 MPa)
E = Ultimate tensile elongation (Units = %)

Aging / Accident	Tests	A	B	C	D	E	F
R70	T	.90 ± .05	1.10 ± .05	1.24 ± .17	1.41 ± .04	.87 ± .10	.95 ± .02
	E	17 ± 3	47 ± 7	64 ± 5	67 ± 6	26 ± 3	130 ± 11
L5: R70+steam(air)	T	.77 ± .07	.74 ± .02	.88 ± .09	1.02 ± .03	.80 ± .03	.77 ± .07
	E	16 ± 6	35 ± 2	36 ± 5	50 ± 1	27 ± 7	71 ± 2
L6: R70+steam(N_2)	T	.63 ± .05	.71 ± .04	.83 ± .08	.99 ± .09	.80 ± .03	.71 ± .04
	E	12 ± 5	34 ± 1	49 ± 5	54 ± 5	24 ± 1	100 ± 10
R28	T	.74 ± .15	.97 ± .04	1.40 ± .11	1.63 ± .06	.93 ± .06	1.36 ± .11
	E	8 ± 1	23 ± 1	62 ± 3	65 ± 5	14 ± 1	147 ± 12
L7: R28+steam(air)	T	.58 ± .06	.74 ± .05	.76 ± .14	.92 ± .08	.75 ± .06	.93 ± .05
	E	8 ± 2	32 ± 2	35 ± 5	57 ± 6	20 ± 3	83 ± 5
L8: R28+steam(N_2)	T	.64 ± .09	.71 ± .10	.88 ± .02	.94 ± .08	.85 ± .07	1.12 ± .05
	E	11 ± 1	30 ± 1	61 ± 8	54 ± 5	21 ± 2	94 ± 5
L9: R+steam(air)	T	.68 ± .08	.53 ± .04	.54 ± .05	.84 ± .04	.80 ± .09	.92 ± .07
	E	10 ± 2	38 ± 4	44 ± 6	63 ± 8	32 ± 2	132 ± 7
L10: R28+steam(N_2)	T	1.20 ± .14	1.07 ± .11	.90 ± .08	1.24 ± .25	.84 ± .13	1.45 ± .25
	E	20 ± 1	52 ± 2	44 ± 1	61 ± 12	26 ± 4	97 ± 4

T_o (units = 10 MPa) = 1.63 ± .08
E_o (units = %) = 383 ± 16

CPE: Weight Gains (%)

ACCIDENT SIMULATIONS

	R70→ST(AIR)	R70→ST(N2)	R28→ST(AIR)	R28→ST(N2)	R+ST(AIR)
UNAGED	8.88	13.15	3.58	1.13	14.65
R120	10.37	10.65	7.94	3.52	24.68
R70→120	9.89	10.27	11.93	6.70	25.73
120→R70	5.70	11.27	7.88	6.22	21.12
R27→120	10.93	10.14	8.85	6.13	22.80
120→R27	7.51	10.34	6.06	4.80	16.27

CPE: Ultimate Tensile Properties

T = Ultimate tensile strength (Units = 10 MPa)
E = Ultimate tensile elongation (Units = %)

Aging / Accident	Tests	A	B	C	D	E	F
R70	T	1.37 ± .02	1.44 ± .07	1.59 ± .22	2.27 ± .03	1.67 ± .08	1.58 ± .13
	E	18 ± 3	21 ± 1	19 ± 4	34 ± 2	28 ± 3	88 ± 11
L5: R70+steam(air)	T	1.30 ± .05	1.63 ± .15	1.39 ± .07	1.70 ± .09	1.60 ± .06	.97 ± .03
	E	17 ± 2	36 ± 4	31 ± 1	31 ± 2	30 ± 1	53 ± 2
L6: R70+steam(N_2)	T	1.14 ± .06	1.46 ± .11	1.67 ± .27	1.79 ± .13	1.50 ± .18	1.17 ± .10
	E	20 ± 6	28 ± 2	33 ± 5	38 ± 2	32 ± 7	61 ± 4
R28	T	1.28 ± .03	1.65 ± .14	2.28 ± .09	1.93 ± .25	1.81 ± .06	1.96 ± .19
	E	10 ± 1	22 ± 1	30 ± 1	23 ± 2	51 ± 3	21 ± 1
L7: R28+steam(air)	T	1.21 ± .12	1.18 ± .03	1.62 ± .09	1.44 ± .19	1.49 ± .08	1.22 ± .03
	E	12 ± 2	18 ± 1	31 ± 1	22 ± 2	21 ± 1	34 ± 2
L8: R28+steam(N_2)	T	1.19 ± .14	1.36 ± .08	1.42 ± .15	1.61 ± .06	1.73 ± .07	1.27 ± .03
	E	11 ± 2	20 ± 1	18 ± 2	22 ± 1	28 ± 2	32 ± 1
L9: R+steam(air)	T	1.22 ± .10	1.26 ± .09	1.06 ± .03	1.20 ± .03	1.40 ± .08	1.28 ± .05
	E	15 ± 2	35 ± 4	30 ± 2	32 ± 2	44 ± 5	63 ± 7
L10: R28+steam(N_2)	T	.76 ± .07	1.47 ± .07	1.90 ± .02	2.09 ± .01	1.66 ± .14	2.62 ± .17
	E	12 ± 2	31 ± 1	45 ± 5	42 ± 1	29 ± 5	82 ± 2

T_o (units = 10 MPa) = 1.48 ± .06
E_o (units = %) = 357 ± 11

Mechanical Measurement

PRC (82I1)

Aging / Accident		Tests	U	A	B	C	D
Blank samples after aging		T	1.3	1.2	0.9	1.1	1.0
		E	370	267	30	269	43
L1	R70 °C	T	1.0	1.1	1.0	1.1	1.15
		E	240	58	26	57	27
L1	R70 °C→LOCA	T	1.0	1.0	0.6	1.1	0.86
		E	55	3.5	8.1	6.0	3.5
L2	LOCA	T	1.1	1.1	0.95	1.1	1.05
		E	306	307	5	256	26
L2	LOCA→R70 °C	T	1.1	1.4	0.5	1.3	1.0
		E	185	13	0	13	3.5
L3	LOCA + R	T	1.1	0.9	0	1.1	0.6
		E	38	1.5	0	5.0	4.0
L4	R23 °C	T	1.0	1.1	1.0	1.1	1.2
		E	185	40	19	27	28
L4	R23 °C→LOCA	T	1.0	1.0	0.94	1.0	0.9
		E	57	25	12	30	30

T = Tensile strength (MPa)
E = Elongation at break (%)

Mechanical Measurement

EPDM (82I2)

Aging / Accident	Tests	U	A	B	C	D
Blank samples after aging	T	0.6	0.3	0.4	0.5	0.2
	E	240	82	0	118	0
L1 R70 °C	T	0.3	0.23	0.25	0.25	0.27
	E	76	49	0	55	0
L1 R70 °C→LOCA	T	0	0	0.2	0	0.2
	E	0	0	0	0	2.2
L2 LOCA	T	0.6	0.2	0.2	0.35	0.2
	E	254	23	0	88	0
L2 LOCA→R70 °C	T	0.23	0.2	0.2	0.3	0.2
	E	70	20	0	55	0
L3 LOCA + R	T	0.07		0.2		0.1
	E	9	0	0	0	0
L4 R23 °C	T	0.4	0.3	0.3	0.4	0.3
	E	65	55	0	57	0
L4 R23 °C LOCA	T	0.3	0.1	0.25	0.1	0.2
	E	70	13	20	3.5	0

T = Tensile strength (MPa)
E = Elongation at break (%)

Mechanical Measurement

Fire-Proof EPDM (82I9)

Aging Accident	Tests	U	A	B	C	D
Blank samples after aging	T	0.6	0.7	0.4	0.8	0.4
	E	245	83	32	84	34
L1 R70 °C	T	0.6	0.5	0.4	0.5	0.4
	E	63	58	23	61	26
L1 R70 °C→LOCA	T	0.4	0.2	0.26	0.25	0.2
	E	56	20	16	33	17
L2 LOCA	T	0.6	0.6	0.4	0.7	0.4
	E	214	71	30	81	32
L2 LOCA→R70 °C	T	0.6	0.4	0.35	0.5	0.4
	E	84	41	21	49	23
L3 LOCA + R	T	0.1	0	0	0	0
	E	12	0	0	0	0
L4 R23 °C	T	0.7	0.7	0.4	0.75	0.45
	E	67	51	19	52	22
L4 R23 °C LOCA	T	0.65	0.4	0.3	0.5	0.4
	E	74	56	30	61	30

T = Tensile strength (MPa)
E = Elongation at break (%)

Mechanical Measurement

VAMAC (82H3)

Aging / Accident	Tests	U	A	B	C	D
Blank samples after aging	T	1.8	1.8	1.8	1.8	1.8
	E	312	245	238	207	215
L1 R70 °C	T	1.9	2.05	2.0	2.0	1.95
	E	238	157	152	143	135
L1 R70 °C→LOCA	T	1.7	1.8	1.8	1.8	1.8
	E	249	189	181	165	163
L2 LOCA	T	1.8	1.7	1.8	1.7	1.8
	E	297	240	247	222	232
L2 LOCA→R70 °C	T	2.0	2.0	2.0	1.8	2.1
	E	187	160	176	152	153
L3 LOCA + R	T	1.8	1.8	1.8	1.8	1.8
	E	248	224	218	208	198
L4 R23 °C	T	1.8	1.8	1.9	1.7	1.8
	E	122	108	109	109	106
L4 R23 °C LOCA	T	0.65	0.4	0.3	0.5	0.4
	E	140	122	128	125	133

T = Tensile strength (MPa)
E = Elongation at break (%)

Mechanical Measurement

EPR (82H4)

Accident / Aging	Tests	U	A	B	C	D
Blank samples after aging	T	1.7	1.3	0.8	1.4	0.8
	E	174	99	81	93	73
L1 R70 °C	T	1.5	1.2	0.7	1.2	0.8
	E	103	62	35	59	36
L1 R70 °C→LOCA	T	1.3	0.7	0.6	0.7	0.5
	E	122	51	35	45	32
L2 LOCA	T	1.1	1.2	0.8	1.2	0.8
	E	198	108	73	102	64
L2 LOCA→R70 °C	T	1.1	0.8	0.6	1.1	0.7
	E	75	39	31	55	35
L3 LOCA + R	T	1.2	0.7	0.7	0.8	0.6
	E	113	65	61	71	52
L4 R23 °C	T	1.6	1.2	0.8	1.4	0.8
	E	97	53	36	59	30
L4 R23 °C LOCA	T	1.5	1.0	0.7	1.1	0.7
	E	106	51	36	55	33

T = Tensile strength (MPa)
E = Elongation at break (%)

Strength at Break Measurement

Polydiallylphtalate (82H5)

Accident \ Aging	U	A	B	C	D
Blank samples after aging	4.6	4.8	5.0	4.8	4.7
L1 R70 °C	6.9	6.7	7.4	6.0	6.5
L1 R70 °C→LOCA	3.1	3.1	3.2	3.1	3.5
L2 LOCA	4.1	4.3	5.7	4.8	4.7
L2 LOCA→R70 °C	5.6	4.0	5.0	5.2	4.5
L3 LOCA + R	4.1	3.7	4.0	3.7	3.7
L4 R23 °C	6.1	7.0	6.5	7.0	7.4
L4 R23 °C LOCA	3.9	4.0	3.6	3.5	3.6

Units = MPa

Strength at Break Measurement

P.P.S. (82H6)

Accident \ Aging	U	A	B	C	D
Blank samples after aging	8.7	8.0	8.1	8.0	7.8
L1 R70 °C	9.2	9.0	9.2	8.7	8.7
L1 R70 °C→LOCA	4.5	5.4	5.5	5.7	5.9
L2 LOCA	5.2	4.7	5.2	5.2	4.6
L2 LOCA→R70 °C	5.8	4.9	5.1	4.9	5.1
L3 LOCA + R	4.8	4.4	5.0	5.6	5.3
L4 R23 °C	9.7	9.2	9.3	9.3	9.3
L4 R23 °C LOCA	5.9	5.2	5.2	5.9	5.3

Units + MPa

Mechanical Measurement

HYPALON (82G10)

Accident / Aging	Tests	U	A	B	C	D
Blank samples after aging	T	0.9	0.7	0.6	0.7	0.7
	E	422	249	205	204	214
L1 R70 °C	T	0.72	0.67	0.65	0.63	0.66
	E	195	35	23	28	30
L1 R70 °C→LOCA	T	0.45	0.42	0.38	0.4	0.3
	E	142	29	26	23	24
L2 LOCA	T	0.72	0.52	0.42	0.51	0.50
	E	355	165	97	146	120
L2 LOCA→R70 °C	T	0.97	0.66	0.53	0.73	0.70
	E	63	24	11	25	22
L3 LOCA + R	T	0.60	0.31	0.26	0.38	0.34
	E	258	69	56	84	65
L4 R23 °C	T	0.71	0.71	0.71	0.68	0.77
	E	170	36	34	42	39
L4 R23 °C LOCA	T	0.50	0.49	0.42	0.42	0.49
	E	105	33	25	24	19

T = Tensile strength (MPa)
E = Elongation at break (%)

Permanent Set After Compression
(In Percent)

VAMAC (82J3)

Accident \ Aging	U	A	B	C	D
Blank samples after aging	9.6	56	71	68	76
L1 R70 °C	82	86	95	87	88
L1 R70 °C→LOCA	75	86	92	89	85
L2 LOCA	29	72	74	75	70
L2 LOCA→R70 °C	85	87	88	87	86
L3 LOCA + R	83	85	82	87	87
L4 R23 °C	85	90	94	85	83
L4 R23 °C LOCA	86	88	91	84	88

Permanent Set After Compression
(In Percent)

VAMAC (82J4)

Accident \ Aging	U	A	B	C	D
Blank samples after aging	8.2	67	71	58	57
L1 R70 °C	78	85	90	85	90
L1 R70 °C→LOCA	78	90	87	91	84
L2 LOCA	32	74	73	69	75
L2 LOCA→R70 °C	89	88	90	90	90
L3 LOCA + R	85	89	88	88	88
L4 R23 °C	82	91	91	91	88
L4 R23 °C LOCA	84	86	89	88	87

DISTRIBUTION:

U.S. Government Printing Office
Receiving Branch (Attn: NRC Stock)
8610 Cherry Lane
Laurel, MD 20707
375 copies for RV

Ansaldo Impianti
Centro Sperimentale del Boschetto
Corso F.M. Perrone, 118
16161 Genova
ITALY
Attn: C. Bozzolo

Ansaldo Impianti
Via Gabriele D'Annunzio, 113
16121 Genova
ITALY
Attn: S. Grifoni

ASEA-ATOM
Department KRD
Box 53
S-721 04
Vasteras
SWEDEN
Attn: A. Kjellberg

ASEA-ATOM
Department TQD
Box 53
S-721 04
Vasteras
SWEDEN
Attn: T. Granberg

ASEA KABEL AB
P.O. Box 42 108
S-126 12
Stockholm
SWEDEN
Attn: B. Dellby

Atomic Energy of Canada, Ltd.
Chalk River Nuclear Laboratories
Chalk River, Ontario K0J 1J0
CANADA
Attn: G. F. Lynch

Atomic Energy of Canada, Ltd.
1600 Dorchester Boulevard West
Montreal, Quebec H3H 1P9
CANADA
Attn: S. Nish

Atomic Energy Research Establishment
Building 47, Division M.D.D.
Harwell, Oxfordshire
OX11 ORA,
ENGLAND
Attn: S. G. Burnay

Bhabha Atomic Research Centre
Health Physics Division
BARC
Bombay-85
INDIA
Attn: S. K. Mehta

British Nuclear Fuels Ltd.
Springfields Works
Salwick, Preston
Lancs
ENGLAND
Attn: W. G. Cunliff, Bldg 334

Brown Boveri Reaktor GMBH
Postfach 5143
D-6800 Mannheim 1
WEST GERMANY
Attn: R. Schemmel

Bundesanstalt fur Materialprufung
Unter den Eichen 87
D-1000 Berlin 45
WEST GERMANY
Attn: K. Wundrich

CEA/CEN-FAR
Departement de Surete Nucleaire
Service d'Analyse Fonctionnelle
B.P. 6
92260 Fontenay-aux-Roses
FRANCE
Attn: M. Le Meur (40 copies)
J. Henry

CERN
Laboratorie 1
CH-1211 Geneve 23
SWITZERLAND
Attn: H. Schonbacher

Canada Wire and Cable Limited
Power & Control Products Division
22 Commercial Road
Toronto, Ontario
CANADA M4G 1Z4
Attn: Z. S. Paniri

Centro Elettrotecnico
Sperimentale Italiano
Research and Development
Via Rubattino 54
20134 Milan,
ITALY
Attn: Carlo Masetti

Commissariat a l'Energie Atomique
ORIS/LABRA
BP N° 21
91190 Gif-Sur-Yvette
FRANCE
Attn: G. Gaussens (10 copies)
J. Chenion
F. Carlin

Commissariat a l'Energie Atomique
CEN Cadarche DRE/STRE
BP N° 1
13115 Saint Paul Lez Durance
FRANCE
Attn: J. Campan

Conductores Monterrey, S. A.
P.O. Box 2039
Monterrey, N. L.
MEXICO
Attn: P. G. Murga

Electricite de France
(S.E.P.T.E.N.)
12, 14 Ave. Dubrieroz
69628 Villeurbarnie
Paris, FRANCE
Attn: H. Herouard
M. Hermant

Electricite de France
Direction des Etudes et Recherches
1, Avenue du General de Gaulle
92141 CLAMART CEDEX
FRANCE
Attn: J. Roubault
L. Deschamps

Electricite de France
Direction des Etudes et Recherches
Les Renardieres
Boite Postale n° 1
77250 MORET SUR LORING
FRANCE
Attn: Ph. Roussarie
V. Deglon
J. Ribot

EURATOM
Commission of European Communities
C.E.C. J.R.C.
21020 Ispra (Varese)
ITALY
Attn: G. Mancini

FRAMATOME
Tour Fiat - Cedex 16
92084 Paris La Defense
FRANCE
Attn: G. Chauvin
E. Raimondo

Furukawa Electric Co., Ltd.
Hiratsuka Wire Works
1-9 Higashi Yawata - 5 Chome
Hiratsuka, Kanagawa Pref
JAPAN 254
Attn: E. Oda

Gesellschaft fur Reaktorsicherheit (GRS) mbH
Glockengasse 2
D-5000 Koln 1
WEST GERMANY
Attn: Library

Health & Safety Executive
Thames House North
Milbank
London SW1P 4QJ
ENGLAND
Attn: W. W. Ascroft-Hutton

ITT Cannon Electric Canada
Four Cannon Court
Whitby, Ontario L1N 5V8
CANADA
Attn: B. D. Vallillee

Imatran Voima Oy
Electrotechn. Department
P.O. Box 138
SF-00101 Helsinki 10
FINLAND
Attn: B. Regnell
K. Koskinen

Institute of Radiation Protection
Department of Reactor Safety
P.O. Box 268
00101 Helsinki 10
FINLAND
Attn: L. Reiman

Instituto de Desarrollo y Diseno
Ingar - Santa Fe
Avellaneda 3657
C.C. 34B
3000 Santa Fe
REPUBLICA ARGENTINA
Attn: N. Labath

Japan Atomic Energy Research Institute
Takasaki Radiation Chemistry
Research Establishment
Watanuki-machi
Takasaki, Gunma-ken
JAPAN
Attn: N. Tamura
K. Yoshida
T. Seguchi

Japan Atomic Energy Research Institute
Tokai-Mura
Naka-Gun
Ibaraki-Ken
319-11
JAPAN
Attn: Y. Koizumi

Japan Atomic Energy Research Institute
Osaka Laboratory for Radiation Chemistry
25-1 Mii-Minami machi,
Neyagawa-shi
Osaka 572
JAPAN
Attn: Y. Nakase

Kalle Niederlassung der Hoechst AG
Postfach 3540
6200 Wiesbaden 1,
WEST GERMANY
Biebrich
Attn: Dr. H. Wilski

Kraftwerk Union AG
Department R361
Hammerbacherstrasse 12 + 14
D-8524 Erlangen
WEST GERMANY
Attn: I. Terry

Kraftwerk Union AG
Section R541
Postfach: 1240
D-8757 Karlstein
WEST GERMANY
Attn: W. Siegler

Kraftwerk Union AG
Hammerbacherstrasse 12 + 14
Postfach: 3220
D-8520 Erlangen
WEST GERMANY
Attn: W. Morell

Motor Columbus
Parkstrasse 27
CH-5401
Baden
SWITZERLAND
Attn: H. Fuchs

National Nuclear Corporation
Cambridge Road
Whetstone
Leicester LE8 3LH
ENGLAND
Attn: A. D. Hayward
J. V. Tindale

NOK AG Baden
Beznau Nuclear Power Plant
CH-5312 Doettingen
SWITZERLAND
Attn: O. Tatti

Norsk Kabelfabrik
3000 Drammen
NORWAY
Attn: C. T. Jacobsen

Nuclear Power Engineering Test Center
6-2, Toranomon, 3-Chome
Minato-ku
No. 2 Akiyana Building
Tokyo 105
JAPAN
Attn: K. Takumi

Ontario Hydro
700 University Avenue
Toronto, Ontario M5G 1X6
CANADA
Attn: R. Wong
B. Kukreti

Oy Stromberg Ab
Helsinki Works
Box 118
FI-00101 Helsinki 10
FINLAND
Attn: P. Paloniemi

Radiation Center of
Osaka Prefecture
Radiation Application-
Physics Division
Shinke-Cho, Sakai
Osaka, 593, JAPAN
Attn: S. Okamoto

Rappinl
ENEA-PEC
Via Arcoveggio 56/23
Bologna
ITALY
Attn: Ing. Ruggero

Rheinisch-Westfallscher
Technischer Uberwachunge-Vereln e.V.
Postfach 10 32 61
D-4300 Essen 1
WEST GERMANY
Attn: R. Sartori

Sydkraft
Southern Sweden Power Supply
21701 Malmo
SWEDEN
Attn: O. Grondalen

Technical University Munich
Institut for Radiochemie
D-8046 Garching
WEST GERMANY
Attn: Dr. H. Heusinger

UKAEA
Materials Development Division
Building 47
AERE Harwell
OXON OX11 ORA
ENGLAND
Attn: D. C. Phillips

United Kingdom Atomic Energy Authority
Safety & Reliability Directorate
Wigshaw Lane
Culcheth
Warrington WA3 4NE
ENGLAND
Attn: M. A. H. G. Alderson

Waseda University
Department of Electrical Engineering
4-1 Ohkubo-3, Shinjuku-ku
Tokyo
JAPAN
Attn: K. Yahagi

1200 J. P. VanDevender
1800 R. L. Schwoebel
1810 R. G. Kepler
1811 R. L. Clough
1812 L. A. Harrah
1812 K. T. Gillen
1813 J. G. Curro
2155 J. E. Gover
2155 O. M. Stuetzer
6200 V. L. Dugan
6300 R. W. Lynch
6400 A. W. Snyder
6410 J. W. Hickman
6417 D. D. Carlson
6420 J. V. Walker
6440 D. A. Dahlgren
6442 W. A. Von Riesemann
6444 L. D. Buxton
6446 L. L. Bonzon (10)
6446 W. H. Buckalew
6446 L. D. Bustard (20)
6446 J. W. Grossman
6446 E. H. Richards
6446 F. V. Thome
6446 F. J. Wyant
6447 D. L. Berry
6447 P. R. Bennett
6449 K. D. Bergeron
6450 J. A. Reuscher
8024 M. A. Pound
3141 C. M. Ostrander (5)
3151 W. L. Garner

NRC FORM 335 (2-84) NRCM 1102, 3201, 3202

U.S. NUCLEAR REGULATORY COMMISSION

BIBLIOGRAPHIC DATA SHEET

SEE INSTRUCTIONS ON THE REVERSE

1 REPORT NUMBER (Assigned by TIDC and Vol. No., if any)
NUREG/CR-4091
SAND84-2291

2 TITLE AND SUBTITLE
The Effect of Alternative Aging and Accident Simulations on Polymer Properties

3 LEAVE BLANK

4 DATE REPORT COMPLETED
MONTH: April YEAR: 1985

5 AUTHOR(S)
L. D. Bustard, J. Chenion, F. Carlin, C. Alba, G. Gaussens, M. LeMeur

6 DATE REPORT ISSUED
MONTH: May YEAR: 1985

7 PERFORMING ORGANIZATION NAME AND MAILING ADDRESS (Include Zip Code)
Sandia National Laboratories
Albuquerque, New Mexico 87185

8 PROJECT TASK WORK UNIT NUMBER

9 FIN OR GRANT NUMBER
A-1051

10 SPONSORING ORGANIZATION NAME AND MAILING ADDRESS (Include Zip Code)
Electrical Engineering Branch
Division of Engineering Technology
Office of Nuclear Regulatory Research
U.S. Nuclear Regulatory Commission
Washington, DC 20555

11a TYPE OF REPORT

b PERIOD COVERED (Inclusive dates)
March 1982-April 1985

12 SUPPLEMENTARY NOTES

13 ABSTRACT (200 words or less)

The influence of accident irradiation, steam, and chemical spray exposures on the behavior of twenty-three age-preconditioned polymer sample sets (twenty-one different materials) has been investigated. The test program varied the following conditions:

1. Accident simulations of irradiation and thermodynamic (steam and chemical spray) conditions were performed both sequentially and simultaneously.
2. Accident thermodynamic (steam and chemical spray) exposures were performed both with and without air present during the exposures.
3. Sequential accident irradiations were performed both at 28°C and 70°C.
4. Age preconditioning was performed both sequentially and simultaneously.
5. Sequential aging irradiations were performed both at 27°C and 70°C.
6. Sequential aging exposures were performed using two sequences: (1) thermal followed by irradiation and (2) irradiation followed by thermal.

We report both general trends applicable to a majority of the tested materials as well as specific results for each polymer. Our data base consists of ultimate tensile properties at the completion of the accident exposure for three XLPO and XLPE, five EPR and EPDM, two CSPE (HYPALON®), one CPE, one VAMAC, one polydiallylphtalate, and one PPS material. We also report bend test results at completion of the accident exposures for two TEFZEL® materials and permanent set after compression results for three EPR, one VAMAC, one BUNA N®, one SILICONE, and one VITON® material.

14 DOCUMENT ANALYSIS - a KEYWORDS/DESCRIPTORS

b IDENTIFIERS/OPEN ENDED TERMS

15 AVAILABILITY STATEMENT
Unlimited

16 SECURITY CLASSIFICATION
(This page) U
(This report) U

17 NUMBER OF PAGES
160

18 PRICE

*U.S. GOVERNMENT PRINTING OFFICE: 1985-0-576-037/20,027